

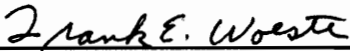
**METAL-PLATE-CONNECTED JOINT AND LUMBER SAFETY FACTORS  
AND THEIR INFLUENCE ON WOOD TRUSS SAFETY FACTORS**

by

Thomas D. Skaggs

Dissertation submitted to the Faculty of the  
Virginia Polytechnic Institute and State University  
in partial fulfillment of the requirements for the degree of  
**DOCTOR OF PHILOSOPHY**  
in  
Biological Systems Engineering

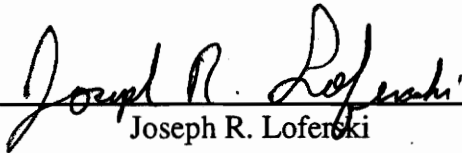
APPROVED:



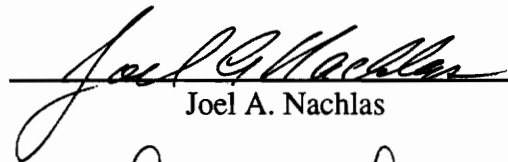
Frank E. Woeste, Chairman



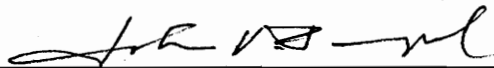
J. Daniel Dolan



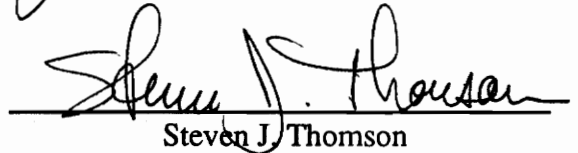
Joseph R. Loferski



Joel A. Nachlas



John V. Perumpral



Steven J. Thomson

February, 1995  
Blacksburg, Virginia

C.2

LD  
5655  
V856  
1995  
S634  
C.2

# **METAL-PLATE-CONNECTED JOINT AND LUMBER SAFETY FACTORS AND THEIR INFLUENCE ON WOOD TRUSS SAFETY FACTORS**

by

Thomas D. Skaggs

Frank E. Woeste, Chair

(ABSTRACT)

A model that simulates test of metal-plate-connected wood trusses was developed. The truss test model built on previous research efforts to simulate ultimate failure of structural systems. For years, lumber failure models have used failure equations that were derived from design equations. This approach was applied to the strengths of metal plate connected joints. The model uses actual steel properties data for modelling the strength of the joints, and uses the most current lumber data to model the lumber strength and stiffness properties in the trusses. One of the unique features of the model is the use of basic fundamental engineering properties to predict the strengths of the individual components of the structural systems. These general principles allow the model to be used for many truss configurations. This flexibility differs from several current metal plate connected wood truss models in the literature.

Although the safety factor for lumber is the smallest of all the truss components, many of the simulated truss failures were controlled by plate failures. The metal plate connected joints were the weakest link in the truss system. To improve the overall strength of a truss, the plates would need to be strengthened.

Two different truss configurations were used for the simulations. Both truss simulations performed well, when compared to actual test data.

# ACKNOWLEDGEMENTS

I would like to thank my graduate committee for their guidance and assistance during my research. The members of my committee were: Frank E. Woeste, J. Dan Dolan, Joe R. Loferski, Joel A. Nachlas, John V. Perumpral, and Steven J. Thomson. Special thanks go to Frank Woeste. Frank helped me tremendously during my Ph.D. studies. Not only did he help me with my research efforts, but he also gave me the opportunity to help him teach his undergraduate courses. Having this opportunity helped me to learn how important it is to transfer research knowledge to "real world people". I hope that some of Frank's finer traits have rubbed off on me so I'll be a more efficient person. I've had the opportunity to get to know several of my committee members both socially and professionally. I've enjoyed this relationship, and I'm looking forward to staying in contact with them. I have also taken several of the committee members' classes, and I believe they are some of the best professors I've had at Virginia Tech. They have all helped me in my educational experience at Virginia Tech.

During my research I had the opportunity to meet several technical directors of truss plate manufacturing companies. Dave Brakeman, P.E. of Lumbermate, Don Scott, P.E., of Truswal Systems and Stu Lewis, P.E. of Alpine helped me in this research. I could not have finished without their technical support. They provided data for my model, and more importantly provided me knowledge so I could develop the model. Special thanks go to Stu Lewis, and the family at Alpine Engineered Products. I had the opportunity to work with Stu for a couple of weeks in the summer of 1993. I learned more in those two weeks than I could have learned in two years in Blacksburg. Although my future areas of research will likely not



be in the area of metal-plate-connected wood trusses, I hope I'll have the opportunity to work with Stu again.

I would like to thank Phil McClellan for his help toward the end of my time in Blacksburg. I would have had a hard time finishing without his help. My family also deserves special thanks, they helped me both personally and financially. Now that I am finished with school, I hope my parents will take the opportunity to do more fishing and square dancing.

I would like to acknowledge the friendship and support of some of my fellow graduate students. Some of the "basement bunch" that stand out are Faycal Bouraoui, Jean Bruggeman, Dan Ess, Kevin Brannan, Jim Kern and Chris Sims. Whether our discussions were politics, sports, guitars, or our research, the conversations were always stimulating and enlightening. They helped to make my free time in Blacksburg more enjoyable.

Finally, I would like to thank Dr. Perumpral and the Biological Engineering Department for their financial support. I was very fortunate to have the opportunity to study in the department. The department gave me the chance to serve on several committees and learn some of the intricacies of becoming a faculty member.

# TABLE OF CONTENTS

	Page
TABLE OF CONTENTS .....	v
LIST OF FIGURES .....	vii
LIST OF TABLES .....	x
INTRODUCTION .....	1
BACKGROUND .....	1
OVERVIEW OF SAFETY FACTORS .....	2
OBJECTIVES .....	5
LITERATURE REVIEW .....	7
WOOD JOINT STUDIES .....	7
WOOD TRUSS RELIABILITY STUDIES .....	14
SYSTEM RELIABILITY STUDIES .....	17
STEEL PROPERTIES STUDY .....	20
BUILDING CODE REQUIREMENTS FOR TRUSS TESTS .....	24
JUSTIFICATION .....	27
INTRODUCTION .....	27
CURRENT SAFETY FACTORS .....	28
Overview .....	28
Steel Net Section .....	29
Steel Shear .....	32
Tooth Withdrawal .....	35
Truss Lumber .....	39
SUMMARY .....	43
CONCLUSIONS .....	45
STEEL PROPERTIES STUDY .....	47
INTRODUCTION .....	47
INITIAL STEEL SURVEY .....	47
ADVANCED STEEL STUDY .....	51
SAS Analysis .....	53
Summary Statistics .....	54
Best-Fit Statistical Distributions .....	59
Grade B Yield Strength Data .....	61
Grade B Ultimate Strength Data .....	72
Grade 60 Strength Data .....	89

<b>SUMMARY</b> .....	96
<b>CONCLUSIONS</b> .....	97
<b>MODEL DEVELOPMENT</b> .....	99
<b>INTRODUCTION</b> .....	99
<b>GENERATING PROPERTIES FOR THE PROBABILISTIC MODEL</b> .....	100
<b>Lumber Strength Properties</b> .....	101
<b>Tooth Withdrawal</b> .....	109
<b>Steel Properties</b> .....	111
<b>STRUCTURAL ANALYSES OF THE TRUSS</b> .....	112
<b>Estimating the End Forces</b> .....	114
<b>Modes of Failure and Failure Criteria</b> .....	117
Modelling Lumber Failures .....	117
Modelling Heel Joint Failures .....	126
Modelling Tension Splice Joint Failures .....	133
Modelling Compression Splice Joint Failures .....	137
Modelling Peak Joint Failures .....	138
Modelling Web Joint Failures .....	143
<b>SIMULATED LOADING OF THE TRUSS</b> .....	143
<b>MODEL ASSUMPTIONS</b> .....	145
<b>MODEL VERIFICATION AND VALIDATION</b> .....	147
<b>INTRODUCTION</b> .....	147
<b>MODEL VERIFICATION</b> .....	150
<b>MODEL VALIDATION</b> .....	152
<b>RESULTS AND DISCUSSION</b> .....	159
<b>VALIDATION TRUSS</b> .....	159
<b>SCISSOR TRUSS</b> .....	162
<b>SUMMARY AND CONCLUSIONS</b> .....	169
<b>SUMMARY</b> .....	169
<b>CONCLUSIONS</b> .....	170
<b>MODEL LIMITATIONS</b> .....	171
<b>FUTURE RESEARCH</b> .....	172
<b>REFERENCES</b> .....	174
<b>TRUSS TEST MODEL SOURCE CODE</b> .....	181
<b>VITA</b> .....	207

# LIST OF FIGURES

		Page
Figure 3.1	Probability density function derived from the literature for the ultimate tensile strength of HS steel based on minimum specified properties. ....	31
Figure 3.2	Probability density function derived from the literature for the shear strength of HS steel based on minimum specified properties. ....	34
Figure 3.3	Weibull density function representing tooth-withdrawal joint strength. The distribution shape was determined from the Suddarth et al. (1981) test data. ....	38
Figure 3.4	Probability density function for the ultimate tensile strength of lumber based on In-grade test data (Evans and Green, 1987). ....	42
Figure 3.5	A comparison of the probabilities of failure for the four failure modes of the joint at different design load multiples. ....	44
Figure 4.1	Histogram of all of the Grade B yield strength data supplied by truss plate manufacturer II with the best-fit distribution overlain. ....	63
Figure 4.2	Histogram of the Grade B yield strength data produced by steel manufacturer W with the best-fit distribution overlain. ....	65
Figure 4.3	Histogram of the Grade B yield strength data produced by steel manufacturer X with the best-fit distribution overlain. ....	67
Figure 4.4	Histogram of the Grade B yield strength data produced by steel manufacturer Y with the best-fit distribution overlain. ....	69
Figure 4.5	Histogram of the Grade B yield strength data produced by steel manufacturer Z with the best-fit distribution overlain. ....	71
Figure 4.6	Histogram of all of the Grade B ultimate strength data supplied by truss plate manufacturer II with the best-fit distribution overlain. ....	74
Figure 4.7	Histogram of the Grade B yield strength data produced by steel manufacturer W with the best-fit distribution overlain. ....	76

Figure 4.8	Histogram of the Grade B yield strength data produced by steel manufacturer X with the best-fit distribution overlain. . . . .	79
Figure 4.9	Histogram of the Grade B yield strength data produced by steel manufacturer Y with the best-fit distribution overlain. . . . .	81
Figure 4.10	Histogram of the Grade B yield strength data produced by steel manufacturer Z with the best-fit distribution overlain. . . . .	83
Figure 4.11	Probability density function representing the smallest mean ultimate strength and the largest mean ultimate strength. . . . .	85
Figure 4.12	Scatter-plot of ultimate strength versus yield strength for Grade B steel supplied by truss plate manufacturer II. . . . .	87
Figure 4.13	Histogram of the Grade 60 yield strength data supplied by truss plate manufacturer II with the best-fit distribution overlain. . . . .	91
Figure 4.14	Histogram of the Grade 60 ultimate strength data supplied by truss plate manufacturer II with the best-fit distribution overlain. . . . .	93
Figure 4.15	Scatter-plot of ultimate strength versus yield strength for Grade 60 steel supplied by truss plate manufacturer II. . . . .	95
Figure 5.1	Schematic diagram of a PPSA4 member showing end force notation. . . . .	115
Figure 5.2	Shear and moment diagrams for a typical truss panel. . . . .	118
Figure 5.3	Schematic view of a heel joint in a pitched chord truss. . . . .	127
Figure 5.4	Close up view of a truss plate used for a heel joint of a pitched chord truss. . . . .	128
Figure 5.5	Schematic view of a tension splice joint. . . . .	133
Figure 5.6	Detailed view of half of the tension splice joint with forces applied. . . . .	134
Figure 5.7	Detailed view of half of the tension splice with the moment converted to an equivalent coupled force. . . . .	136
Figure 5.8	Schematic view of a peak joint in a pitched chord truss. . . . .	139

<b>Figure 5.9</b>	<b>Expanded view of the plate with the pertinent forces for possible failure modes. . . . .</b>	<b>140</b>
<b>Figure 5.10</b>	<b>Graphical representation of the lengths <math>L_1</math> and <math>L_2</math>. . . . .</b>	<b>142</b>
<b>Figure 6.1</b>	<b>Schematic diagram of a truss used for verification and validation of the truss test model. . . . .</b>	<b>148</b>
<b>Figure 6.2</b>	<b>Histogram of the multiple of live load capacity for the validation truss, lumber failure controlled for all trials. . . . .</b>	<b>153</b>
<b>Figure 6.3</b>	<b>Histogram of the multiple of live load for the validation truss. . . . .</b>	<b>155</b>
<b>Figure 7.1</b>	<b>Histogram of the multiple of live load capacity for the validation truss, lumber failure controlled for all trials with no calibration of the fictitious members. . . . .</b>	<b>160</b>
<b>Figure 7.2</b>	<b>Histogram of the multiple of live load for the validation truss with no calibration of the fictitious members. . . . .</b>	<b>161</b>
<b>Figure 7.3</b>	<b>Schematic diagram of a truss used for verification and validation of the truss test model. . . . .</b>	<b>163</b>
<b>Figure 7.4</b>	<b>Histogram of the multiple of live load capacity for the scissor truss. . . . .</b>	<b>165</b>
<b>Figure 7.5</b>	<b>Histogram of the multiple of live load for the scissor truss assuming that there is no interaction between the tensile strength and the shear strength in the peak joints. . . . .</b>	<b>167</b>

# LIST OF TABLES

		Page
Table 2.1	Summary of building code requirements for test safety factors of metal-plate-connected wood trusses. ....	24
Table 3.1	Minimum tensile-strength properties of steel truss plates. ....	30
Table 3.2	Minimum shear-strength properties of steel truss plates. ....	33
Table 4.1	Summary of the truss plate manufacturers steel survey response in terms of yield strength. ....	49
Table 4.2	Summary of the truss plate manufacturers steel survey response in terms of ultimate strength. ....	50
Table 4.3	Summary of yield strength properties for Grade B steel from truss plate manufacturer II. ....	52
Table 4.4	Summary of ultimate strength properties for Grade B steel from truss plate manufacturer II. ....	53
Table 4.5	Summary of yield strength properties for Grade 60 steel from truss plate manufacturer II. ....	57
Table 4.6	Summary of ultimate strength properties for Grade 60 steel from truss plate manufacturer II. ....	57
Table 4.7	Best fit statistical distributions for Grade B steel yield strength from truss plate manufacturer II, and the probabilities of values occurring below nominal yield strength. ....	62
Table 4.8	Best fit statistical distributions for Grade B steel ultimate strength from truss plate manufacturer II, and the probabilities of values occurring below nominal ultimate strength. ....	73
Table 4.9	Best fit statistical distributions for Grade 60 steel from truss plate manufacturer II, and the probabilities of values occurring below nominal strengths. ....	90
Table 6.1	Plate values used for the validation truss. ....	149

**Table 6.2**      **Summary of simulated failures for the validation truss. . . . .** 157

**Table 7.1**      **Plate values used for the scissor truss trials. . . . .** 164

**Table 7.2**      **Summary of simulated failures for the scissor truss. . . . .** 168



# CHAPTER I

## INTRODUCTION

### BACKGROUND

Metal-plate-connected (MPC) truss design involves the selection of lumber for the truss chords and webs, followed by the design of joints to safely transmit the forces developed in the truss members. An adequate design requires that the webs and chords be selected such that the lumber members are not overstressed, and that the joints are not overstressed. Critical lumber stresses include tension, compression, bending, and shear stresses. Critical joint stresses are steel tension, steel shear, tooth withdrawal, and net-section of the lumber at the joint. The theoretical design safety factors, using the various published allowable design values for the four stress conditions of the joints, are not equal. Also, the theoretical design safety factors for the lumber members do not match the safety factors used for the joint designs. Even though the safety factors used to design the components of a truss vary, trusses designed under this system have performed well in service.

Sometimes it is necessary to demonstrate that a constructed truss will carry some multiple of the design loads. This multiple will be referred to as the "truss-test safety factor." Truss-test safety factors are specified either by the code of jurisdiction or by an industry standard, or the code of jurisdiction may reference an industry standard. Truss-test safety factors specified by the codes that are applicable to wood trusses range from 2-times live load to more than 3-times total load. These code-specified test safety factors are typically higher than the safety factors used to design the individual components of the truss. This situation

raises two questions: 1) Should a truss, made of many individual components, have a higher test safety factor than the safety factors used to design the components and 2) What is the relationship between the theoretical design safety factors of the components and the expected truss-test safety factor?

## **OVERVIEW OF SAFETY FACTORS**

Safety factors have been used successfully in many areas of engineering to manage risk even though their basis has been subjective and difficult to rationalize. For purposes of this discussion, a system is considered safe when the "capacity" exceeds the "load". Safety factors are simple methods to account for uncertainty in loads and capacities. Although the concept of a safety factor is simple, it is not always applied to the capacity and to the load variables in the same way.

Some designs apply a safety factor to the load variable, but have no safety factor applied to the capacity variable. For example, a culvert may be designed based on a 50-year mean recurrence interval flow rate (a load), but the culvert will be sized based on its "average" capacity. In this case, the load contains a built-in safety factor equal to the 50-year event divided by the average flow, and the safety factor on the culvert capacity is 1.0.

In the case of a grain bin design, the safety factor on the load is typically 1.0, but the capacity contains the safety factor used in the steel design codes of practice. In both of these examples, the designers apparently believe that the "risks" are managed properly.

In most structural designs, safety factors are used on both the load and the capacity. For example, a typical residential floor (living area) is designed for 40 psf live load. The

average live load on a residential floor is about 11 psf (Corotis and Doshi, 1977). Therefore the safety factor on the load based on the average live load is  $40/11$ , or 3.64. For lumber, the theoretical design safety factor is the result of dividing the fifth percentile of the test strength distribution by the allowable stress adjusted to a ten minute test duration. The published value for a bending stress safety factor is 1.3<sup>1</sup> (ASTM, 1993d), which is a number much less than what would be obtained had the safety factor been based on the average strength. The two factors of safety can be combined to make one. The safety factor of a joist assuming the average service live load and a 1.3 safety adjustment on the fifth percentile of the capacity distribution is  $3.64 \times 1.3$  or 4.73.

Two points can be made from the residential floor design example. The first point is that structural designers adjust both the load and the capacity sides of the design equation. This approach should inherently be superior to adjusting only one side of the design equation because the adjustments account for variability in both the applied load and the capacity of the structural material used. The second point is that the basis of a safety factor is as important as the magnitude of the safety factor. Had the safety factor for the structural material (assuming a southern pine wood joist) been based on the "In-grade" average strength of the joists (Green and Evans, 1987), rather than the fifth percentile, the combined safety factor for the joist design problem would be in the range of 8 to 13.

---

<sup>1</sup>The 1.3 safety factor is not widely understood. The well-known 2.1 associated with lumber stresses is the product of 1.6 for a normal duration adjustment and 1.3, the safety factor. See the last sentence of paragraph 6.2 in ASTM D 245-92 (1993d) for further discussion.

The safety factor most frequently quoted and referenced in codes and standards is the "design safety factor" (DSF). The DSFs for structural applications range from as low as 1.25 for manned aircraft (Allen and Haisler, 1985) to as high as 6.0 for nails subjected to withdrawal loading conditions over a long period of time (Forest Products Laboratory, 1987). Apparent safety factors of bolted lumber connections have been found to be as high as 8.1 (Gutshall, 1994). The DSF is the ratio of the average capacity (generally from a short term test), or a nominal value less than the average, to the allowable design capacity for the material.

One problem with understanding and setting safety factors stems from the fact that a proportional relationship may not exist between the size of the DSF and the amount of protection against the anticipated risks. For example, few people would question the safety record of commercial aircraft in the United States even though the DSF values used are close to 1.25. And it is not rational that nails, with a DSF of 6.0 on withdrawal capacity, have a risk of failure less than that for a commercial aircraft. The aircraft versus nail example suggests that probably the best tool for evaluating or specifying design safety factors is in-service experience because even though nails and airplanes are designed with greatly contrasting DSF values, both appear to provide safe and acceptable levels of service.

In summary, a universal rule for determining the appropriate DSF for a structural application is not available. The actual safety of a design depends upon the many aspects of the structural components as part of a system that includes the statistical basis of the DSF. A DSF based on the average capacity of a structural material may be much greater than another factor based on the lower tail of the distribution (such as the fifth percentile), yet the

latter design with a lower DSF may provide a greater level of protection against the risks of failure. In-service experience should be given substantial consideration when evaluating and setting safety factors for structural design.

## **OBJECTIVES**

The main objective of this research is to analyze the relationship between safety factors for the "parts" versus "the whole" truss. The intent of structural safety factors will be reviewed as background. Theoretical-design safety-factors for joints will be documented and probability distributions for steel strength will be derived based on the research literature and codes-of-practice for steel design. A probability distribution for tooth withdrawal resistance will be developed from research literature. The theoretical-design safety-factor for lumber strength will be presented and a probability distribution representing lumber strength will be defined. These probability curves will be used to calculate the theoretical failure probabilities of the joints and lumber when subjected to various multiples of design load. The truss-test safety-factors specified by the codes will be summarized and using a probabilistic model it will be demonstrated that a link between the code requirements for a truss test and the design of the truss parts is not evident.

The specific objectives of this research are:

- 1.) To outline and discuss safety factors currently used for metal-plate-connected joint design.
- 2.) To develop a procedure for relating joint and lumber safety factors to truss safety factors.
- 3.) To verify and validate the developed probability-based truss model.
- 4.) To perform sensitivity analyses on the validated model.

# CHAPTER II

## LITERATURE REVIEW

### WOOD JOINT STUDIES

Maraghechi and Itani (1984) developed a two-dimensional, three degrees-of-freedom finite-element model for simulating metal connector plates (MCPs). The linear-elastic-spring constants were found using three types of tests: bending, shear, and axial tests for estimating the rotational, shear, and axial spring constants, respectively. The researchers found that the shear-spring stiffness had little effect on the overall behavior of a truss analog. Their method calculated forces in the plate elements; however, no suggestions were given relating the forces to allowable steel stresses.

Beineke and Suddarth (1979) compared several theories on the tooth loading distribution along the length of an axial loaded MCP. They explored several different nonlinear-theoretical models, and found the results were all similar. They then attempted to validate the theoretical models by testing plates with different lengths. The theoretical models failed to predict the relationship between plate length and axial displacement; therefore, the researchers used simple linear regression that fit the data better than the more complex models. A recommendation was made to test joints with the shortest plates used in design and longest plates used for design, and then apply linear regression to find a best-fit line. Another suggestion was to transform the truss plate to an equivalent wood cross section for modeling the deflection of tension joints. Their research focused on stiffness of joints, but not strengths.

Crovella and Gebremedhin (1990) developed a tension joint model for MCPs. This model treated the plate as an elastic foundation, and was validated by testing tension-splice joints. Finite element analysis was also conducted. They found that the elastic foundation model consistently predicted both joint stiffness and stress distributions in the teeth as accurately as finite element analysis.

Groom and Polensek (1992) developed a theoretical model to predict the load transfer between the wood and teeth of MCPs loaded in tension. The teeth were modeled as a beam on an inelastic foundation, and the Runge-Kutta method was used to solve the governing differential equations. Four modes of failure were considered as potential limit states. These were 1) tooth withdrawal, 2) wood strength, 3) plate tension, and 4) plate bending that causes rotation of the plate and subsequently the tooth to withdraw. The researchers stated that the teeth could be modeled analogous to rivets in a steel plate. Predictions made by the theoretical deflection model compared well to test results for joints that failed in tooth withdrawal; however, the model poorly predicted the behavior of joints that exhibited wood type failures.

McCarthy and Wolfe (1987) tested southern pine joints in tension with six different configurations. Four of the joint configurations were standard TPI (1992) joints, while the two remaining joint configurations were non-standard, with plate to grain orientations of 30 and 60 degrees. These joints are similar to heel-joints; however, they were tested in pure tension. A Hankinson (1921, as cited by McCarthy and Wolfe) type interpolation was used to estimate parameters for a nonlinear load versus displacement model (originally developed by Foschi, 1977b) for plate angles other than those tested.



Wolfe et al. (1991) stated that although many failures are caused by the connections, there has been a major emphasis in modeling truss lumber failures. They imply research is lacking in the field of combined loading of joints and indicate that there is no standard procedure for testing joints for combined loading arrangements. The researchers developed special grips to test splice joints in combined bending and tension. This was achieved by axially loading the specimen above the neutral axis causing eccentricity; thus, inducing moment in the splice joint. These grips were designed to be portable, lightweight and adaptable so they could be used with a variety of testing machines. These special grips were designed for 2 x 4 lumber and 20 gauge MCPs. Wolfe (1990) used these special testing grips to test 62 southern-pine joints plated with 3- by 5.25-inch 20 gauge metal connector plates. There were five different joint configurations, ranging from pure tension to pure bending with three levels of combined tension and bending. From these data a proposed interaction equation was developed to predict failure for combined bending and tension, for example, a bottom chord splice joint. Equation 2.1 represents the proposed criterion.

$$\frac{t}{T} + \frac{m^a}{M} \leq 1.0 \quad (2.1)$$

where:

- t = eccentric axial load,
- T = axial strength of the connection,
- m = bending moment,
- M = pure bending moment capacity of the connection, and
- a = exponent derived by test.

The axial tension capacity,  $T$ , is determined by testing joints in pure tension. The bending moment capacity is found by testing joints in pure tension, and the exponent,  $a$ , is found by a least squares regression technique fit the pure tension data, the pure moment data, and the combined tension and bending data. Wolfe (1990) derived the appropriate parameters for the interaction equation by testing southern pine 2 by 4 lumber. These joints were plated with two 3- by 5.25-inch 20 gauge metal connector plates. Based on the test data,  $T$ ,  $M$ , and  $a$  were found to be 6,700 lbs, 8,700 in-lbs, and 1.28, respectively.

In a later publication, Wolfe et al (1991) analyzed the Wolfe (1990) data and developed a more general failure criteria. It should be noted that Equation 2.2 appears differently in the Wolfe et al. (1991) publication and for consistency is rewritten here as:

$$\left(\frac{t}{T}\right)^a + \left(\frac{m}{M}\right)^b \leq 1.0 \quad (2.2)$$

Wolfe re-fit the data and found  $a$  and  $b$  provided a best fit as 0.83 and 1.16, respectively.

Gupta (1994) tested 41 southern pine 2 by 4 joints in combined tension and bending. The joints were constructed with 3- by 4-inch 20 gauge metal connector plates. The researcher tested joints in pure bending, pure tension, and four different levels of combined bending and tension by eccentrically loading the joints in tension. Gupta found  $T$  equal to 6305 lbs,  $M$  equal to 10,943 in-lbs,  $a$  equal to 8.3011 and  $b$  equal to 0.6083. Gupta theorized that the large value of  $a$  was caused by the testing method. Most of the test specimens were loaded closer to pure tension than to pure bending; therefore, intermediate values of combined tension and bending were lacking.

These proposed failure criteria are joint specific; therefore, they require testing of each joint configuration to find  $T$ ,  $M$ ,  $a$ , and  $b$ . This could be a drawback for expanding these methods to different size plates.

Triche (1984) constructed 2 x 4 MSR western-hemlock splice joints for testing in pure bending. Triche modified a finite element model developed by Foschi (1977a, 1977b) called Structural Analysis of Trusses (SAT). Triche applied the modified model to tension-splice joints and found good agreement in terms of deflection. SAT incorporates a nonlinear element stiffness matrix for the finite element representing the joint that requires an iterative technique to solve the global stiffness matrix. Although he used a nonlinear joint element, it was illustrated that the joints behaved in a linear fashion, in terms of deflection, within the design range. A per-tooth stress relationship was also developed that could be used for design purposes. When the tooth load exceeds tooth allowable load, the design is considered inadequate.

Gebremedhin et al. (1992) tested southern-pine joints in tension and shear, and fit Foschi's (1977b) nonlinear model to the data. The researchers tested the four standard TPI (1992) joints as well as special joints at several different lumber-axis and plate-axis orientations. Several of the specimens resembled heel-joints with roof slopes of 30, 45 and 60 degrees. Only three replications were tested, which follows the TPI (1992) recommendation. The 30 degree heel-joints all failed in tooth withdrawal. The authors reported that a linear relationship of load versus deflection is valid up to the critical slip. Critical slip is reached when the total slip of the joint equals 0.030 inches.

McAllister (1989) fit Foschi's (1977b) nonlinear model to joint deflection test data. The study consisted of joints constructed from southern pine dimension lumber, laminated veneer lumber (LVL) manufactured from southern-pine, and a composite yellow poplar and Douglas-fir flake board. The researcher tested three different types of truss plates, two different types of load/plate axis orientations, and two load/wood grain orientations. The researcher found no significant difference between either ultimate loads, loads at critical slip, or nonlinear model parameters within a specific plate. McAllister theorized that the similarities in the joint behavior could be explained by similar specific gravities of the three different lumber samples.

Cramer et al. (1990) pointed out that the current design philosophies for small truss plates are based on simplified but reasonable assumptions; however, they questioned the adequacy of using these simple design procedures for large trusses. Large trusses are generally used for longer spans with fewer redundancies, hence system truss reliability could be sacrificed by using these simplifying assumptions. The researchers suggested that deformation of joints can be broken into three parts, 1) wood deformation, 2) steel deformation, and 3) a combination, wood-to-steel deformation due to tooth deformation. The size effects of truss plates were analyzed with the aid of a 2-D finite element model. A nonlinear spring was used to model the wood-to-steel interface, but the authors suggested that obtaining the nonlinear spring constants could be cumbersome. The theoretical model supported the following conclusions: as plate contact area increases, the contribution of deformation from wood-to-steel interface decreases; however, the deformation contribution due to steel increases. The researchers theorized that small plates act as rigid bodies; hence,

the stress distributions of the teeth are uniform throughout the plate. As plate size increases, the stress distributions for the teeth are no longer uniform.

Lau (1987) tested white-spruce and lodgepole-pine joints in tension and shear. He also tested joints in a specially designed steel frame that resembled heel-joints. The joints were pin connected to the test frame, and the pin holes were reinforced with truss plates to provide additional strength and reduce deformation. The load was applied with a hydraulic jack at the point where the reactions would normally be located on the heel-joint, and only the vertical displacements of the joints were recorded. Lau calibrated SAT to CSA standard tension joints (1980, as cited by Lau) that are identical to standard TPI (1992) tension joints. He then succeeded in predicting the deflection of three member shear test specimens using the calibrated model. SAT adequately predicted the shear test deflections for plate orientations ranging from 0 to 165 degrees with 15 degree increments. SAT was also used to predict the vertical deflections of the heel-joints. SAT was not as successful at predicting the deflections of the heel joints as in predicting the deflections of the simple shear joints. The author theorized that the friction between the top and bottom-chord members influenced the joint deformation, and SAT did not include frictional forces between chord members. The simple shear tests should have had minimal friction; thus, a smaller error was introduced by not including frictional forces in SAT. Lau was enthusiastic about this method of testing because of the efficiency in testing heel-joints.

Gupta and Gebremedhin (1990) developed a test rack for the purpose of testing 2 x 4 lumber heel-joints, tension-splice joints and web joints. The heel-joint configurations were supported by a roller-type reaction at the bottom-chord and loaded at the centroid of the top-

chord by a compressive force. The moments that are induced in the heel-joint from bending moments in the chords are not simulated. All three joint configurations were tested during their research. The heel-joint failures were dominated by the tooth withdrawal failure mode, with ninety-five percent of the web joints failing by tooth withdrawal from the tension web and 94% of the tension joints failing in tooth withdrawal.

## **WOOD TRUSS RELIABILITY STUDIES**

Triche and Suddarth (1988) incorporated SAT into PPSA (Suddarth and Wolfe, 1984). This fusion model was called PPSAFT (PPSA-Foschi-Triche), and was used to predict deflections for four different truss configurations. The deflections of two parallel-chord trusses, one scissor truss and one 60 ft triple fink truss were predicted adequately. The modulus of elasticity (MOE) of the lumber were measured to be included as input into PPSAFT. The joint parameters were also estimated from a nonlinear regression performed on data collected from experimental tests for each lumber/plate type combination. Although Triche (1984) presented a Hankinson (1921) style interpolation to be used for joints without test data, Triche and Suddarth (1988) did not use these types of interpolations.

Sheppard (1969) investigated a simple procedure for testing light-gauge-metal heel plates. He compared the results of testing 24 ft trusses and 8 ft triangular trusses. These test consisted of 24 matched specimens with two repetitions each. The joint configurations were identical for the two trusses, with the only differences between the trusses being the spans and the fact that the smaller triangular trusses had no web members. Also heel-joint failures were forced to occur in a specific joint by placing a large MCP on the opposite end of the truss. It

was found that the heel-joints on the smaller triangular trusses were 8% stronger than the full size trusses. This could indicate that although the triangular trusses had identical geometry in the heel-joints, the behavior of the smaller trusses does not exactly emulate the behavior of the bigger trusses.

Rojiani and Tarbell (1985) studied the reliability of triple-W and flat Howe trusses. The researchers studied several different reliability formulations. These included: 1) mean-value first-order second-moment method (MVFOSM) with all variables assumed to be independent, 2) MVFOSM method with correlated variables, 3) advanced FOSM method with correlated variables having normal distributions, and 4) advanced FOSM method with independent variables and non-normal distributions. The non-normal distributions were chosen from historical data, and the load duration was modeled as a random variable with the assumed loading being snow. Modeling the load duration effect as a random variable, in essence, induces correlation between the snow load and the resistances of the wood members. The researchers found that the risk levels for wood trusses were comparable to steel and concrete. Another finding was the reliability indices were much higher for the webs of the trusses than for the chords. Generally advanced non-normal FOSM methods yielded higher reliability indices than the advanced normal FOSM method.

Gupta et al. (1992) fit statistical distributions to data collected by Gupta and Gebremedhin (1990) for three different joint configurations. They found that the heel-joints and web joints were best fit by a normal distribution, and none of the distributions tested seemed to fit the tension joints data. The distributions studied by the researchers were normal, two-parameter lognormal, and three parameter Weibull. The authors suggested using the

actual data for sampling when simulating tension joint strength. Gupta and Gebremedhin (1992) used the data for simulation of trusses with the same joint configurations. The researchers conducted a reliability study with these joints, but indicate that these test data should only be used for simulated trusses with these specific joint configurations.

Suddarth et al. (1981) tested six different metal-plate-connected parallel-chord floor trusses. These trusses were part of a research program that was designed to validate PCT-80 (TPI, 1987). Three replications of each of the six different trusses were tested to ultimate failure. The researchers defined an ultimate load factor that is based on the multiple of live load carried at truss failure, in addition to the design dead load. These load factors ranged from 2.40 to 4.94 for the eighteen test specimens, and ten of the eighteen trusses exceeded an ultimate load factor of 3.0. Fourteen of the eighteen trusses failed by peeling of the plate, also known as tooth withdrawal. The authors also conducted another study as part of the research plan that tested 322 tensile joints. The objectives of this study were to observe the amount of variability in terms of both strength and stiffness. It was found that the coefficient of variation (COV) ranged from ten to fifteen percent for three out of the four lumber grades studied. The COV was recorded as high as twenty percent for the smallest of the four lumber samples (N = 21). This sample was from an "Illinois Sample" that did not contain lumber from the southern pine species group. This "Illinois Sample" contained a collage of lumber including, "No. 1 and Construction grade S-dry Douglas fir, No.1 S-green Douglas fir, Construction and Standard grade S-dry Hem fir and No. 1, No. 2, Construction and Standard grade S-dry spruce-pine-fir". The authors suggest that this joint testing program is the first for a study of this kind, and suggest that their findings are more exploratory than statistically



based on random sampling. This joint test study is the cornerstone for the truss industry assumption of a COV equal to fourteen percent for tooth withdrawal (Lewis, 1993)

Zhao et al. (1992) used the tension joint data collected by Suddarth et al. (1981) for a bottom truss chord reliability study. The researchers grouped the data from the four lumber samples into one large pool, and fit a two-parameter Weibull distribution. By normalizing the fitted distribution, these adjusted data were used to simulate joint strengths. The study was designed to analyze the effect of bottom-chord span length on truss reliability. This normalization technique was used to extrapolate the original test data to a format that could be used in simulating tension joints that were not identical to the original test specimens.

## SYSTEM RELIABILITY STUDIES

Schuëller (1985) presented a paper that made several suggestions about examining the reliability of structural systems. He points out that structural systems can fail in many modes, and presented a method to estimate the upper and lower boundaries for the true probability of failure. Assuming that the modes of failure are completely dependent, the probability of failure ( $P_f$ ) can be estimated by Equation 2.3.

$$P_f = \max_{i=1}^n (P_{fi}) \quad (2.3)$$

where:

$P_f$  = system probability of failure and  
 $P_{fi}$  = probability of failure for the  $i^{\text{th}}$  mode.

Similarly, the probability of failure for a system where the modes of failure are completely independent can be estimated by Equation 2.4.

$$P_f = 1 - \prod_{i=1}^n (1 - P_{f,i}) \quad (2.4)$$

In an actual structural system, all modes of failure are neither totally independent, nor completely dependent. Equations 2.3 and 2.4 can be used to construct a boundary on the estimate of the  $P_f$  of the truss as a single unit. Schuëller also states that if there are only a few dominate modes of failure, the bounds will be close to the estimate of probability of failure; however if several modes have similar  $P_f$  values, the correlation between the modes must be taken into account.

Schuëller suggests that Monte Carlo simulations yield an accurate estimate of the true  $P_f$  if the simulated sample size is sufficiently large. Monte Carlo simulation is advantageous because such mechanical aspects as large deformation, second order effects, and material nonlinearities can be included to improve the accuracy of the model. Schuëller finally enumerated what he considered the needs for a structural system reliability model. The model should:

- 1.) Not limit the distributions of the loads and resistances.
- 2.) Have the capability to analyze different levels of correlations for both the loads and the resistances.
- 3.) Contain minimal mechanical idealizations.
- 4.) Have the capacity to analyze large structural systems, as in practice.
- 5.) Be efficient in terms of computational effort.

The Schuëller states that criterion 3 is important in order to gain acceptance of the model by practicing engineers.

Ellingwood et al. (1980) presented a report to the National Bureau of Standards pertaining to loads for a probability-based design procedure. This report was used in developing the first Load and Resistant Factor Design (LRFD) steel manual (AISC, 1986). The researchers studied structural steel, glued-laminated (glulam) timber beams, and reinforced concrete. This study was limited to ultimate limit state failures and ignored serviceability considerations. The authors stated that it is not practical to have the same reliability index for all building materials, and "there is no reason to force the design profession to adopt a uniform value." The researchers suggested that the optimal load and resistance factors could differ for each building material; however it would be preferable to have the same factors for all materials to simplify the design process. Developing a limit-state-design procedure involves:

- 1.) Identification of all modes of failure or ways in which the structure might fail to fulfill its intended purpose (limit states)
- 2.) Determination of acceptable levels of safety against occurrence of each limit state.
- 3.) Consideration by the designer of the significant limit states.

The significant finding relating to wood engineering was that the calculated reliability of glulam was similar to that of light-metal structures.

## STEEL PROPERTIES STUDY

Several research projects have been devoted to characterizing the properties of structural steel. Ellingwood et al. (1980) and Kennedy and Baker (1984) both focused on the development of limit-state-design criteria for structural steel. Although these two research studies concentrated on the properties of structural steel, they may not be indicative of the properties of steel coils that are used to manufacture truss plates. Little data are reported on the properties of steel coils; therefore, for comparison purposes, the Ellingwood et al. (1980) and the Kennedy and Baker (1984) findings were used as a starting point to characterize the properties of the steel used to manufacture truss plates.

Two main properties of steel that are commonly analyzed are yield strength and the ultimate strength. Although both of these properties are important, Kennedy and Gad Aly (1980) state, "The most significant strength property used in determining the capacity of a structural member is the yield point." Similarly, Galambos and Ravindra (1978) state, "The principal material property affecting the resistance of a steel structure is the yield stress." Both of these studies dealt with developing an ultimate strength criteria for design purposes. Since the objectives of this research are to realistically simulate steel failures, the more pertinent parameter is ultimate strength. Therefore, both the yield strength and the ultimate strength will be examined in detail.

Determining the yield strength is a more subjective measurement than the ultimate strength because it can be measured in several ways. For example, there is the static yield point, the dynamic yield point (Kennedy and Gad Aly, 1980), the lower yield point and the upper yield point (Salmon and Johnson, 1990). Standard coupon tests measure the dynamic

yield point; however, the static yield point is the more germane parameter in terms of limit state design (Galambos and Ravindra, 1978; Kennedy and Gad Aly, 1980). Static yield stress is defined as the yield stress under zero strain rate. The static yield stress is obtained in the laboratory by stopping the test, hence stopping the straining, after the stress versus strain curve has reached the plastic plateau (Galambos and Ravindra, 1978). Both Kennedy and Gad Aly (1980) and Galambos and Ravindra (1978) cite a relationship developed from test data by Rao et al. (1966) that relates the dynamic yield strength to static yield strength. The relationship is a linear function of straining rate, developed for rates between 100 and 800 in/in/sec. Salmon and Johnson (1990) explain that some steels do not adhere to the idealized elastic-plastic stress versus strain curve; therefore, there is no specific yield point, but a yielding region. Steels that exhibit this characteristic use the offset strain of 0.2%; or alternatively, a 0.5% extension under load to define the yield strength. ASTM Standard A446 (1991a) that outlines the properties of Grades A, B and C steel sheets, uses the 0.2% offset strain or 0.5% extension under load method to define yield strength.

Ellingwood et al. (1980) developed a National Bureau of Standards publication regarding the development of probability based load criteria. The report summarized the work of numerous research projects and made recommendations for characterizing material properties. In the publication, the authors conservatively characterized the means and COVs (coefficient of variations) of the tensile and static yield strengths of structural steel. The authors assumed that both the static yield strength and the ultimate strength followed a lognormal distribution. Based on research performed by Galambos and Ravindra (1978) on a summary of hot-rolled sections, the ratio of mean static yield strength to nominal yield

strength was 1.05 for steel flanges and the ratio for steel webs was assumed to be 1.10 with a COV of 0.11. Again, the Ellingwood et al. (1980) report was based on conservative estimates of the static yield strength. The original study by Galambos and Ravindra (1978) was a compilation of data based on a summary of yield tests where dynamic yield strengths were reported. These data represent many shapes, several U. S. mills and a time span of 40 years. The ratio of the mean mill dynamic yield strength to specified yield strength ranged from 1.21 to 1.22 for webs of rolled shapes with a COV ranging from 0.09 to 0.11. The ratio of dynamic yield strength to specified yield strength for structural steel plates and high strength plates ranged from 1.03 to 1.15 with COVs ranging from 0.04 to 0.12. Galambos and Ravindra (1978) converted the dynamic yield strength to static yield strength by reducing the test data by four ksi; however, they stated that the strain rates were not reported for the original data. The four ksi reduction was based on a loading rate of 800 in/in/sec which was the upper limit of the loading rate in which the relationship was developed (Rao et al., 1966). Based on research presented by AISI (1978, as cited by Ellingwood et al., 1980), the ratio of mean ultimate strength to nominal ultimate strength for hot-rolled sections was 1.10 with a COV of 0.11.

Kennedy and Baker (1984) characterized the static yield strength properties for welded sections. These sections were produced from rolled plates that are manufactured similar to the procedure used for producing steel coils. The researchers re-analyzed 3370 mill test specimens originally reported by Kennedy and Gad Aly (1980). The tensile coupons were taken from individual heats of Grade 44 steel produced at a steel mill. Before the re-analysis was performed, the data were scaled by the nominal yield strength (44 ksi) for normalization

purposes. The scaling procedure was identical to calculating the ratio of the data to the nominal yield strength. The researchers found that the ratio of the yield strength to the nominal yield strength could be “excellently” fit by a lognormal distribution with the estimated mean and COV of 1.10 and 0.10, respectively. Kennedy and Baker (1984) truncated their lognormal distribution at 0.954. The truncation was performed because the researchers stated that it is highly unlikely that the yield strength of Grade 44 steel could be 2 ksi less than nominal due to steel mill quality control procedures. Hence, normalized yield strengths less than 0.954 (42 ksi/44 ksi) were not considered valid for this particular study. Kennedy and Gad Aly (1980) assumed that the dynamic yield strength would be 2 ksi greater than the static yield strength. By examining the original data in terms of the dynamic yield strength, the researchers observed ratios of dynamic yield strength to nominal yield strength for plates in the range of 1.12 to 1.18 with COVs ranging from 0.079 to 0.083. The researchers reported the ratios of dynamic yield strength to nominal yield strength for webs from W-sections were in the range of 1.15 to 1.20 with COVs ranging from 0.064 to 0.083.

The reports on strength properties of structural steel agree somewhat. Both Ellingwood et al. (1980) and Kennedy and Baker (1984) reported using a lognormal distribution to model the steel strength. Both of these reports also found that the ratio of mean static yield strength to nominal yield strength was between 1.05 and 1.10 and the COV was close to 0.10. Since these conclusions were intended for design, they were conservatively calculated. Galambos and Ravindra (1978) and Kennedy and Gad Aly (1980) reported ratios of the mean dynamic yield strength to nominal yield strength in the range of 1.03 to 1.22 with COVs ranging from 0.04 to 0.12.

## BUILDING CODE REQUIREMENTS FOR TRUSS TESTS

In the United States, there are three major model building codes that cities and counties either adopt or modify. These codes are designed to ensure public safety and welfare (Breyer, 1993). The three major codes are, 1) the Standard Building Code, SBC (SBCCI, 1991), 2) The BOCA National Building Code (1993) and 3) The Uniform Building Code, UBC (ICBO, 1991a). Table 2.1 represents a summary of the major code requirements applicable for tests of metal-plate-connected wood trusses. This table includes the applicable loading for the tests and the required test safety factors.

**Table 2.1 Summary of building code requirements for test safety factors of metal-plate-connected wood trusses.**

Code	Section applicable	Loading	SF
SBC (SBCCI, 1991)	§2503.1	Live	2.0
BOCA (1993)	§1710.3.1	Dead + Live	2.5
UBC (ICBO, 1991a)	§2510(f)	Dead + Live	3.0 <sup>a</sup>

<sup>a</sup> ICBO (1991b) requires the truss capacity to exceed dead load plus 3.0 times design load.

The SBC code is generally used as the model code for the southern regions of the United States. Building officials can require load tests for any construction whenever there is a reason to question the safety for the intended use (SBCCI, 1991). The code requires that a structural test "shall sustain, without structural failure or excessive deflection, a superimposed load equal to two times the live load."

The BOCA model building code is predominately used in the northern and eastern regions of the United States. This code specifies the allowable superimposed load (dead +



live) is equal to the failure load divided by 2.5 (BOCA, 1993). This provision is applicable for tests of all structural components.

The UBC is used in the western parts of the United States. Unlike the other two model building codes, the UBC (ICBO, 1991a) specifically addresses metal-plate-connectors, instead of generalized structural systems. The UBC requires a truss test to withstand basic dead load plus 3.0 times total design load (ICBO, 1991b). Traditionally the UBC has been the most conservative of the building codes for metal-plate-connected wood trusses. The UBC-specified average safety factor for truss-plate tooth-holding tests is 4.0 instead of the safety factor of 3.0 specified by TPI (1992) and used by other major model building codes.]

A precedent does exist for setting truss-test safety-factors for steel bar joists in one code. UBC standard 27-4 (ICBO, 1991b) pertains to open web steel joists. This standard specifies that the structural system must provide a minimum safety factor of 1.65. The minimum safety factor for the "parts" of the steel joist apparently came from the reciprocal of the 0.60 factor ( $1/0.60$ ) used in steel design which is equal to 1.67. Seely (1935) summarizes the misconception of relating the safety factors of "parts" to the safety factors of the "whole" as follows:

The use of this term (factor of safety) and the idea of safety which it conveys, however, is likely to be misleading. For example, if a factor of safety of 4 based on the ultimate strength is used in selecting a working stress for structural steel, a structure designed on the basis of this working stress will not in general satisfactorily resist loads four times as great as those that produce the working stress, because the members in the structure will yield and take large permanent deformations before their ultimate strengths are reached and the distribution of the loads to the various members is thereby radically changed.

This statement suggests that for structural steel the safety factors of the "parts" are not directly related to safety factors of the "whole", and that truss-test safety-factors should logically be less than the joint design safety factor.

# CHAPTER III

## JUSTIFICATION

### INTRODUCTION

The theories that Ellingwood et al. (1980) presented for developing a limit state design are applicable to metal-plate-connected wood trusses. Through years of in-use performance, structural tests, and engineering analysis and judgment, the modes of failure for a truss have been identified, thus satisfying criterion 1, (identification of all failure modes before developing a limit state design criteria). The second criterion, determination of acceptable levels of safety against each limit state, is more difficult to achieve. This criterion is subjective since an acceptable level of safety is dependent on many factors, including the opinions of the truss engineer, the builder, the customer, and the building code officials. The three major building codes do not agree on the required levels of safety. Safety factors for the design load of full size trusses are 2.0, 2.5, and 3.0 for the SBC (SBCCI, 1991), BOCA (1993), and UBC (ICBO, 1991b) model building codes, respectively.

The lack of agreement from the codes could cause confusion among truss engineers, add to truss cost, and cause unnecessary litigation. The need to obtain multiple code approvals is just one example of the added costs. Since the model building codes have different safety factors, each engineered product must undergo the code approval process (BOCA, 1991; ICBO ES 1991, 1992, 1993). These two reports contain different design values for tooth withdrawal. Obtaining multiple code approval is required because the model building codes do not necessarily accept reports from other coding agencies. These different

design values can confuse the truss engineer assuming the design market is subjected to different codes. Finally, conflicting safety margins in the codes have a potential to cause litigation that adding more cost to housing nationwide.

## **CURRENT SAFETY FACTORS**

Before a rigorous study of joint- and truss-safety factors can be conducted, the purpose of safety factors should be discussed along with present safety factors used for metal-plate-connected joint design. An outline of the methods that are currently used to determine design values will also aid in understanding joint safety factors. Since a joint can fail in four different modes, each will be discussed separately.

### **Overview**

The actual safety of a design depends upon many aspects of the structural component, and how the component behaves in the structural systems. The statistical basis of the design safety factor, DSF, is also important. For instance, a DSF based on the average capacity of a structural material may be much greater than another factor based on the lower tail of the distribution (such as the fifth percentile), yet the latter design with a lower DSF may provide a greater level of protection against the risks of failure. In-service experience should be given substantial consideration when evaluating and setting safety factors for structural design.

Part of the difficulty in accurately estimating the design safety factor of the "parts" of a truss stem from the fact that theoretical-minimum strength values based on published safety factors do not necessarily reflect actual strength values. For instance, lumber is sometimes

graded No. 1 & Better. The design value is based on No. 1 grade lumber; however, the strength of the lumber in the No. 1 & Better designation is generally stronger than lumber in a pure No. 1 grade. This causes the true safety factor to be much larger than the theoretical safety factor. Another example of the difficulty is estimating design safety is ASTM standards (1993a, 1993c) specify minimum yield and ultimate strengths for steel sheets. However, it is common for manufacturers to produce stronger steel than minimum required (Ellingwood et al., 1980; Kennedy and Baker, 1984). Although these two cases effectively increase the safety factor of a truss, they complicate analysis of safety factors for wood trusses.

### Steel Net Section

The steel-net-section design values for metal-connector-plates are based on three samples loaded in axial tension (TPI, 1992). Typical grades of steel used for manufacturing truss plates are Grades A, B, C, and high strength (HS) steel (ICBO Evaluation Service, 1991, 1992, 1993). Table 3.1 (Column 2 and 3) gives the specified properties for the four grades. The properties of Grades A, B, and C are governed by ASTM A 446 (1993a). The high strength properties are governed by ASTM A 816 (1993c) Grade 60 steel. The safety factor for steel in tension can be estimated by Equation 3.1.

$$SF_{\pi} = \frac{F_u}{0.6 \cdot F_y} \quad (3.1)$$

where:

$SF_{st}$  = safety factor for steel in tension,  
 $F_u$  = ultimate tensile strength of steel, and  
 $F_y$  = yield strength of steel.

The yield strength of steel for design is reduced to 60 percent of the published  $F_y$  for the grade. This is specified by TPI (1992) and is based on the allowable stress design of steel members. The safety factors range from 1.94 to 2.34 for the four steel grades studied.

**Table 3.1 Minimum tensile-strength properties of steel truss plates.**

Steel	$F_y$ (ksi)	$F_u$ (ksi)	design (ksi)	SF	$P_f$
Grade A <sup>a</sup>	33	45	19.8	2.27	5.20e-17
Grade B <sup>a</sup>	37	52	22.2	2.34	4.94e-18
Grade C <sup>a</sup>	40	55	24.0	2.29	2.74e-17
HS <sup>b</sup>	60	70	36.0	1.94	3.04e-12

<sup>a</sup> ASTM A 446 Designation

<sup>b</sup> ASTM A 816 Grade 60 designation

Both Ellingwood et al. (1980) and Kennedy and Baker (1984) reported that the ultimate strength of steel followed a lognormal distribution with a coefficient of variation (COV) of approximately 10 percent. Both researchers also reported that the mean ultimate-strength of steel is approximately equal to 1.10 times the nominal  $F_u$ . Figure 3.1 represents a probability density function (PDF) of the ultimate tensile strength of steel based on an assumed COV of 10 percent and a mean ultimate-strength to nominal- $F_u$  ratio of 1.10.

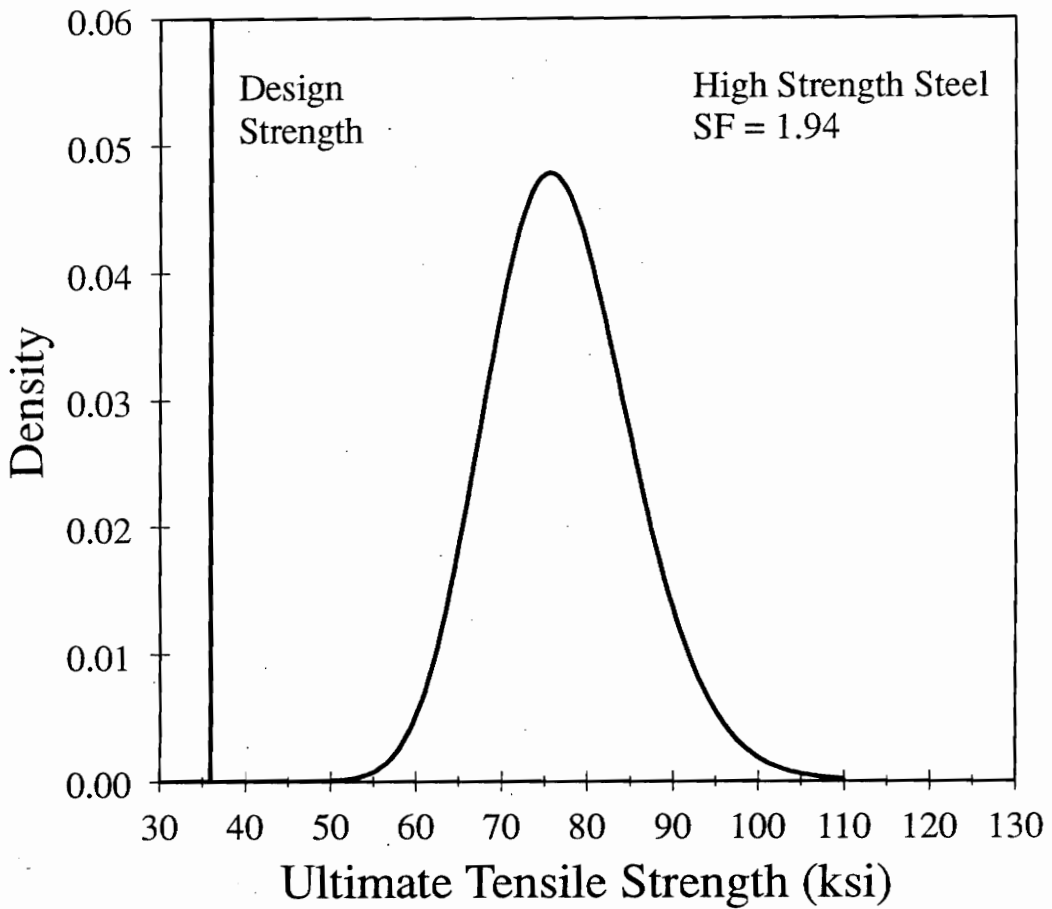


**Figure 3.1** Probability density function derived from the literature for the ultimate tensile strength of HS steel based on minimum specified properties.

The line extending the height of the graph represents the allowable design strength ( $0.60 \cdot F_y$ ). The safety factor for HS steel is equal to 1.94 with respect to the ultimate-strength mean-value. The probabilities of failure ( $P_f$ ) at design allowable loads (Table 3.2, rightmost column) were estimated using an IMSL (1987) subroutine. The calculated  $P_f$ 's at allowable design loads are extremely small, essentially zero.

### Steel Shear

Design values for steel shear are based on three-member test specimens. Six replications of each test specimen are required with plate orientations of 0, 30, 60, 90, 120, and 150 degrees (TPI, 1992). The same grades of steel that were studied for steel net-section failure were studied for shear failure (refer to Table 3.2). The safety factor for steel metal-connector-plates in shear is estimated by Equation 3.2.

$$SF_{st} = \frac{0.577 \cdot F_u}{0.4 \cdot F_y} \quad (3.2)$$

where:

$SF_{sv}$  = safety factor for steel in shear.

Again the  $0.4 \cdot F_y$  factor is from TPI (1992) which is based on the allowable-stress steel-design methodology. The  $0.577 \cdot F_u$  term is also from the TPI (1992) specification, but it is based on the maximum octahedral shearing stress (Boresi and Sidebottom, 1985).



**Table 3.2 Minimum shear-strength properties of steel truss plates.**

Steel	$F_y$ (ksi)	$F_u$ (ksi)	design (ksi)	SF	$P_f$
Grade A <sup>a</sup>	33	45	13.2	1.97	1.44e-12
Grade B <sup>a</sup>	37	52	14.8	2.03	1.96e-13
Grade C <sup>a</sup>	40	55	16.0	1.98	8.40e-13
HS <sup>b</sup>	60	70	24.0	1.68	1.34e-08

<sup>a</sup> ASTM A446 Designation

<sup>b</sup> ASTM A 816 Grade 60 designation

The safety factors range from 1.68 to 2.03. These safety factors for steel in shear are consistently lower (by a factor of 0.87) than the steel tension safety factors. Figure 3.2 represents the PDF for the ultimate shear strength of steel ( $0.577 \cdot F_u$ ). The vertical line on the left represents the design shear strength ( $0.4 \cdot F_y$ ). The safety factor for HS steel in shear is 1.68. This case produces the lowest of all the steel-failure safety factors considered. The  $P_f$  values were estimated for the shear failures following the same procedure as for the steel-net-section failure mode. Again, as for the tension case, the calculated failure rates at allowable design loads are extremely small (Table 3.2, rightmost column).

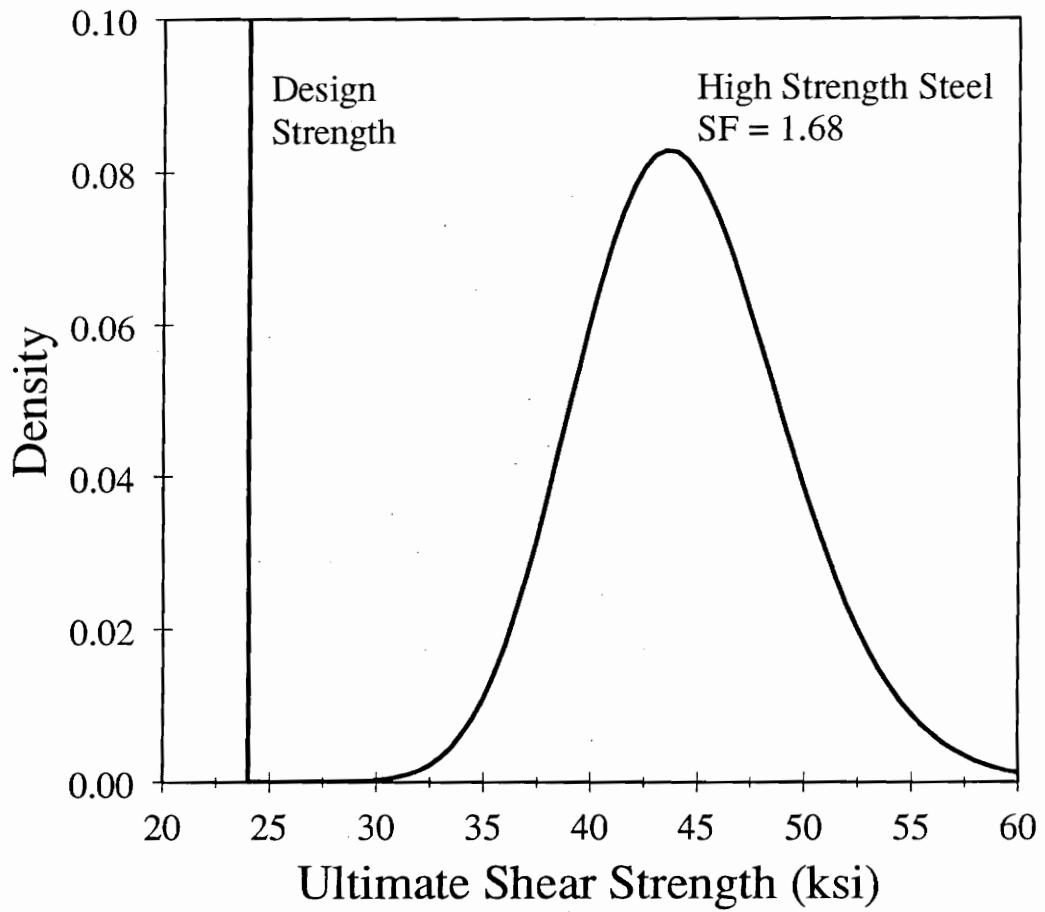


**Figure 3.2** Probability density function derived from the literature for the shear strength of HS steel based on minimum specified properties.

## **Tooth Withdrawal**

The tooth-withdrawal design values are based on tests with five replicate specimens (TPI, 1992) loaded in tension. The design load is determined by taking the minimum of the average sample ultimate load divided by 3.0 and the average load at critical slip (0.030 in) divided by 1.6. When the ultimate test load average divided by 3.0 limits the allowable design value for a specific plate type, the test-average tooth-withdrawal strength is 3.0 times the published allowable for the plate. This procedure for determining tooth withdrawal design values implies that the published design values contain a safety factor of 3.0 based on the average ten-minute test strength.

Alternately, the Truss Plate Institute defines a safety factor with respect to the fifth percentile of the tooth-withdrawal strength distribution (BOCA, 1989). Using the fifth percentile of the distribution (and consequently a smaller safety factor) is a good approach; however, engineers and regulatory persons are accustomed to larger factors-of-safety for connections based on the average test strength. Regardless of the safety factor analysis approach used, the net result is that the ten-minute test strength is equal to 3.0 times the published design values for the plate.

To define a theoretical tooth-withdrawal strength distribution, the Suddarth et al. (1981) test data consisting of 322 metal plated joints tested in tension were analyzed by Zhao et al. (1992). These data were analyzed to determine the best probability model available that would describe tooth-withdrawal variation. They fitted several distributions to the data and found that the 2-parameter Weibull yielded the best fit. The Weibull scale ( $\sigma$ ) and shape ( $\eta$ ) parameters were 5.400 kips and 8.663, respectively. The mean value of the fitted distribution

was determined to be 5.106 kips. With this information the parameters of another Weibull distribution having the same COV and shape as the original but a different average strength ( $x_b$ ) can be calculated by:

$$\begin{aligned}\eta^* &= \eta \\ \sigma^* &= 5.400 / 5.106 * x_b \\ &= 1.056 * x_b\end{aligned}\tag{3.3}$$

where:

$$\begin{aligned}\eta^* &= \text{new shape parameter equal to the original shape parameter and} \\ \sigma^* &= \text{new scale parameter such that the average of the distribution is } x_b.\end{aligned}$$

A distribution of theoretical ten-minute tooth-withdrawal strengths relative to design load is obtained by using the 3.0 safety factor based on the average from TPI (1992). Assuming the joints are the minimum size required by the design loads, the Weibull parameters for the distribution of tooth withdrawal strength as a multiple of design load are:

$$\begin{aligned}\eta^* &= \eta = 8.663 \\ \sigma^* &= 1.058 * x_b \\ &= 3.174\end{aligned}\tag{3.4}$$

This resulting Weibull distribution is shown in Figure 3.3. The probability of failure of the joint at any multiple of design load is given by Equation 3.5.

$$P_f = 1 - \exp\left(-\left(\frac{MDL}{\sigma^*}\right)^{\eta^*}\right)\tag{3.5}$$

where:

MDL = The load level as a multiple of design load.

For example, the probability of failure at design load (MDL = 1) is:

$$P_f = 1 - \exp\left(-\left(\frac{1}{3.174}\right)^{8.663}\right) = 4.5 \times 10^{-5} \quad (3.6)$$

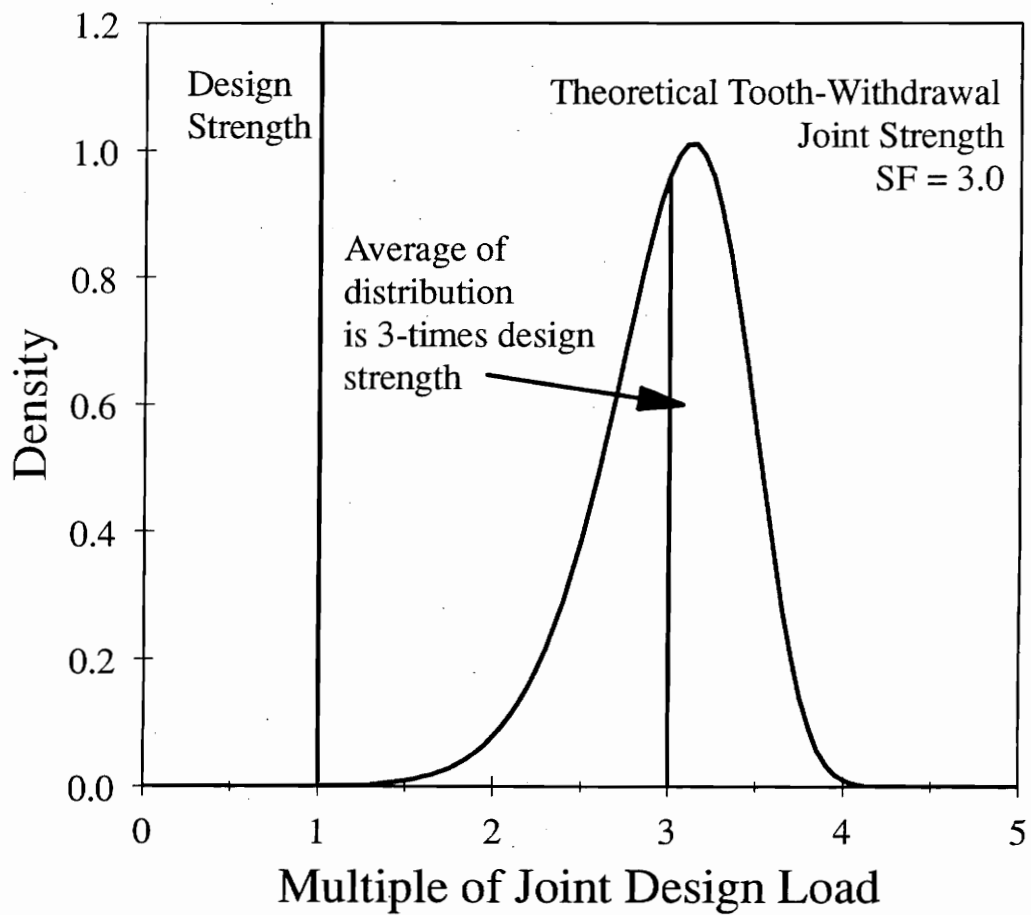


**Figure 3.3** Weibull density function representing tooth-withdrawal joint strength. The distribution shape was determined from the Suddarth et al. (1981) test data.

## Truss Lumber

For this discussion, the net-section design values for lumber at the joints are based on the tensile strengths of lumber. The design tensile strengths of lumber are found in the National Design Specification, NDS (AFPA, 1991). These design values are derived from the fifth percentiles of destructively tested lumber samples of softwood species. Lumber design values based on the "In-grade" test data (Green and Evans, 1987) are derived as follows: the fifth percentile of the lumber test data is estimated and divided by 2.1 to yield the design tensile strength. The 2.1 factor is based on a load duration factor of 1.6 and a safety factor of 1.3. The 1.6 load duration factor adjusts the test data, with an assumed test duration of ten minutes, to a ten year (normal) load duration. Designs having a load duration other than 10-years are adjusted accordingly. This implies that the theoretical safety factor for lumber strength (for any assumed load duration) is 1.3 with respect to the fifth percentile as the base value.

An investigation of the actual safety factors of lumber was conducted using data collected and published in a recent In-grade test-program summary (Green and Evans, 1987). Various grades and sizes of southern-pine were considered for this investigation, and summarized in Table 3.3.

**Table 3.3 Summary of lumber tension properties from In-grade test data (Green and Evans, 1987) and the NDS (AFPA, 1991).**

Size	Grade	N	Best-fit <sup>a</sup>	5 <sup>th</sup> %tile (ksi)	Design <sup>b</sup> (ksi)	SF	P <sub>f</sub>
2 x 4	SS	415	3P-W <sup>c</sup>	3.242	2.560	1.27	1.60e-02
	No.1	99	LN <sup>d</sup>	2.028	1.680	1.21	1.44e-02
	No.1&Btr	413	LN	2.709	1.680	1.61	2.82e-03
	No.2	413	LN	1.620	1.320	1.23	1.84e-02
2 x 6	No.2	412	LN	1.425	1.160	1.23	2.11e-02
2 x 8	SS	411	2P-W <sup>e</sup>	2.829	2.080	1.36	1.56e-02
	No.1	40	3P-W	1.570	1.320	1.19	1.89e-02
	No.1&Btr	413	2P-W	2.443	1.320	1.85	6.28e-03
	No.2	413	LN	1.322	1.040	1.27	1.89e-02
2 x 10	SS	413	2P-W	3.069	1.760	1.74	3.54e-03
	No.1	33	LN	1.482	1.160	1.28	1.15e-02
	No.1&Btr	411	2P-W	2.691	1.160	2.32	1.59e-03
	No.2	413	LN	1.252	0.920	1.36	1.27e-02

<sup>a</sup> Determined by Kolmogorov-Smirnov and Anderson-Darling test statistics

<sup>b</sup> NDS (AFPA, 1991) design strength adjusted to 10 minute load duration

<sup>c</sup> Three-parameter Weibull Distribution

<sup>d</sup> Lognormal Distribution

<sup>e</sup> Two-parameter Weibull Distribution

Green and Evans (1987) fit numerous statistical distributions to the lumber data and conducted goodness-of-fit tests. The In-grade test program documentation had no suggestions for selecting a so called "best-fit" distribution; however, the statistics from the Kolmogorov Smirnov (KS) and the Anderson Darling (AD) goodness-of-fit tests were published. By analyzing the KS and AD tests statistics, the "best-fit" distributions were selected for thirteen different lumber samples. The fifth percentiles were also published for the fitted distributions (Green and Evans, 1987). The actual safety factor for the southern pine lumber was calculated by Equation 3.7.



$$SF_w = \frac{x_{0.05}}{F_t \cdot ldf} \quad (3.7)$$

where:

- $SF_w$  = safety factor for lumber,
- $X_{0.05}$  = "best-fit" fifth percentiles (Green and Evans, 1987),
- $F_t$  = NDS (AFPA, 1991) tensile strength design value, and
- $ldf$  = load duration factor, (equal to 1.6).

Since the In-grade tension test data was collected at an approximate ten-minute load duration (Green and Evans, 1987), the NDS design values must be adjusted from a ten year load duration to a ten-minute load duration. Safety factors ranged from 1.19 to 2.32 for the thirteen lumber samples studied. Figure 3.4 represents the probability density function (PDF) for southern pine 2x8 No.2 lumber. The vertical line extending the height of the graph represents the NDS design value adjusted to a ten-minute load duration. The shorter vertical line to the right extending up to the PDF curve represents the fifth percentile for the fitted lognormal distribution. The safety factor for this size and grade was estimated to be 1.27. The probabilities of failures at design load were estimated for each of the thirteen lumber samples. The  $P_f$  associated with the lognormal distribution was estimated using an IMSL (1987) subroutine. The largest calculated probability of failure (given design load) was 2.1% for 2x6 No.2 lumber.

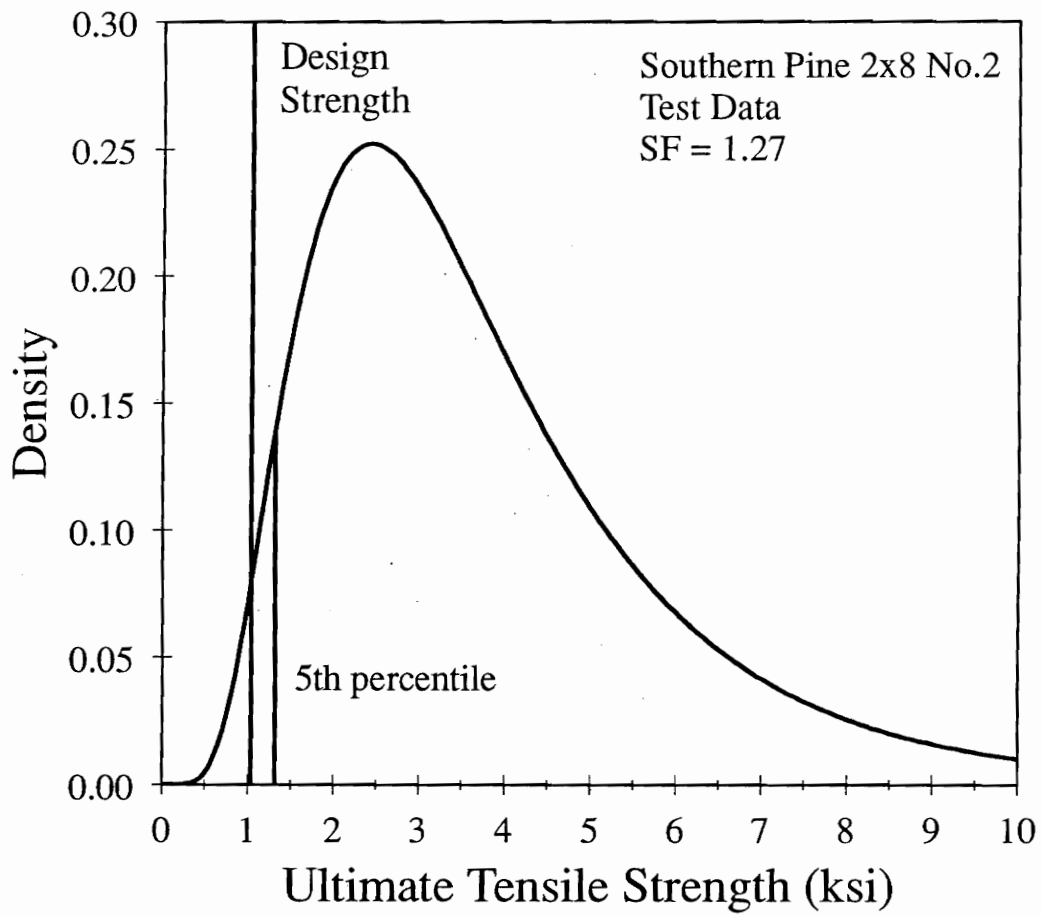


**Figure 3.4** Probability density function for the ultimate tensile strength of lumber based on In-grade test data (Evans and Green, 1987).

All  $P_f$  calculations presented in this study are theoretically based on assumed probability distributions. The assumed distributions are believed to describe the specific mechanical properties studied. The results do not apply to actual truss construction since neither the true PDF of the properties is known, nor is the actual loading of the lumber or joints known precisely.

## SUMMARY

Although the wood net section generally had the smallest safety factor, and the largest (theoretical) probabilities of failure at design load, few of the truss and joint tests reported in the literature failed in this mode. It is unlikely that a maximum strength-reducing knot would be placed in the joint area of a test joint or truss test; therefore, the net-section failure mode should not be expected to dominate since lumber strength is controlled by knots and other natural characteristics. These perfect joints only occur under laboratory conditions, there is no way to guarantee knots or strength reducing characteristics will not be placed in the joint area of an actual truss used in the field.

A plot that compares the theoretical probability-of-failures of the different failure modes at different loading levels is presented in Figure 3.5.

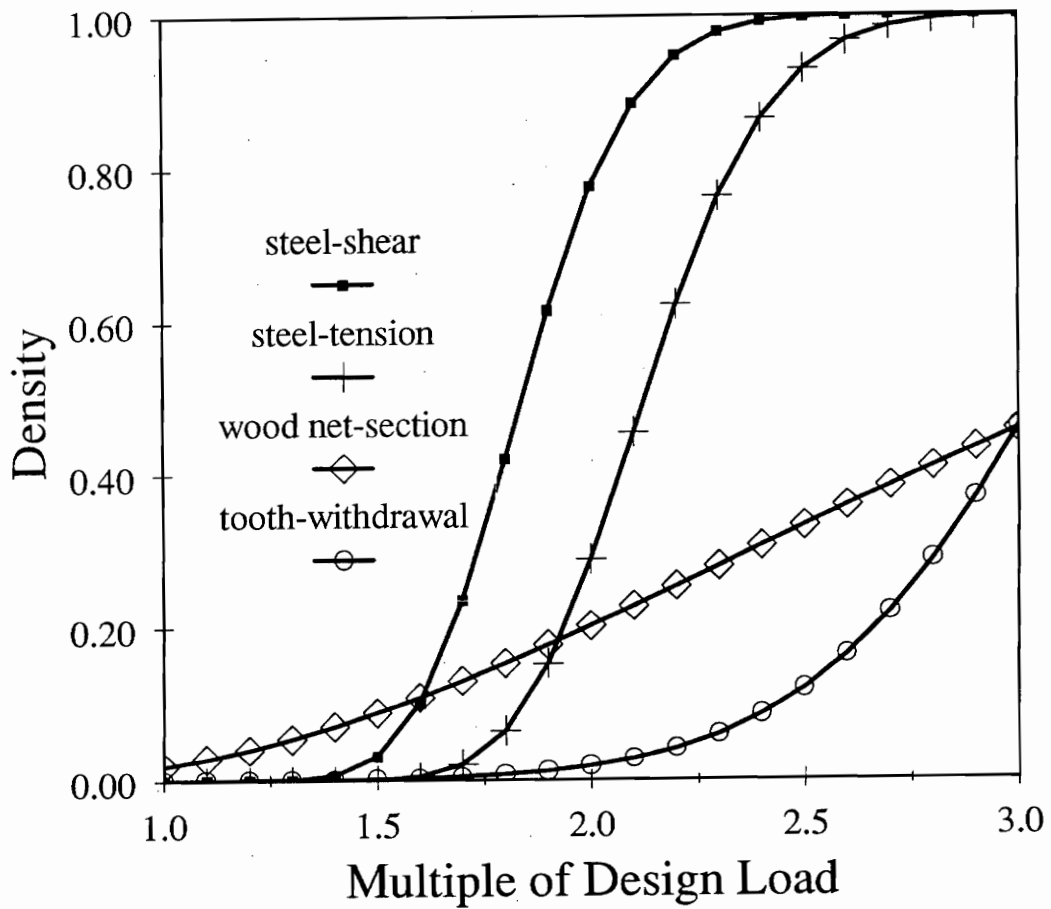


**Figure 3.5** A comparison of the probabilities of failure for the four failure modes of the joint at different design load multiples.

Loading the joint at 3.0-times design load yielded a probability-of-failure for wood net-section and tooth-withdrawal close to 0.40. This same load level predicted a very high likelihood of failure (nearly 1.0) for steel tension and shear for the joint failure modes. These differences in estimated failure rates offer another explanation of why few truss tests exhibit net-section wood type failures, as opposed to plate failures. Interestingly enough, Figure 3.5 suggests that steel-shear failures should be the most critical mode in overload situations. Figure 3.5 was based on the assumption that the joints are loaded at 100 percent of the design capacity for each failure mode in question. Depending on the truss design, the shear mode may not be loaded to 100 percent capacity; therefore, shear failures may not be the dominant failure mode in a truss. Figure 3.5 also assumes that the steel properties are based on ASTM minimum values. This assumption regarding the steel strength in actual tests versus the steel strength assumed in design should be studied in more detail. It has been recorded in the literature (Ellingwood et al., 1980 and Kennedy and Baker, 1984) that the true strength properties of steel are considerable greater than the minimum properties specified by ASTM. A further investigation, reported in Chapter IV, was needed to effectively and accurately model the steel properties for the joints.

## CONCLUSIONS

- 1.) The safety factors used to design the components of trusses are not consistent in either the magnitude or the method of estimating the safety factors.

- 2.) Although the safety factor for lumber is smaller than the safety factors for steel net section, steel shear, and tooth withdrawal, often times, lumber failures do not control truss and joint tests.
- 3.) Safety factors alone, do not indicate which mode of failure dominates. The different failure modes must be accompanied by statistical distributions to aid in identifying the probable failure mode.
- 4.) The analysis in this chapter assumed that the joints loaded to critical values for each of the four modes of failure. This is not a realistic assumption; therefore, a different method is needed to link the behavior of the joints to the behavior of the truss.
- 5.) The assumed steel properties used in this chapter were based on structural steel. Steel properties used to manufacture metal connector plates should be investigated.

# CHAPTER IV

## STEEL PROPERTIES STUDY

### INTRODUCTION

Although the reviewed reports (Kennedy and Gad Aly, 1980; Ellingwood et al., 1980; Galambos and Ravindra, 1978; Kennedy and Baker, 1984) provide valuable information on the strength properties of structural steel, they may not accurately characterize the properties of the steel coils used to manufacture truss plates; therefore, truss plate manufacturers were surveyed on the steels that are used for producing truss plates. The data base was subsequently analyzed to determine minimum strengths, mean strengths and COVs for different grades of steel. Statistical distributions were fit to the data and inferences were drawn from the distributions.

### INITIAL STEEL SURVEY

Since little data have been reported on the strength of steel used to manufacture truss plates, a survey was conducted to form an "in-grade" data base. The survey was designed to query truss plate manufacturers on the properties of the steel that are actually used in their plate production. The collected data can be used to make decisions about methods to model steel properties for realistic Monte Carlo simulations of metal-plate-connected wood trusses.

The survey was sent to all truss plate manufacturers (8 companies) that are members of the Truss Plate Institute (TPI). The survey queried the observed properties of ASTM A446 (1993a) Grades A, B, and C and ASTM A816 (1993c) Grade 60 steel. The truss plate

manufacturers were asked to define the typical lows, averages and typical highs for both yield strength and ultimate strength of the steels used by their company. Typical lows and highs were defined as the lowest and the highest strengths, respectively, out of a sample size of 50. Since truss plate manufacturers generally do not release this type of "in-house" information, a coding procedure was implemented. The respondents were asked to send their replies to a third party and the surveys would be relayed to the author of this dissertation in the order received with a code designation of I, II, III.. Tables 4.1 and 4.2 are summaries of the survey responses for the yield strength and ultimate strength of steel properties, respectively. Truss plate manufacturer (TPM) II sent the raw data for 52 coils of steel. These coils were produced by four different steel manufacturers. The sample sizes for the different steel manufacturers were 4, 5, 19 and 24. These 52 samples were grouped together as one group and the properties for TPM II found in Tables 4.1 and 4.2 were summarized by the author of this dissertation.



**Table 4.1 Summary of the truss plate manufacturers steel survey response in terms of yield strength.**

TPM <sup>a</sup> - Grade <sup>b</sup>	N <sup>c</sup>	Typical Low <sup>d</sup> (ksi)	Average  (ksi)	Avg./ Nominal <sup>e</sup>	Typical High <sup>f</sup> (ksi)
I-A	NR <sup>g</sup>	33.6	43.0	1.30	56.7
I-B	31	35.7	49.0	1.32	57.7
II-B	52	41.2	46.3	1.25	54.0
III-B	32	43.4	46.0	1.24	51.7
III-C	20	46.7	50.0	1.25	51.0
III-60	50	60.2	64.2	1.07	66.7

<sup>a</sup> Truss plate manufacturer designation. Letters assigned by response time (i.e. first response received was designated I).

<sup>b</sup> Grades A, B, and C are based on ASTM Standard A446 and Grade 60 is based on ASTM Standard A816.

<sup>c</sup> Sample size.

<sup>d</sup> Typical low was defined as the lowest yield or ultimate strength out of 50 coils of steel tested.

<sup>e</sup> Nominal yield strengths for Grades A, B, C, and 60 are 33.0, 37.0, 40.0, and 60.0 ksi, respectively.

<sup>f</sup> Typical high was defined as the highest yield or ultimate strength out of 50 coils of steel tested.

<sup>g</sup> No response.

**Table 4.2 Summary of the truss plate manufacturers steel survey response in terms of ultimate strength.**

TPM <sup>a</sup> Grade <sup>b</sup>	N <sup>c</sup>	Typical Low <sup>e</sup> (ksi)	Average (ksi)	Avg./ Nominal <sup>e</sup>	Typical High <sup>f</sup> (ksi)
I-A	NR <sup>g</sup>	48.6	53.9	1.20	61.0
I-B	31	52.0	58.1	1.12	68.3
II-B	52	52.8	57.4	1.10	66.5
III-B	32	53.1	55.5	1.07	59.1
III-C	20	62.5	63.5	1.15	64.5
III-60	50	72.0	78.0	1.11	82.2

<sup>a</sup> Truss plate manufacturer designation. Letters assigned by response time (i.e. first response received was designated I).

<sup>b</sup> Grades A, B, and C are based on ASTM Standard A446 and Grade 60 is based on ASTM Standard A816.

<sup>c</sup> Sample size.

<sup>d</sup> Typical low was defined as the lowest yield or ultimate strength out of 50 coils of steel tested.

<sup>e</sup> Nominal ultimate strengths for Grades A, B, C, and 60 are 45.0, 52.0, 55.0, and 70.0 ksi, respectively.

<sup>f</sup> Typical high was defined as the highest yield or ultimate strength out of 50 coils of steel tested.

<sup>g</sup> No response.

Only one TPM reported a typical low strength that was less than nominal. The minimum was reported by TPM I for the typical low yield strength of ASTM Grade B steel (designated I-B, column 3, Table 4.1). The typical minimum yield strength was reported as 35.7 ksi. The nominal yield strength for Grade B steel is 37 ksi; thus, yielding a ratio of 0.975 (35.7/37.0). The ratio is close to the theoretical threshold minimum (0.954) that Kennedy and Baker (1984) reported, indicating that the steel mill quality control procedures for structural steel suggested by Kennedy and Baker (1984) might be extended to steel coils used to

manufacture truss plates. All other typical low strengths reported by the TPMs exceeded the ASTM minimum strength criteria.

Tables 4.1 and 4.2 also contain two columns of scaled data giving the average strengths divided by the nominal strengths for both yield and ultimate (columns 5). Truss plate manufacturer III reported a ratio of average yield strength to nominal yield strength for Grade 60 steel of 1.07. The ratio is in the range suggested by Galambos and Ravindra (1978) and Kennedy and Gad Aly (1980) for dynamic yield strength. The other responses in terms of yield strength ratios were greater than the maximum ratio (1.22) reported by Galambos and Ravindra (1978). The other responses ranged from 1.24 to 1.30 indicating that for most samples collected from steel coils, the manufacturers are producing steel that is considerably "above-grade" in terms of minimum yield strength.

The ratio of average ultimate strength to nominal ultimate strength was consistent with 1.10 for structural steel reported by AISI (1978). For the four grades of steel that were considered, these ratios ranged from 1.07 to 1.20 for the three different TPMs. The ratios suggest that the steel mills are typically producing steel sheets as close to "on-grade" as structural steel is produced.

## **ADVANCED STEEL STUDY**

Several weeks after the initial steel survey responses were received, TPM II sent another, larger raw data set containing both Grade B and Grade 60 steel. These data were collected from four different steel manufacturers. The total sample size for Grade B steel was 264 with sample sizes from the four steel suppliers of 21, 30, 64 and 149. The total sample

size for Grade 60 steel was 37. The Grade 60 sample consisted of data from two different steel suppliers. One sample size was 35; whereas, the other was from two coil samples of Grade 60 steel. The raw data from the 52 samples from the initial steel survey were independent of the 264 samples that were later sent, and the two data sets contained data from the same four steel manufacturers; therefore, the data were grouped together to form one large sample of 316. The four sub-samples corresponding to the different steel manufacturers contained sample sizes of 26, 54, 83 and 153. The ultimate strength of the steel is an important measurement when modeling the steel strength of truss plates; therefore, the four steel samples were sorted by the average ultimate strengths. For example, the lesser of the four steel samples, in terms of ultimate strength was denoted "W". The next strongest was labeled "X", with "Z" being the largest average ultimate strength of the four steel producers. A summary of the properties of yield strength and ultimate strengths can be found in Tables 4.3 and 4.4, respectively.

**Table 4.3 Summary of yield strength properties for Grade B steel from truss plate manufacturer II.**

Steel Supplier <sup>a</sup>	N <sup>b</sup>	minimum (ksi)	average (ksi)	COV <sup>c</sup>	avg./nominal <sup>d</sup>
W	83	42.9	46.82	0.0490	1.27
X	26	45.0	48.24	0.0299	1.30
Y	54	38.3	42.57	0.0817	1.15
Z	153	41.0	48.33	0.0430	1.31
Combined	316	38.3	46.94	0.0674	1.27

<sup>a</sup> Letters assigned by the sorted ultimate strength averages for Grade B steel (i.e. W represents the steel supplier with the lowest average ultimate strength).

<sup>b</sup> Sample Size.

<sup>c</sup> Coefficient of variation.

<sup>d</sup> Nominal yield strength for Grade B steel is 37 ksi.

**Table 4.4 Summary of ultimate strength properties for Grade B steel from truss plate manufacturer II.**

Steel Supplier <sup>a</sup>	N <sup>b</sup>	minimum (ksi)	average (ksi)	COV <sup>c</sup>	avg./nominal <sup>d</sup>
W	83	52.2	55.08	0.0304	1.06
X	26	55.0	56.35	0.0232	1.08
Y	54	54.0	57.33	0.0471	1.10
Z	153	56.2	59.98	0.0202	1.15
Combined	316	52.2	57.94	0.0465	1.11

<sup>a</sup> Letters assigned by the sorted ultimate strength averages (i.e. W represents the steel supplier with the lowest average ultimate strength).

<sup>b</sup> Sample Size.

<sup>c</sup> Coefficient of variation.

<sup>d</sup> Nominal ultimate strength for Grade B steel is 52 ksi.

### SAS Analysis

A one-way analysis of variance using a fixed effect model (Dunn and Clark, 1987) was conducted on the four samples to determine if there were significant differences in the mean yield and ultimate strengths due to steel manufacturer. The procedure was conducted to determine if some of the steel strength samples could be grouped together for fitting statistical distributions. The SAS procedure general linear models, GLM, (SAS Institute Inc., 1989) was used to perform the one-way analysis of variance. A significant difference between at least one pair of the mean yield strengths was indicated with very strong evidence ( $p \leq 0.0001$ ). A significant difference in at least one pair of the mean ultimate strengths was also indicated with strong evidence ( $p \leq 0.0001$ ).

The one-way analysis of variance will only indicate if there is a significant difference between at least one pair of means, but it does not guarantee that there is a significant difference between all pairs of means. A Fisher's protected least significant difference, LSD,

(Ott, 1988) was conducted on both the yield and ultimate strength data. The test is used to differentiate between means for multiple comparisons. It should only be used after the original one-way analysis of variance finds a significant difference in at least one pair of means. The test is designed to preserve the original error rate; hence, the name "protected". Fisher's protected LSD is based on performing a series of t-tests on each pair of means for the multiple comparisons. The test indicated that the mean yield strengths for steel suppliers X and Z were statistically similar ( $\alpha = 0.05$ ). Fisher's protected LSD was conducted on the ultimate strength data also. The test indicated that all pairs of means were statistically different ( $\alpha = 0.05$ ). From the findings a decision was made to treat the four steel samples as independent. This decision agrees with intuition, because each steel mill could have a different manufacturing process; thus, there is no logical link between the steel suppliers, other than they are producing steel of the same ASTM Grades.

### **Summary Statistics**

Table 4.3 presents summary statistics for the yield strength of steel from the four steel suppliers. The minimum yield strength recorded for the 316 samples was 38.3 ksi. The observation was found in the steel provided by supplier Y. Steel supplier Y also had the smallest average yield strength of 42.57 ksi and the largest COV of the four suppliers (COV = 0.082). The COVs for the steel coil samples were found to be similar to the COVs reported by Kennedy and Gad Aly (1980) and Galambos and Ravindra (1978). The COV of the entire sample of yield strength was 0.067. The smallest ratio of average to nominal yield strength was 1.15. The value is also in the range of steel properties reported by Galambos and

Ravindra (1978) and Kennedy and Gad Aly (1980). In terms of averages and low values, these yield strength data are similar to the data reported by the two other truss plate manufacturers (I and III). It appears that the steel reported by TPM II is representative of the three truss plate manufacturers that responded to the initial survey. The yield strength properties observed from the steel coil samples are similar to the actual structural steel properties reported by Galambos and Ravindra (1978) and Kennedy and Gad Aly (1980).

Similar to the yield strength data, the summary statistics for the ultimate strength data can be found in Table 4.4. The minimum observed ultimate strength was found in a sample supplied by steel manufacturer W. The observed minimum ultimate strength of 52.2 ksi was still greater than the ASTM minimum of 52 ksi. Steel supplier W also contained the lowest average ultimate strength of 55.08. The largest COV for ultimate strength was found to be 0.047 for steel supplier Y which also exhibited the largest COV for yield strength. The average ultimate-strength to nominal-ultimate strength ratio for steel supplier W was 1.06 which is smaller than predicted by Ellingwood et al. (1980). When all data are grouped together, the average ultimate to nominal strength was equal to 1.11, which is closer to the value Ellingwood et al. (1980) reported for structural steel than the individual samples are close to Ellingwood's results. Based on the summary statistics from Table 4.4, these data are similar in terms of minimum and average to the data from the initial TPM steel survey. It appears that these data can be used as a representative sample of steel used by truss plate manufacturers. Since no yield or ultimate strength values were found below the nominal strength, it appears that the quality control procedures used by the steel suppliers for coils

produce similar results to the procedures discussed by Kennedy and Baker (1984) for structural steel.

The summary statistics for Grade 60 steel can be found in Tables 4.5 and 4.6. The steel suppliers were assigned the same label for Grade 60 steel as the original labels assigned to the Grade B steel. Only data from two of the four Grade B suppliers were reported, which were steel suppliers W and X. The minimum yield strength recorded for Grade 60 steel was 59.4 ksi, which corresponded to steel supplier X. Although the value is below the ASTM specified minimum yield strength for Grade 60 steel (minimum  $F_y = 60$  ksi), the "below-grade" yield strength sample could still be acceptable by ASTM standards. A note in ASTM standard A816 (1993c) explains why it is possible to observe values lower than minimum by the following statement, "Because testing within the body of the coil cannot be performed by the producer, recognition must be given to the fact that some portions of coils could fall below the specified minimums." When the data were grouped together, the average to nominal ratio was found to be 1.05 with a COV of 0.045. These statistics are close to the values suggested for structural steel by Galambos and Ravindra (1978) and Kennedy and Gad Aly (1980).



**Table 4.5 Summary of yield strength properties for Grade 60 steel from truss plate manufacturer II.**

Steel Supplier <sup>a</sup>	N <sup>b</sup>	minimum (ksi)	average (ksi)	COV <sup>c</sup>	avg./nominal <sup>d</sup>
W	35	60.5	63.48	0.0436	1.06
X	2	59.4	59.45	0.0012	0.99
Combined	37	59.4	63.26	0.0449	1.05

<sup>a</sup> Letters assigned by the sorted ultimate strength averages for Grade B steel (i.e. W represents the steel supplier with the lowest average ultimate strength).

<sup>b</sup> Sample Size.

<sup>c</sup> Coefficient of variation.

<sup>d</sup> Nominal yield strength for Grade 60 steel is 60 ksi.

**Table 4.6 Summary of ultimate strength properties for Grade 60 steel from truss plate manufacturer II.**

Steel Supplier <sup>a</sup>	N <sup>b</sup>	minimum (ksi)	average (ksi)	COV <sup>c</sup>	avg./nominal <sup>d</sup>
W	35	70.0	73.27	0.0294	1.05
X	2	68.7	69.55	0.0173	0.99
Combined	37	68.7	73.07	0.0311	1.04

<sup>a</sup> Letters assigned by the sorted ultimate strength averages for Grade B steel (i.e. W represents the steel supplier with the lowest average ultimate strength).

<sup>b</sup> Sample Size.

<sup>c</sup> Coefficient of variation.

<sup>d</sup> Nominal ultimate strength for Grade 60 steel is 70 ksi.

The summary information for ultimate strength of Grade 60 steel can be found in Table 4.6. Steel supplier X produced the lowest observed value of 68.7 ksi, but steel supplier W had five observations at exactly the ASTM minimum of 70 ksi. The data were grouped together and the average to nominal ultimate strength ratio was 1.04 with a COV of 0.031. These data appear to have a smaller ratios of mean ultimate strength to nominal strength than suggested by Ellingwood et al. (1980) and a COV that is also lower, but the Ellingwood et

al. (1980) report had different objectives than this report. The Ellingwood et al. (1980) report was intended as a recommendation for ultimate state design values; hence, the authors objectives for their study were different from the objectives of this report. Whereas, this study was conducted to quantify actual "in-grade" steel properties for modeling steel used by truss plate manufacturers.

## **Best-Fit Statistical Distributions**

A common method to model a population of random variables is to fit statistical distributions to a sample of data taken from the population. To obtain an accurate statistical model, the sample must be representative of the population. Selecting the "best-fit" distribution can be somewhat objective. Worley et al. (1990) suggest that, "it is a good practice to try more than one distribution and/or method of estimating distribution parameters." There are several computer packages that are capable of estimating statistical distribution parameters. Two of these developed at Virginia Tech are GDA (Worley et al., 1990) and VTFIT (Cooke et al., 1993).

Five different distributions were selected as possible candidates as "best-fit" distributions for the steel data. These were normal, 2- and 3-parameter lognormal and 2- and 3-parameter Weibull. GDA (Worley et al., 1990) uses a maximum likelihood estimation technique to estimate the model parameters for the five distributions analyzed. VTFIT (Cooke et al., 1993) uses a maximum likelihood estimation technique to estimate the parameters of the normal, 2-parameter lognormal and the 2-parameter Weibull. Cooke et al. (1993) explains that there are certain cases in which the maximum likelihood functions become unstable; therefore, VTFIT estimates the 3-parameter lognormal and the 3-parameter Weibull using a technique that maximizes the natural logarithm of the multinomial distribution function. GDA was used to estimate the parameters of all five distributions; whereas, VTFIT was used to perform additional estimates for the parameters of the 3-parameter lognormal and the 3-parameter Weibull. VTFIT and GDA estimate the parameters for the normal, 2-parameter

lognormal and the 2-parameter Weibull using the same algorithm; therefore, to prevent the duplication of effort, it was not necessary to use VTFIT for these three distributions.

Several formal goodness-of-fit tests that can be used to select the "best-fit" distribution. Formal goodness-of-fit procedures are used to statistically test if the data could have come from a hypothesized distribution. Three popular goodness-of-fit tests are the Kolmogorov-Smirnov (KS), the Anderson-Darling (AD), and the Shapiro-Wilk (SW) tests (Evans et al., 1989). Although test statistics can be calculated for any distribution, the critical values, used for making decisions about the null hypotheses, are only defined for a limited number of distributions (Cooke et al., 1993). Hoyle et al. (1979) suggested that goodness-of-fit tests, specifically the Shapiro-Wilk, should be used as a tool to help identify potential "best-fit" distributions. By examining the visual aids, if none of the candidates appear to have an apparent lack-of-fit, the maximum log-likelihood estimate can be used to select the "best-fit" distribution from the potential candidates. If no distribution examined meets the goodness-of-fit criteria, the maximum log-likelihood estimate can be used to make a choice, if necessary.

Since the one-way analysis of variance and Fisher's protected LSD tests indicated that there were differences due to steel manufacturers, the sample of Grade B steel was broken into sub-samples, sorted by steel mill. The five distributions previously discussed were then fit to the yield and ultimate strengths of the coil samples supplied by the four steel mills. The maximum log-likelihood estimate was used as an aid in selecting the "best-fit" distribution. GDA estimates the critical values of the KS, AD and SW goodness-of-fit tests using relationships developed at the U. S. Forest Products Laboratory (Evans et al., 1989) for the 2- and 3-parameter Weibull. Evans et al. (1989) performed a series of simulations for

selecting the best fit distributions, from the simulation results, the authors suggested that the AD statistics works best for the 2-parameter Weibull, and the SW is the best goodness-of-fit test for the 3-parameter Weibull. The test results will be reported when Weibull distributions are determined as the "best-fit" distributions. Finally, histograms with the distributions overlain were plotted as another criteria for deciding the "best-fit" distribution. The "best-fit" distribution did not always correspond to the distribution with the maximum log-likelihood estimate. The parameters for the "best-fit" distribution were estimated using the maximum likelihood estimates (in other words GDA was used), unless otherwise noted.

#### Grade B Yield Strength Data

Table 4.7 summarizes the best fit distributions for the yield strength of Grade B steel. Assuming the "best-fit" distribution adequately models the population, the probabilities that a sample taken from a coil of steel will be below the nominal yield strength was estimated (column 4, Table 4.7). An IMSL (1987) function was used to estimate these probabilities for the normal and 2- and 3-parameter lognormal distributions; whereas, the closed form solution was used for the 2- and 3-parameter Weibull distributions (Law and Kelton, 1991). Although there were differences due to steel suppliers, all data were grouped together so distributions could be fit to all the data sent by TPM II. Figure 4.1 represents a histogram of the yield strengths of Grade B steel with the "best-fit" distribution overlain. The 3-parameter Weibull was selected to model these data based on the maximum log-likelihood estimate. The KS, AD and SW goodness-of-fit test were conducted on the null hypothesis that these data could come from the 3-parameter Weibull distribution with the fitted parameters. The results of the

KS and AD goodness-of-fit tests rejected the 3-parameter Weibull distribution at  $\alpha = 0.01$ . The SW test failed to reject the hypothesized distribution at  $\alpha = 0.01$ , however the distribution was rejected at  $\alpha = 0.05$ . The probability that a sample taken from a coil exhibits a yield strength less than 37 ksi was estimated as 0.0034, indicating that about three steel samples in one-thousand could be "below-grade".

**Table 4.7 Best fit statistical distributions for Grade B steel yield strength from truss plate manufacturer II, and the probabilities of values occurring below nominal yield strength.**

Steel Supplier <sup>a</sup>	N <sup>b</sup>	Best-fit <sup>c</sup>	$P\{F_y\} \leq \text{Nominal Strength}^d$
W	83	3P-Weibull	undefined <sup>e</sup>
X	26	3P-Lognormal	8.87e-29
Y	54	3P-Lognormal	7.11e-06
Z	153	3P-Lognormal	3.21e-18
Combined	316	3P-Weibull	3.36e-03

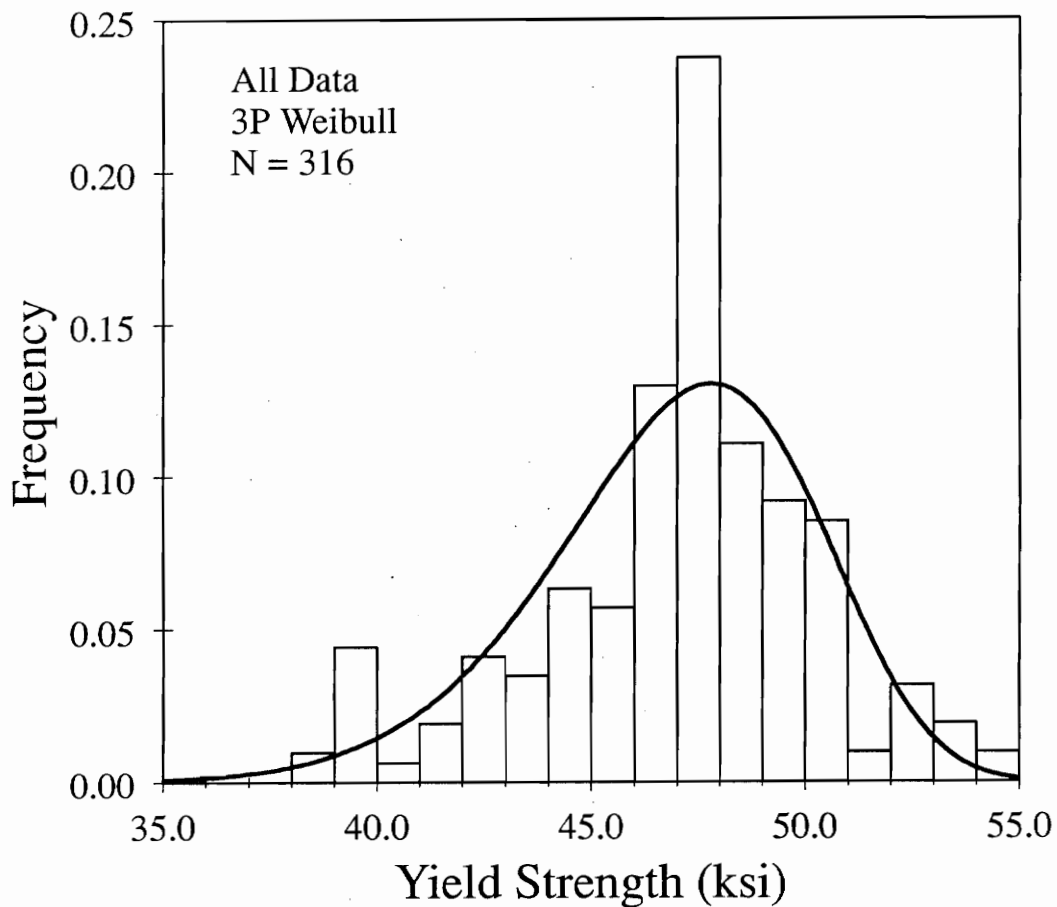
<sup>a</sup> Letters assigned by the sorted ultimate strength averages for Grade B steel (i.e. W represents the steel supplier with the lowest average ultimate strength).

<sup>b</sup> Sample Size.

<sup>c</sup> Best fit based on goodness-of-fit tests and maximum log-likelihood functions.

<sup>d</sup> Nominal yield strength for Grade B steel is 37 ksi.

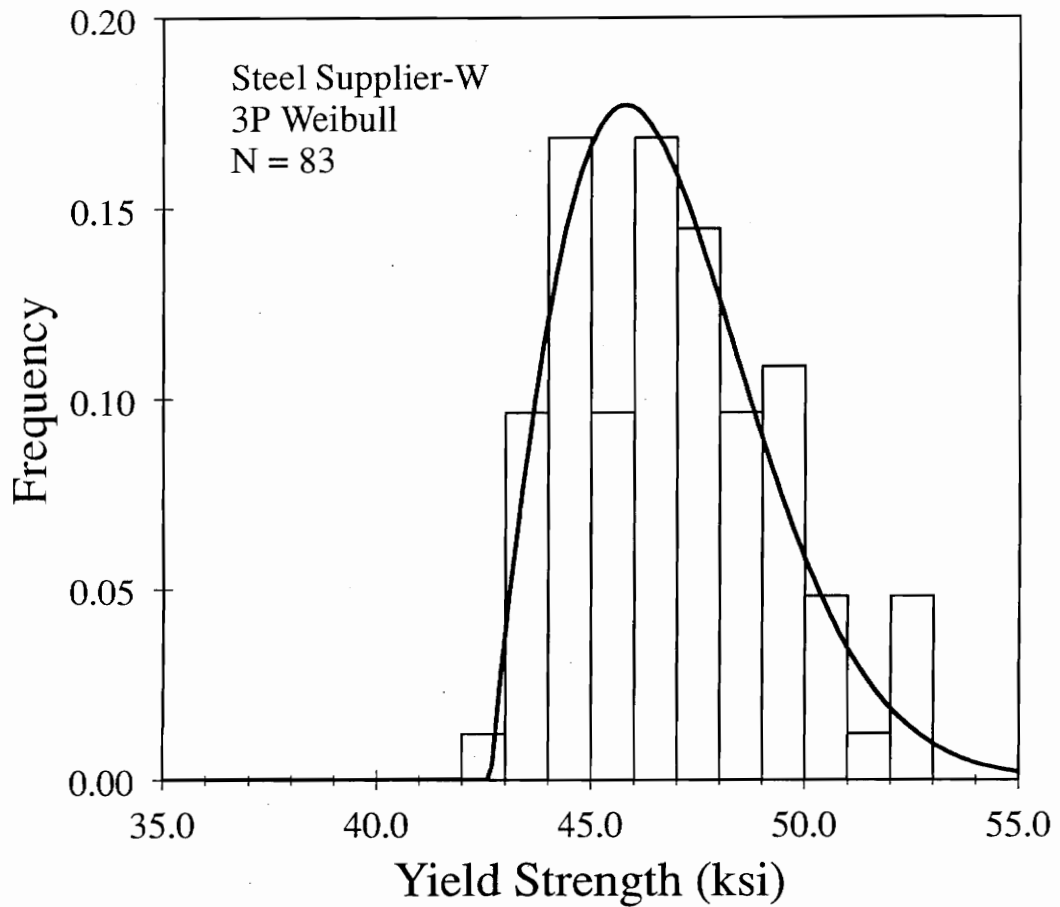
<sup>e</sup> Location parameter is greater than the nominal yield strength; therefore, the probability is undefined.



**Figure 4.1** Histogram of all of the Grade B yield strength data supplied by truss plate manufacturer II with the best-fit distribution overlain.

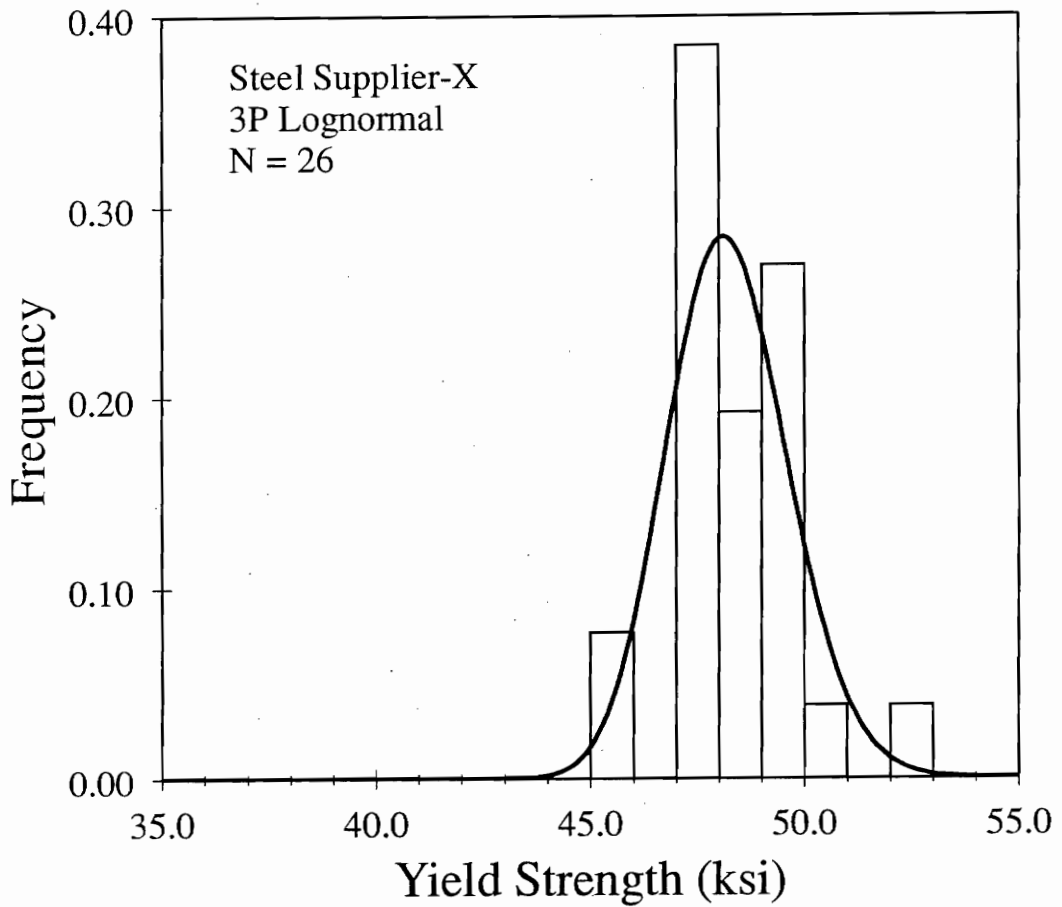
Figure 4.2 is a histogram representing the yield strength of Grade B steel supplied by steel manufacturer W. The 3-parameter Weibull distribution gave the maximum log-likelihood function of the distributions studied. The KS, AD and SW goodness-of-fit tests were used to test the hypothesis that the data followed the 3-parameter Weibull distribution. The results from the KS and AD tests both failed-to-reject the distribution at  $\alpha = 0.05$ , however the distribution was rejected at  $\alpha = 0.10$ . The SW test, which Evans et al. (1989) suggests is the best test for the 3-parameter Weibull, supplied strong evidence to reject the distribution at  $\alpha = 0.01$ . The probability that a sample from a coil produced by supplier W will be below 37 ksi is undefined, due to the fact that the 3-parameter Weibull has a shift parameter (location) greater than 37 ksi. The probability of an observation occurring below the location parameter is not mathematically defined.





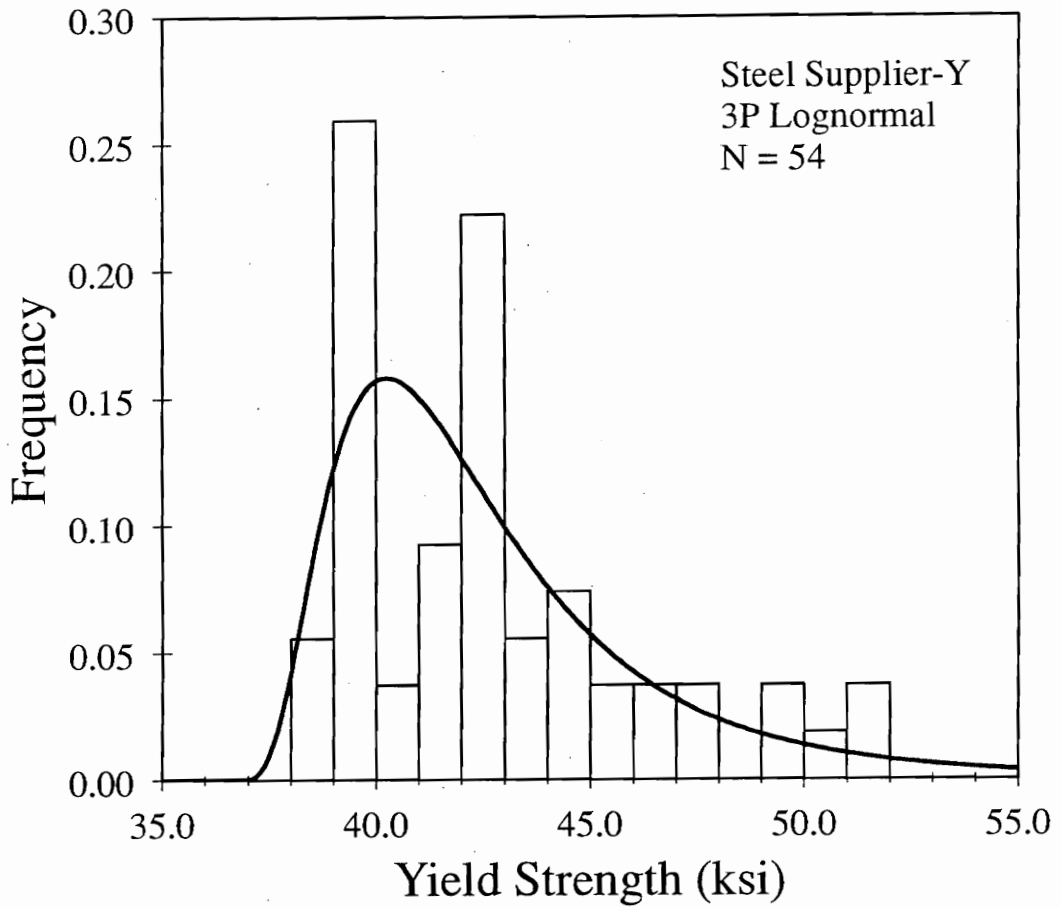
**Figure 4.2** Histogram of the Grade B yield strength data produced by steel manufacturer W with the best-fit distribution overlain.

Figure 4.3 represents a histogram of the yield strength of samples taken from coils supplied by steel manufacturer X. The 3-parameter lognormal was chosen as the "best-fit" based on the maximum log-likelihood estimate. Visual examination of Figure 4.3 shows an apparent lack-of-fit; however, the histogram is based on a sample size of 26; therefore, it is not surprising that no distribution studied fit the data well. Assuming the 3-parameter lognormal adequately fits the data, the probability that a sample from a coil produced by steel manufacturer X is "below-grade" is very small ( $8.87e-29$ ). The probability alone does not mean much, but it can be used as a relative comparison between the probabilities that other manufacturers will produce coils in which samples can be collected that will be less than nominal yield strength.



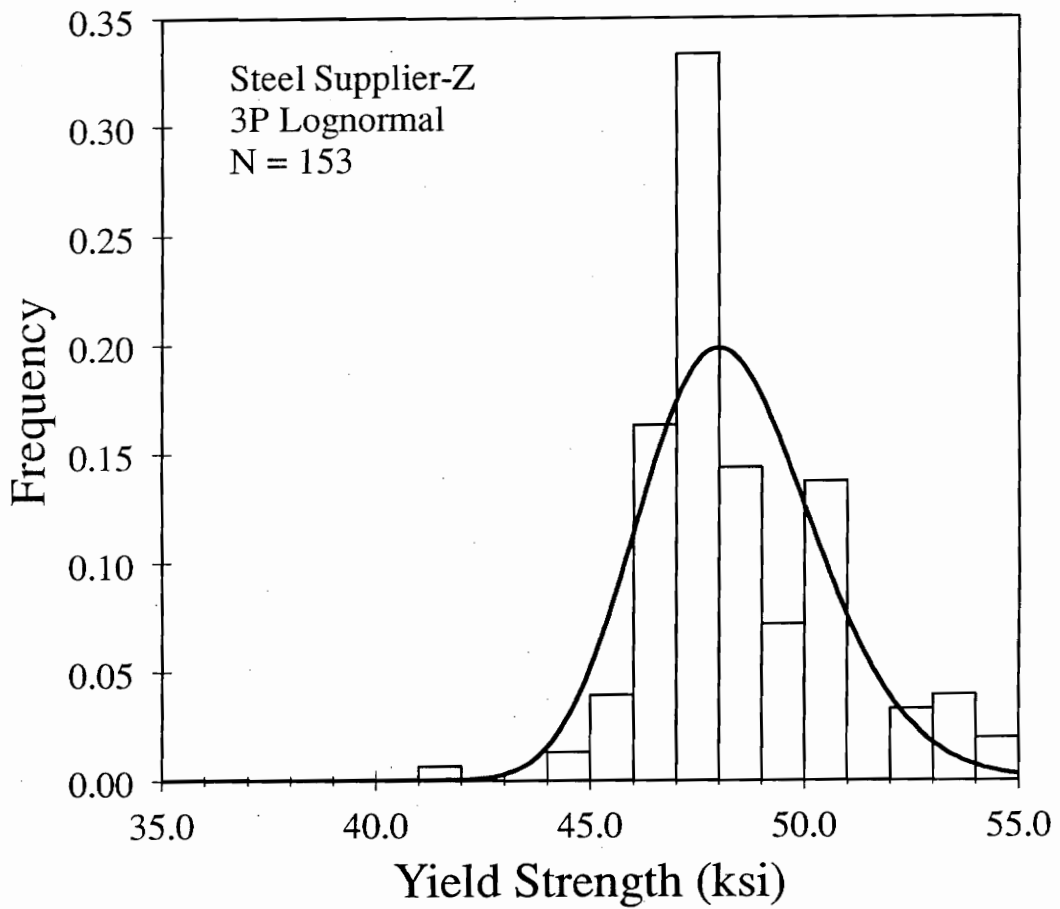
**Figure 4.3** Histogram of the Grade B yield strength data produced by steel manufacturer X with the best-fit distribution overlain.

Figure 4.4 is a histogram that represents the steel yield strength supplied by mill Y, with the "best-fit" probability density function overlain. The 3-parameter Weibull distribution yielded the maximum log-likelihood function; however, the shape parameter was estimated as 1.0. A shape parameter equal to 1.0 is a limiting case of the Weibull, that produces the exponential distribution. An exponential distribution is skewed right, and generally would be a poor model for strength data. The results of the KS, AD and SW tests provided strong evidence that the 3-parameter Weibull distribution was a poor fit for the data by rejecting the hypothesized distribution at  $\alpha = 0.01$ . The small sample size ( $N = 54$ ) could have caused sampling error; therefore, the 3-parameter Weibull was deemed as inadequate. The next largest log-likelihood estimate was the 3-parameter lognormal. Examining the visual also shows some lack-of-fit; however, the 3-parameter lognormal was chosen as the "best-fit". The probability that a sample can be collected from a coil supplied by Y exhibiting a yield strength less than 37 ksi was estimated as  $7.11e-6$ .



**Figure 4.4** Histogram of the Grade B yield strength data produced by steel manufacturer Y with the best-fit distribution overlain.

Figure 4.5 represents the histogram of the yield strength of coil samples provided by steel mill Z. This is the largest sample size of the sub-samples of yield strength data with a sample size of 153. The 3-parameter lognormal was chosen as the "best-fit" distribution based on the maximum log-likelihood estimate. The probability that steel mill Z will produce a coil having a test sample with a yield strength of less than 37 ksi is  $3.21e-18$ . The number is also very small, but it can be used for comparison purposes.



**Figure 4.5** Histogram of the Grade B yield strength data produced by steel manufacturer Z with the best-fit distribution overlain.

The probability of each steel mill producing coils having test samples with a yield strengths less than nominal was either small or undefined. If all the Grade B steel is considered as one sample, observing a coil test sample with a yield strength less than nominal could occur about 3 times in one-thousand replications. Although this frequency is not large, it could be significant and provides evidence that it is possible that a truss plate manufacturer could receive a coil of Grade B steel containing a section that is below the ASTM minimum yield strength.

#### Grade B Ultimate Strength Data

Table 4.8 lists the "best-fit" statistical distributions for the ultimate strength of Grade B steel sent by truss plate manufacturer II. Table 4.8 also contains a column (column 4) that estimates the probability of observing a sample from a coil of steel with a ultimate strength less than the ASTM nominal of 52 ksi. Figure 4.6 is a histogram that represents the ultimate strength data for Grade B steel sent by TPM II with the "best-fit" distribution overlain. The figure shows definite lack-of-fit for the 3-parameter Weibull. The lack-of-fit might be attributed to the fact that the data actually contains four sub-samples (based on steel supplier) of Grade B ultimate strength data grouped together. GDA, which uses a routine developed by Kline and Bender (1990) to estimate the parameters for the 3-parameter Weibull, failed to execute for the data set; therefore, a program utilizing the Kline and Bender (1990) algorithm was used to estimate the maximum likelihood estimates for the 3-parameter Weibull. The program did not calculate the test statistics for the KS, AD and SW tests; therefore, the results for these test will not be reported. The 3-parameter Weibull was chosen as the "best-



fit" distribution based on the maximum log-likelihood estimate. Even though the estimate is probably not very accurate, the probability of a truss plate manufacturer collecting a sample from a coil of steel with an ultimate strength less than nominal is 0.0024.

**Table 4.8 Best fit statistical distributions for Grade B steel ultimate strength from truss plate manufacturer II, and the probabilities of values occurring below nominal ultimate strength.**

Steel Supplier <sup>a</sup>	N <sup>b</sup>	Best-fit <sup>c</sup>	P{F <sub>u</sub> } ≤ Nominal Strength <sup>d</sup>
W	83	3P-Lognormal	3.74e-03
X	26	2P-Lognormal	1.95e-04
Y	54	3P-Weibull	undefined <sup>e</sup>
Z	153	3P-Weibull	2.06e-06
Combined	316	3P-Weibull	2.44e-03

<sup>a</sup> Letters assigned by the sorted ultimate strength averages for Grade B steel (i.e. W represents the steel supplier with the lowest average ultimate strength).

<sup>b</sup> Sample Size.

<sup>c</sup> Best fit based on goodness-of-fit tests and maximum log-likelihood functions.

<sup>d</sup> Nominal ultimate strength for Grade B steel is 52 ksi.

<sup>e</sup> Location parameter is greater than the ultimate yield strength; therefore, the probability is undefined.

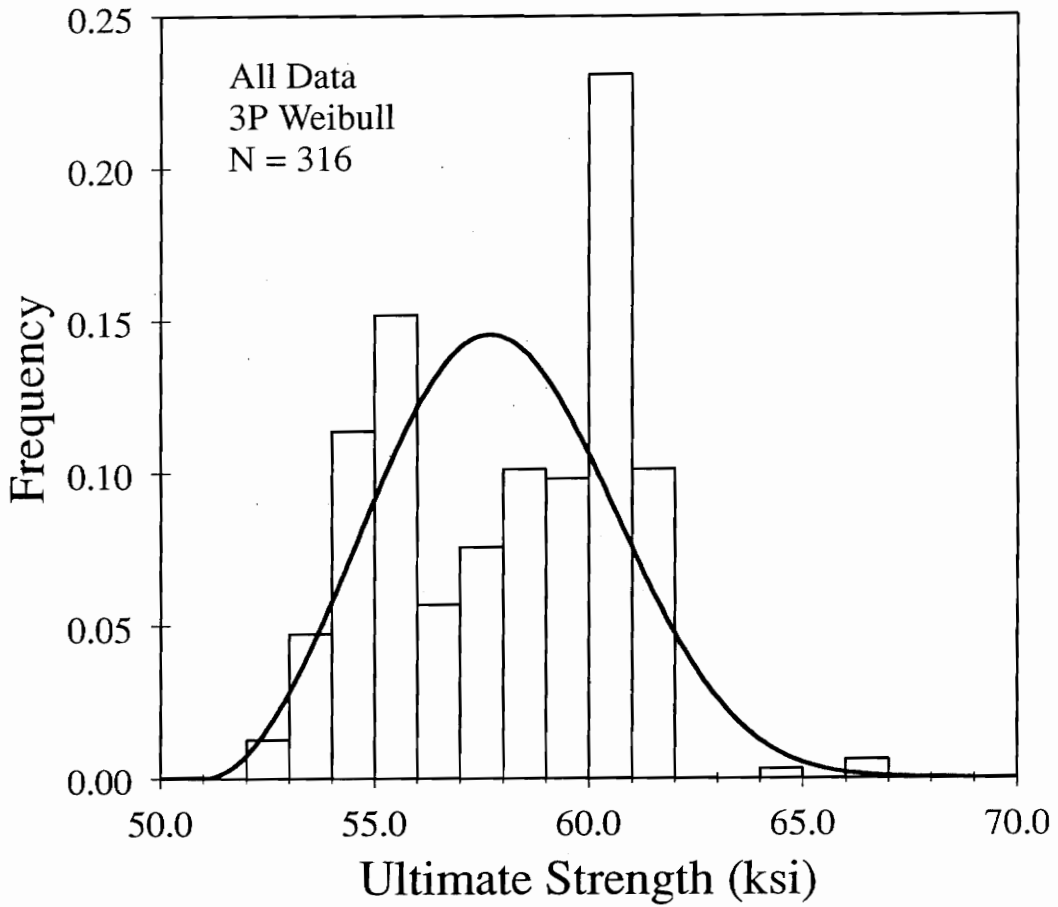


**Figure 4.6** Histogram of all of the Grade B ultimate strength data supplied by truss plate manufacturer II with the best-fit distribution overlain.

Figure 4.7 represents the "best-fit" distribution overlain on the histogram of the ultimate strength of steel produced by mill W. The mill produced the lowest average ultimate strength of the four steel mills; thus, it can be thought of as the controlling steel mill in terms of ultimate strength. A 3-parameter lognormal was chosen as the "best-fit" based on the maximum log-likelihood estimate. By visually assessing the fit of the 3-parameter lognormal, it appears that the fit is reasonable. The probability of a sample from a coil produced by steel mill W having an ultimate strength less than 52 ksi is 0.0037. The percentile is roughly equivalent to 4 coil samples out of one-thousand will be "below-grade".

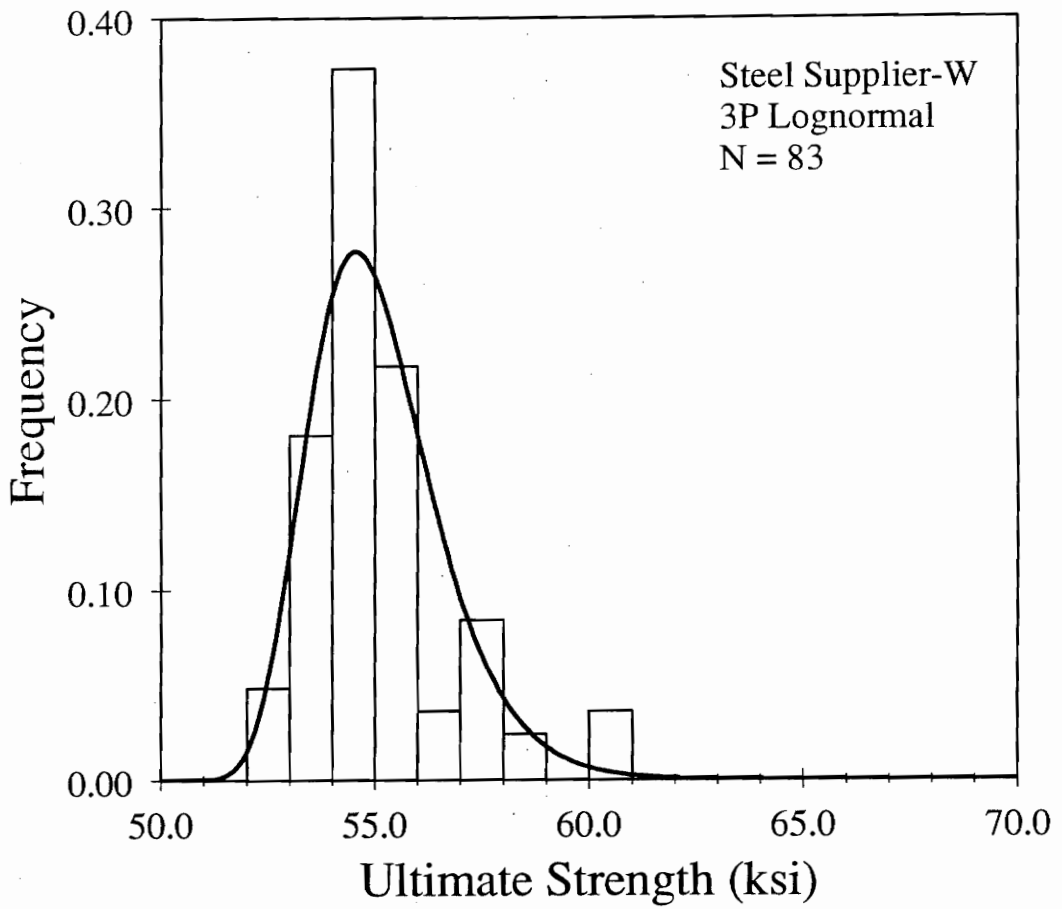
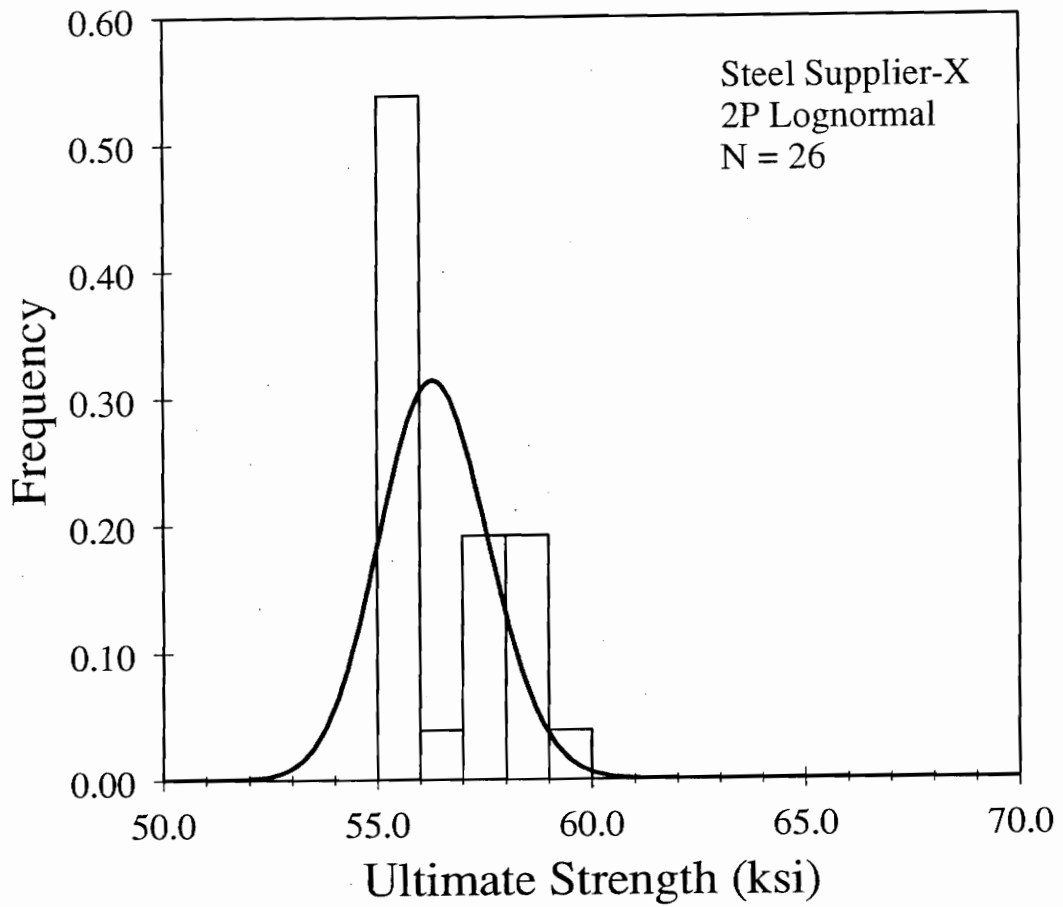


**Figure 4.7** Histogram of the Grade B yield strength data produced by steel manufacturer W with the best-fit distribution overlain.

Figure 4.8 represents a histogram of the ultimate strength of Grade B steel produced by steel mill X with the "best-fit" distribution overlain. The data set is one of the two that VTFIT estimated parameters with a greater log-likelihood function than GDA for a given 3-parameter distribution. In this case, it occurred for the 3-parameter Weibull. VTFIT estimated the shape as being less than 1.0, and GDA estimated the shape as being 1.0 exactly. Examining the histogram reveals that the data is in fact skewed right. This skew could possibly be attributed to sampling error, since the sample size was small ( $N = 26$ ). Theoretically the ultimate strength of steel should not be highly skewed right; therefore, the skewed distributions are more than likely poor candidates. One of the properties of the Weibull is that the probability density function approaches infinity at the location parameter, if the shape is less than 1.0.

Although VTFIT produced log-likelihood estimates greater than GDA, the actual parameters are probably not a realistic model for these data. The next largest log-likelihood function was the 3-parameter lognormal estimated by GDA. Examining the probability density function overlain on the histogram revealed that the density function approached a large number near the location parameter, and the fitted distribution was also highly skewed right; therefore, it was decided that the 3-parameter lognormal was probably not a very good choice for the "best-fit" distribution. The next largest log-likelihood estimate was the 2-parameter lognormal. Although visually, there appears to be lack-of-fit, the 2-parameter lognormal distribution was chosen as the "best-fit". There is also historical evidence that the 2-parameter lognormal is a reasonable model for the ultimate strength of steel (Ellingwood, et al., 1980;

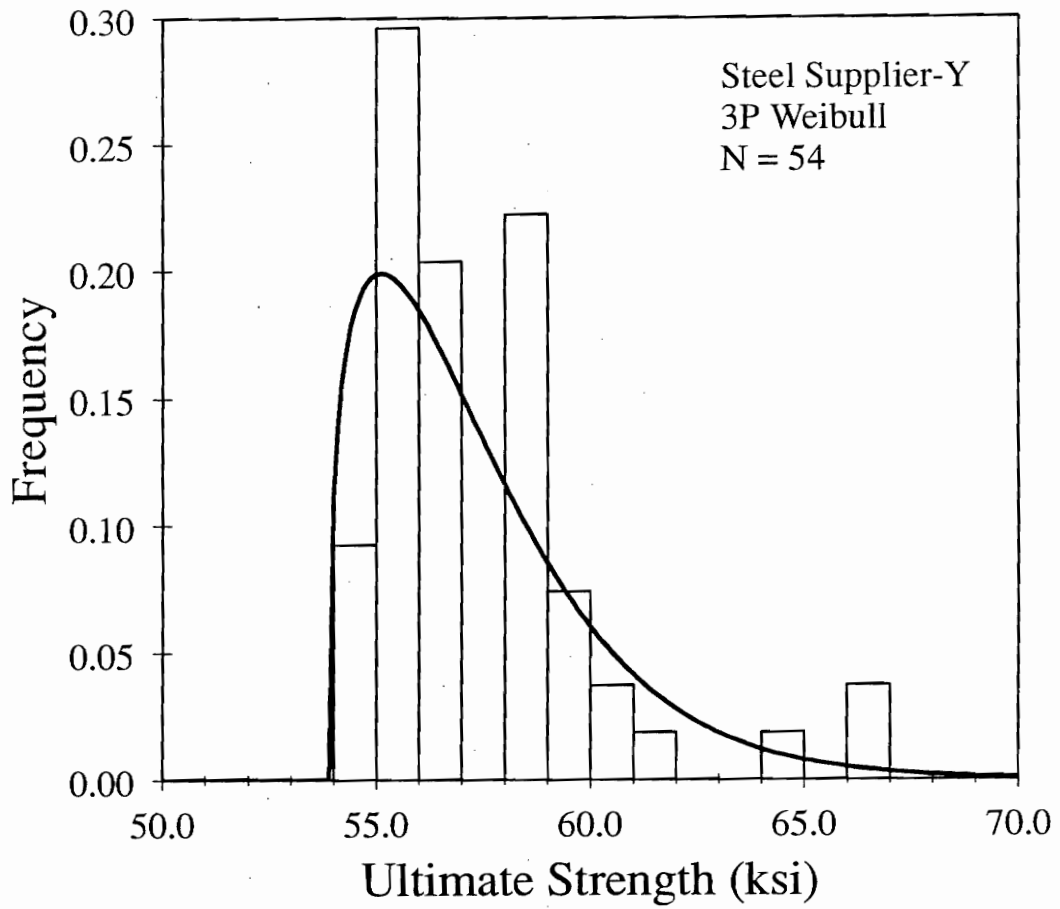
Kennedy and Baker, 1984). The probability of collecting a sample from a steel coil exhibiting an ultimate strength less than 52 ksi was calculated as  $1.95e-4$ .



**Figure 4.8** Histogram of the Grade B yield strength data produced by steel manufacturer X with the best-fit distribution overlain.

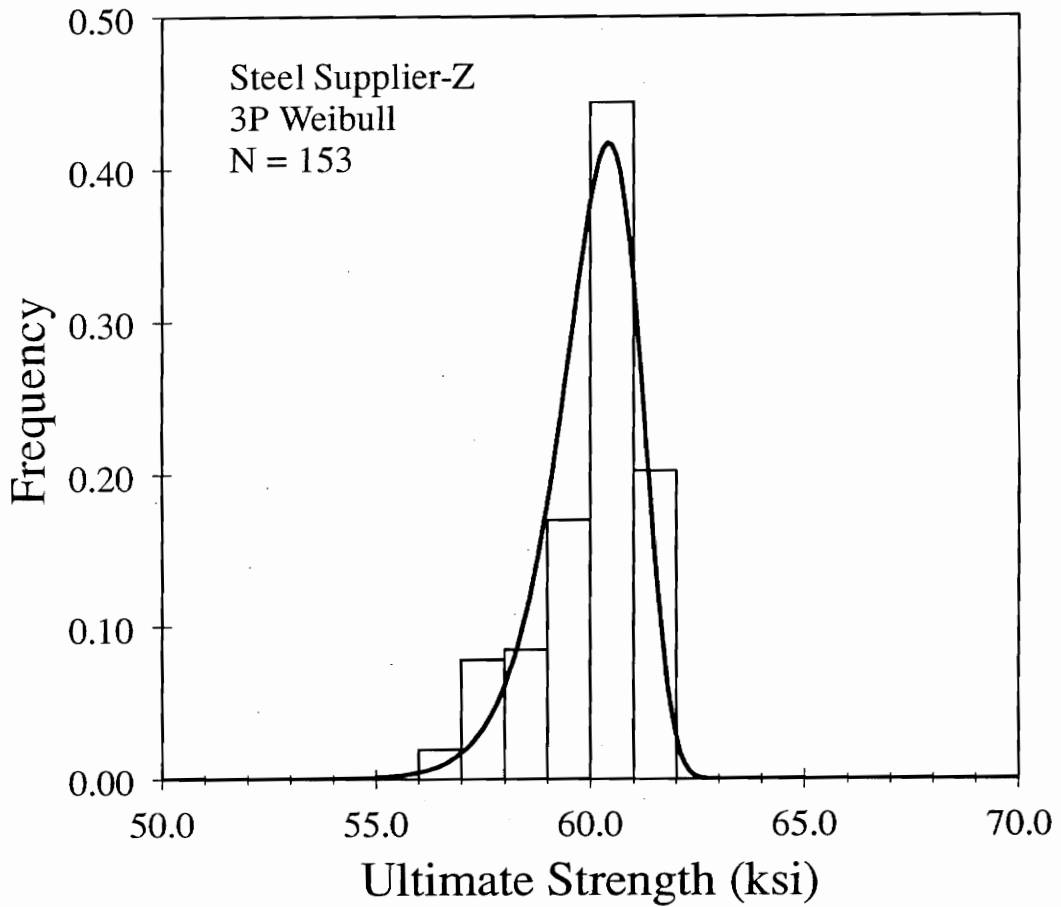
Figure 4.9 represents a histogram of the ultimate strength of steel coil samples produced by steel mill Y with the "best-fit" distribution overlain. The data set is the second of the two data sets in which VTFIT estimated parameters with larger log-likelihood estimates than GDA for a given 3-parameter distribution; however, the estimated parameters for the 3-parameter Weibull estimated by GDA yielded the maximum log-likelihood estimate. The KS, AD and SW goodness-of-fit test were used to test the hypothesis that the data could come from a 3-parameter Weibull distribution with the fitted parameters. The results of the KS test failed-to-reject the distribution at  $\alpha = 0.05$ , but rejected the 3-parameter Weibull at  $\alpha = 0.10$ . The results of the AD test resulted in failing-to-reject the distribution at  $\alpha = 0.01$ , but rejected at  $\alpha = 0.05$ , and the best test for the 3-parameter Weibull (Evans, et al., 1989), the SW test, strongly rejected the distribution, at  $\alpha = 0.01$ . Assuming the 3-parameter Weibull is the "best-fit" distribution, the probability that a sample collected from a coil of steel produced by mill Y having an ultimate strength less than 52 ksi, is undefined. The mathematical abnormality could give an indication that the 3-parameter Weibull may not adequately model the data; however, the sample size is fairly small; hence, sensitive to sampling error.





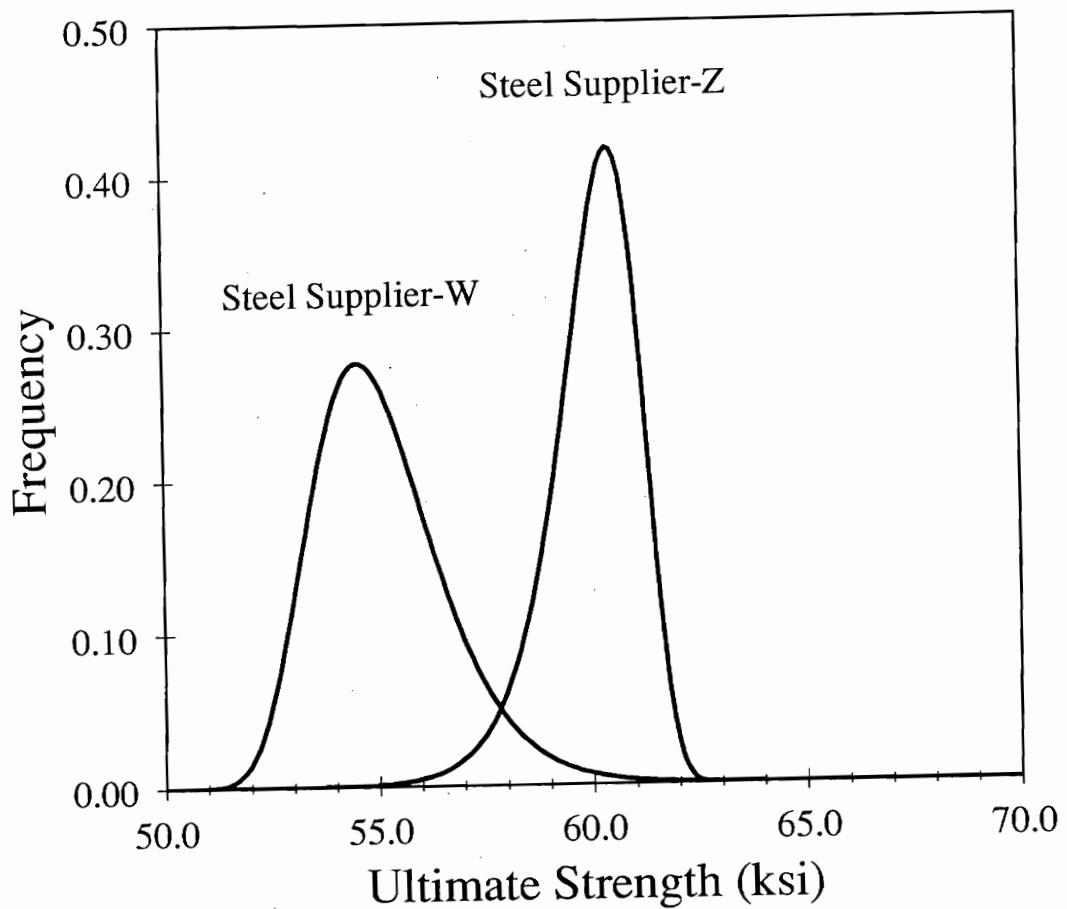
**Figure 4.9** Histogram of the Grade B yield strength data produced by steel manufacturer Y with the best-fit distribution overlain.

Figure 4.10 represents the histogram of the ultimate strength of steel manufactured by steel mill Z with the "best-fit" distribution overlain. The data not only represents the largest sample size ( $N = 153$ ), also is the strongest, on average, of the four sub-samples. The 3-parameter Weibull was selected on the basis of the maximum log-likelihood estimate. GDA failed to execute for the data set; therefore, an algorithm developed by Kline and Bender (1990) was used to estimate the parameters. The program did not estimate the test statistics for the KS, AD and the SW tests; therefore, the conclusions for these test were not reported. The probability that a sample from a coil of steel from mill Z is less than 52 ksi was estimated as  $2.06e-6$ . The number is fairly small; however, it can be used as a comparison to the other probabilities. As might be expected the steel supplier with the largest average ultimate stress, also had the smallest probability of having a coil sample with a ultimate strength less than nominal.



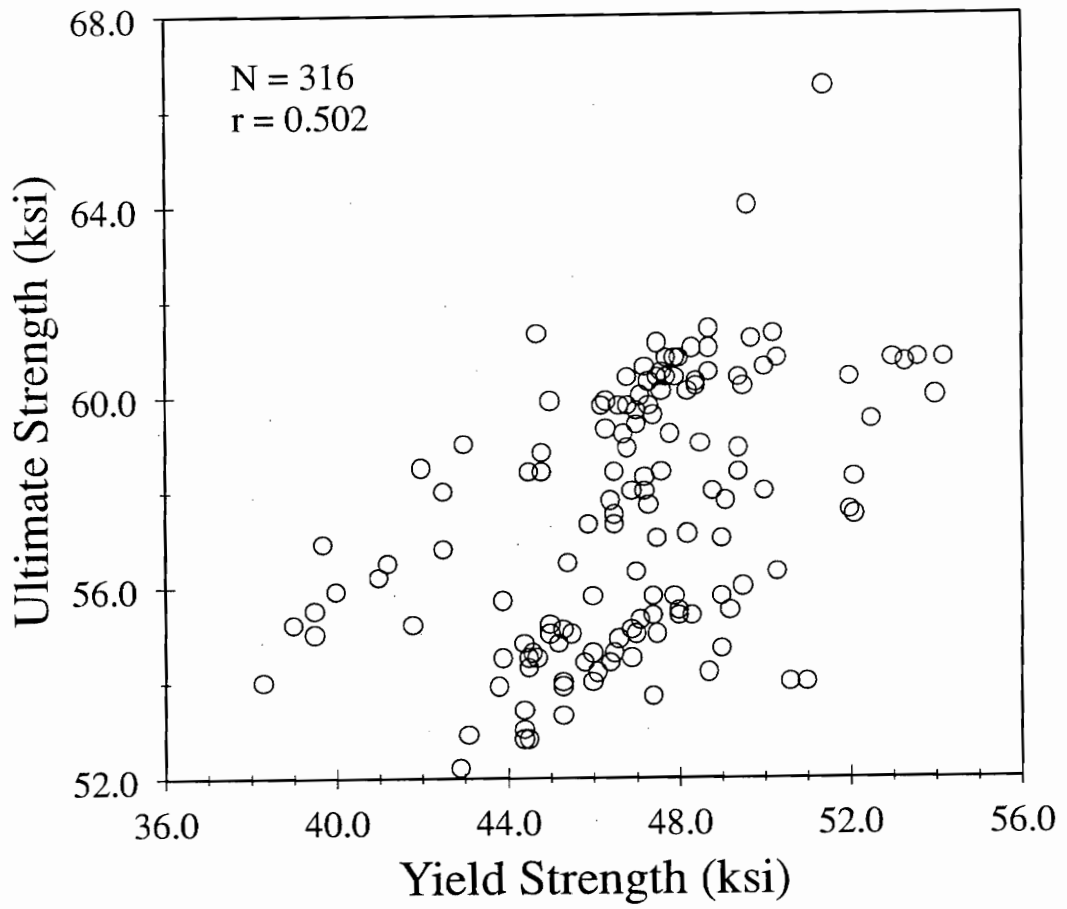
**Figure 4.10** Histogram of the Grade B yield strength data produced by steel manufacturer Z with the best-fit distribution overlain.

Figure 4.11 represents a plot of the "best-fit" probability density functions for steel suppliers W and Z. Steel mills W and Z produced the smallest average ultimate strength and the largest average ultimate strength, respectively, from the data reported by TPM II. The graph illustrates the upper and lower limits of the four different steel mills for Grade B steel. Although steel supplier Z provides an "above-grade" product, the results of steel supplier W cannot be ignored. Truss plates manufactured from coils produced from mill W could possibly be the weakest link in a truss; hence, a simulation cannot assume that steel properties are considerably greater than the nominal ultimate strength.



**Figure 4.11** Probability density function representing the smallest mean ultimate strength and the largest mean ultimate strength.

Figure 4.12 is a scatter plot of ultimate strength versus yield strength for Grade B steel. The graph suggests that the yield strength and ultimate strength could be positively correlated random variables. The variability in the relationship between these two properties is probably due to chemical differences in the heats of steel produced at the mill. The Pearson product-moment method (described in Gibbons, 1993) was used to estimate the correlation coefficient ( $r$ ) by using the SAS procedure CORR (1990). The estimate of  $r$  for the yield and ultimate strengths of Grade B steel was 0.502. The null hypothesis ( $H_0$ ), that there is no correlation ( $\rho = 0$ ) in the population of Grade B yield and ultimate strengths, was tested. The alternative hypothesis ( $H_a$ ) was one-sided since it is expected that there is a positive correlation ( $\rho > 0$ ) for the yield and ultimate strengths of steel. The null hypothesis was very strongly rejected ( $p \leq 0.00005$ ); hence, it can be concluded that yield strength and ultimate strength are positively correlated. An observation from the graph is that steel having a yield strength considerably higher than the nominal yield strength does not guarantee that the ultimate strength will be considerably higher than the nominal ultimate strength; however, there is a general positive trend.



**Figure 4.12** Scatter-plot of ultimate strength versus yield strength for Grade B steel supplied by truss plate manufacturer II.

Edwards (1984) warns that the estimate of the correlation coefficient can be highly influenced when samples of observations are really composed of two or more sub-samples with different means of the two random variables. In a previous section, significant differences were found in the means of the yield and ultimate strengths of Grade B steel, when the data was sorted by steel supplier. Therefore, the SAS procedure CORR was used to estimate the Pearson product-moment correlation coefficient for the steel provided by the four steel suppliers. The correlations were estimated as 0.612, 0.658, 0.790, and 0.460 for steel suppliers W, X, Y, and Z, respectively. Edwards (1984) demonstrates a statistical test, based on the chi-squared statistic, that is used to test if two or more correlation coefficients are equal. More formally, the null hypothesis is that the correlation coefficients are equal for the four different steel suppliers; thus, implying that there is no effect of steel supplier on the correlation of yield strength and ultimate strength. The alternative hypothesis is that at least one pair of correlation coefficients are different. The null hypothesis was rejected ( $p \leq 0.01$ ); therefore, it was assumed that there was a difference in the correlation of yield strength and ultimate strength due to steel supplier.

The four correlation coefficients were then tested for significance ( $H_0: \rho = 0$ ,  $H_a: \rho > 0$ ). All null hypotheses were strongly rejected (maximum  $p \leq 0.00015$  for supplier X). Therefore, it can be concluded that there is a positive relationship between yield strength and ultimate strength for Grade B steel and this relationship holds true for steel from four manufacturers. The estimated correlation coefficients ranged from 0.46 to 0.79.



### Grade 60 Strength Data

Table 4.9 contains the "best-fit" distributions for the yield and ultimate strength of Grades 60 steel and the probabilities that a coil sample will fall below the nominal yield and ultimate strength. These data were supplied by TPM II. Figure 4.13 is a histogram of the yield strength of Grade 60 steel. The maximum log-likelihood estimate was for the 3-parameter Weibull; thus, it was chosen as the "best-fit" distribution. The KS, AD and SW goodness-of-fit test were used to test the hypothesis that the data could be modeled by the 3-parameter Weibull. The results of the KS test failed-to-reject the distribution at  $\alpha = 0.05$ , but rejected the distribution at  $\alpha = 0.10$ . The results of the AD test failed-to-reject the distribution at  $\alpha = 0.01$ , but rejected the distribution at  $\alpha = 0.05$ . The results of the SW test strongly rejected the distributions with  $\alpha = 0.01$ . A visual examination of Figure 4.13 shows a lack-of-fit; however, the sample size is fairly small ( $N = 37$ ). The small sample size could have caused sampling errors. A larger sample size would probably "smooth-out" the histogram so a better fit could be obtained. The probability of a sample taken from a coil of steel having a yield strength less than nominal (60 ksi) is 0.078. The probability indicates that about one sample out of thirteen test specimens will be "below-grade".

**Table 4.9 Best fit statistical distributions for Grade 60 steel from truss plate manufacturer II, and the probabilities of values occurring below nominal strengths.**

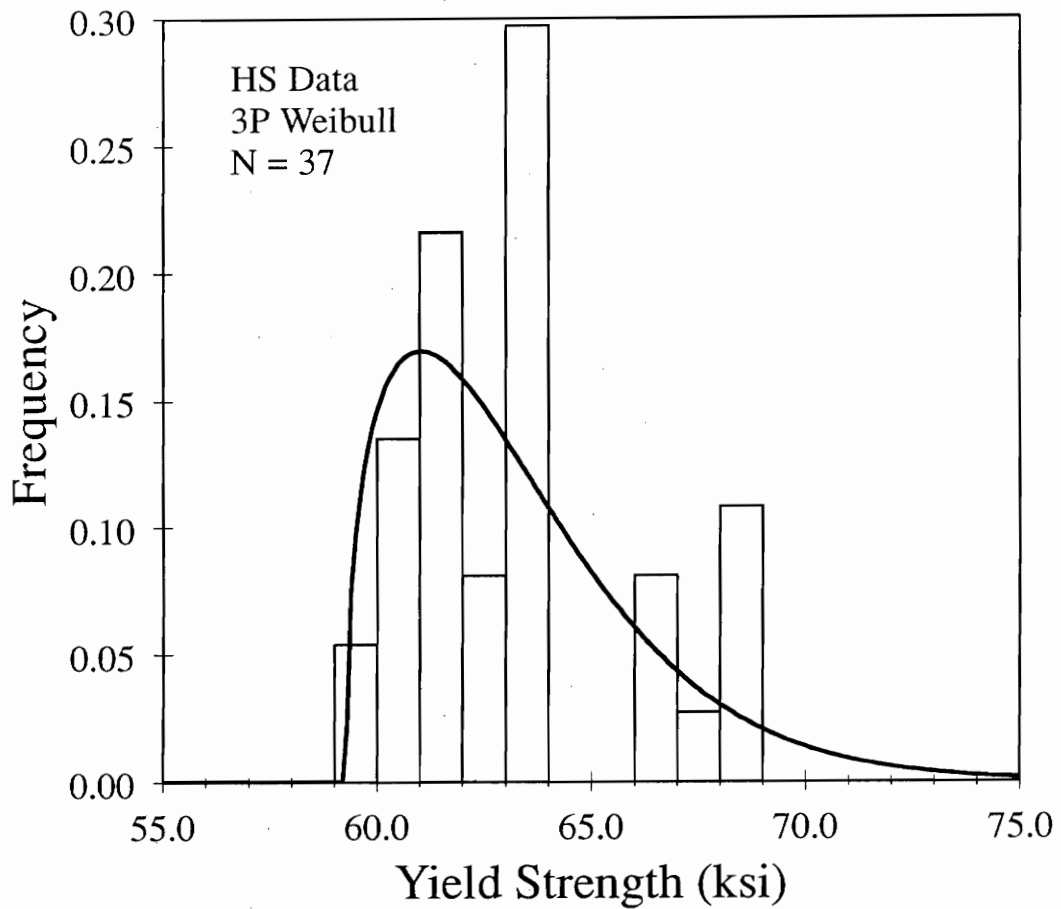
Steel Property <sup>a</sup>	N <sup>b</sup>	Best-fit <sup>c</sup>	Nominal Strength (ksi)	P{F} ≤ Nominal <sup>c</sup>
yield strength	37	3P-Weibull	60	7.73e-02
ultimate strength	37	3P-Weibull	70	7.99e-02

<sup>a</sup> Letters assigned by the sorted ultimate strength averages for Grade B steel (i.e. W represents the steel supplier with the lowest average ultimate strength).

<sup>b</sup> Sample Size.

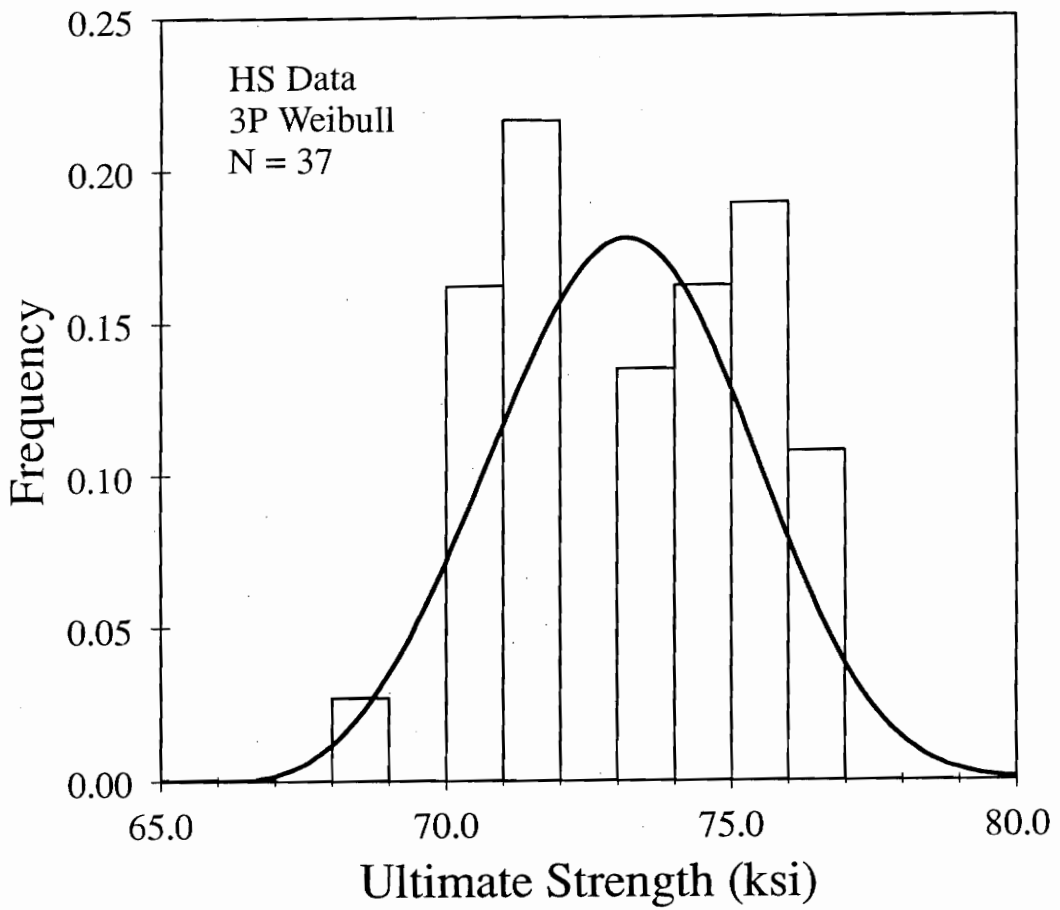
<sup>c</sup> Best fit based on goodness-of-fit tests and maximum log-likelihood functions.

<sup>d</sup> Represents the probability that the yield or ultimate strength for a sample from a sample from <sup>e</sup> coil of steel is less than the nominal yield or ultimate strength, respectively.



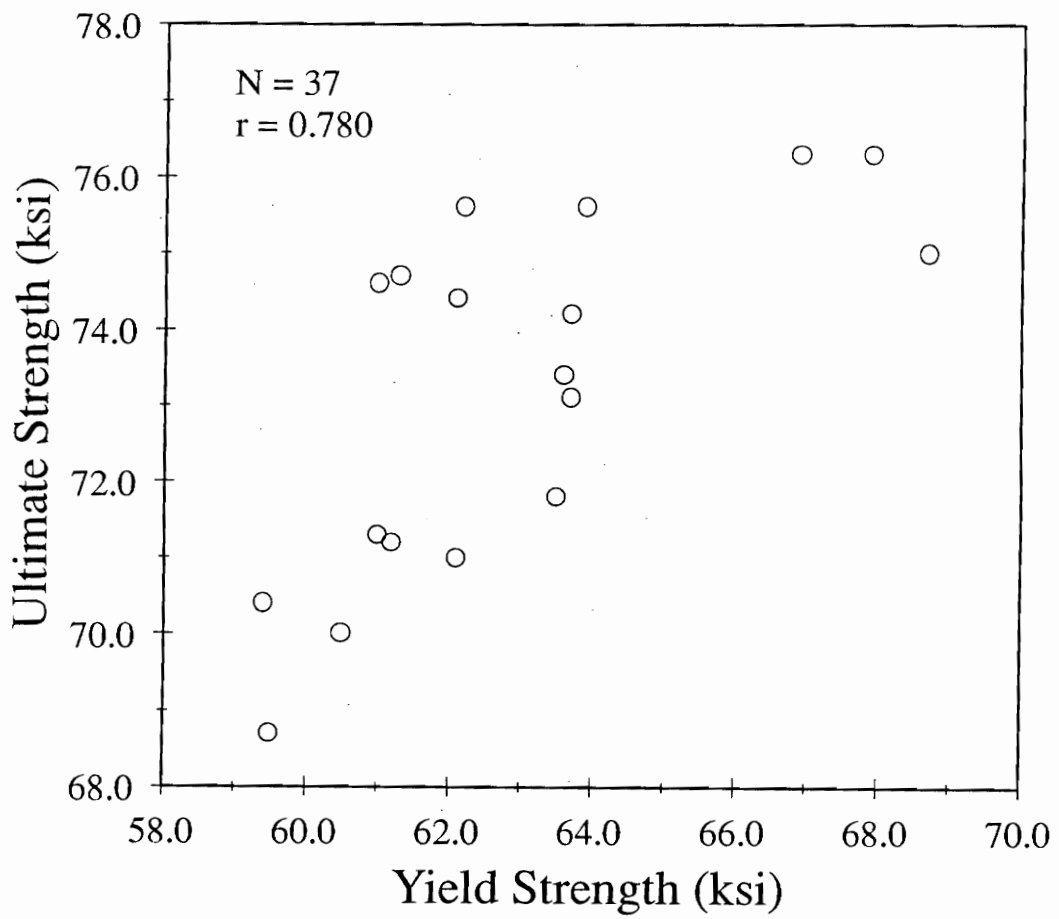
**Figure 4.13** Histogram of the Grade 60 yield strength data supplied by truss plate manufacturer II with the best-fit distribution overlain.

Figure 4.14 is a histogram of the ultimate strength of Grade 60 steel with the "best-fit" distribution overlain. GDA failed to execute with the data set; therefore, a program using the method developed by Kline and Bender (1990) was used to estimate the 3-parameter Weibull parameters. The 3-parameter Weibull had the largest log-likelihood function of the distributions examined. Similar to the Grade 60 yield strength data, the ultimate strength data showed lack-of-fit. The lack-of-fit could probably be attributed to the small sample size. Assuming that the 3-parameter Weibull is an adequate fit, the probability that a truss plate manufacturer will collect a sample from a coil of Grade 60 steel in which the ultimate strength is less than nominal is 0.080. The percentile indicates that one out of every thirteen test samples could be "below-grade" in terms of ultimate strength.



**Figure 4.14** Histogram of the Grade 60 ultimate strength data supplied by truss plate manufacturer II with the best-fit distribution overlain.

Figure 4.15 is a scatter plot of ultimate strength versus yield strength for Grade 60 steel. The plot is similar than the Grade B steel; however, it has less data points than Figure 4.12. The correlation coefficient was estimated as 0.780 using the Pearson product-moment method (described in Gibbons, 1993). The null hypothesis, that the population correlation coefficient is equal to zero ( $\rho = 0$ ), was tested using the SAS procedure CORR (1990). The alternative hypothesis was that there is positive correlation between yield and ultimate strengths ( $\rho > 0$ ) for the population of samples taken from Grade 60 coils of steel. The null hypothesis was strongly rejected ( $p \leq 0.00005$ ); therefore, it can be concluded that the positive trend in the data cannot be attributed to sample randomness. The same conclusions for the Grade B data can be drawn for the Grade 60 data. There is a general positive trend in the data. A steel that has an above average yield strength will tend to have an above average ultimate strength.



**Figure 4.15** Scatter-plot of ultimate strength versus yield strength for Grade 60 steel supplied by truss plate manufacturer II.

## SUMMARY

Some steel suppliers produce coils with properties statistically distributed near the minimum strength requirements specified by ASTM Standards A446 and A816 (1993a, 1993c). For example, from Grade B samples collected from coils produced by steel supplier W, it may be predicted that about four samples out of one-thousand will fall below the ASTM specified minimum ultimate strength (1993a). This study also revealed that Grade 60 coil samples have higher occurrence of non-conforming strength properties than Grade B. These data indicate that about one out of every thirteen samples collected from coils of Grade 60 steel will be below the ASTM Standard minimum ultimate strength (1993c).

Design procedures are developed to allow for "worst-case scenarios" for both the loads and the resistance of the materials, and still provide a design that is structurally safe. Near minimum steel properties represent "worst-case scenarios" for the resistance parameters of metal-connector-plates in wood-truss structural systems. A specific roof or floor structure may contain plates manufactured from any of the four steel suppliers analyzed in this study; however, the truss should pass a code specified test regardless of steel manufacturer. Since the purpose of this study is to arrive at a rational truss test safety factors, steel data from manufacturer W will be used as the controlling ultimate strength distribution for Grade B steel.

The "best-fit" distribution for Grade 60 steel showed a lack-of-fit (Figure 4.14) and was based on a small sample size ( $N = 37$ ). However, the statistical information derived from the 37 samples was judged to be adequate for the purposes of this study. From the 37 coil samples, two were found to be less than the ASTM minimum ultimate strength and five



observations were recorded as 70.0 ksi (the ASTM minimum ultimate strength). Below minimum ultimate strength steel may occur in an actual joint; therefore, the remote possibility of a near minimum (or below) steel will be included in this simulation study aimed at evaluation truss test safety factors.

## CONCLUSIONS

- 1.) Not only are the yield strengths and the ultimate strength random variables, but the relationship between the two is also a random variable. The estimated correlation coefficient for the relationship of yield strength and ultimate strength for Grades B and 60 steels ranged from 0.46 to 0.79.
- 2.) An important attribute in modeling the failure strength of a metal-plate-connected joint is the ultimate strength of steel.
- 3.) It is possible for a truss plate manufacturer to receive a coil of steel that contains a sample having strength slightly below the minimum specified strength.
- 4.) A truss simulation aimed at evaluating code specified truss test safety factors should include steel that is close to minimum specified strengths. Grade B steel will be modeled using the statistical distribution fit to the ultimate strength data from steel supplier W. The ultimate strength of Grade 60 steel

will be modeled using statistical distribution fit to 37 coil samples of Grade 60 steel.

# CHAPTER V

## MODEL DEVELOPMENT

### INTRODUCTION

Intuition suggests that if the modes of failure for metal-plate-connected joints have safety factors in the range of 1.68 to 2.34, it appears that achieving a safety factor for a truss of 2.0, 2.5, or 3.0 for live and 4.0 for dead loads would be unlikely, especially when the theoretical safety factor for wood is 1.3. One of the difficulties in developing a model that relates joint and lumber safety to truss safety is the method to estimate safety. Although safety factors are specified in the model codes and used in designing trusses (TPI, 1992), it is difficult to quantitatively relate safety factors. Safety factors are calculated differently for different modes of failure, for instance lumber safety factors are based on the fifth percentile; whereas, tooth withdrawal safety factors are based on the mean. The other elements that confound safety factors are different variabilities, or for that matter, different parent distributions. Two modes of failure could have similar safety factors based on the mean, but the joint with the highest COV, assuming a symmetric distribution, will have the largest probability of failure,  $P_f$ . A method to relate safety factors of the components and safety factors of the trusses was developed using a probabilistic format.

Schuëller (1985) presented two simple probability models for estimating the  $P_f$  of a system. Both models were idealized by either considering no correlation between the modes of failure or perfect correlation between the modes of failure. Schuëller suggested that Monte Carlo simulation can be used if including correlation is desirable. Researchers have shown that

to accurately model lumber properties, the serial correlation along the length of the lumber must be included for both stiffness (Kline et al., 1986) and strength (Showalter et al., 1987). Schuëller (1985) also suggested that a model should have minimal mechanical idealizations so the model will obtain acceptance by practicing engineers. There have been many theoretical models that attempted to model the physical behavior of metal-plate-connected joints. All of these models have limitations. More specifically, these theoretical models predict deflection well, for certain loading conditions; however, predictions of the ultimate strength of joints are limited. It is possible that a metal-plate-connected joint is so complex, that a physical model has yet to be developed that accurately predicts the mechanical behavior.

An alternative to the theoretical physical joint behavior models is a probabilistic model based on test data for one or more limiting cases. Gupta et al. (1992) and Zhao et al. (1992) used probabilistic models to study the reliability of metal-plate-connected 2 x 4 wood trusses. These models use statistical distributions to simulate the joint strengths, instead of attempting to model the joints using complex physical models. Both Gupta et al. (1992) and Zhao et al. (1992) successfully modelled trusses for their specific objectives; therefore, this research will build on their ideas. More specifically a probabilistic model will be described that includes the lumber strengths and the joint strengths to aid in modeling metal-plate-connected trusses in a test type environment.

## **GENERATING PROPERTIES FOR THE PROBABILISTIC MODEL**

A model for an entire system is only as good as the probabilistic model that represents each individual component. For the case of wood trusses, the lumber components of the truss

must be adequately modelled as well as the behavior of the joints. Modelling the lumber must include the stiffness of the lumber and the strength of the lumber. The joint model will include strength only. To model the resistance of metal-connector-plates, the tooth withdrawal strength, shear strength and tensile strength will be included to model the different types of potential failure modes.

### **Lumber Strength Properties**

The results of a comprehensive testing program, called the In-Grade study, were recently published by Green and Evans (1987). The main objective of this study was to derive design values using full size, 2-inch nominal dimension specimens, as opposed to the older method of deriving lumber properties from small clear wood specimens. The theory behind this study was that testing full size members should better characterize the end use of the lumber. The lumber properties studied were, the tensile strength, the modulus of rupture (bending strength), compression strength, and the modulus of elasticity in flatwise bending. Green and Evans (1987) fit the two- and three-parameter Weibull, lognormal, and normal distributions to numerous different lumber species, grades, and sizes. The Kolmogorov-Smirnov, Anderson-Darling, and Shapiro-Wilke goodness of fit test statistics were calculated for the four different fitted distributions. The In-Grade study is the definitive work to date; therefore, the results of this study were chosen to be used to model the lumber properties for the truss model.

Kline et al. (1986) and Showalter et al. (1987) showed that to accurately model the strength of a piece of lumber, the serial correlation for both the strength and the stiffness

along the length of the piece must be included. However, since the truss simulation is attempting to model the strength of the entire truss, this more accurate lumber model was not used due to the cumbersome nature of generating small segments within each full piece of lumber. The lumber model assumed that the material properties are constant throughout a single piece of lumber. To simulate building a truss from commercially available lumber, each individual piece of lumber is considered independent. For many trusses, one piece of lumber will span more than one truss panel. The model accounts for a piece of lumber spanning multiple truss panels. This concept will be discussed in further detail in the "Truss Analysis Section" below.

Researchers have shown that correlated strength properties affect the predicted load carrying capacity of members under combined loading situations. Suddarth et al. (1978) examined a single member under combined loading, and Hamon et al.(1985) studied the effect of lumber strength correlations on the reliability of roof trusses. Taylor and Bender (1988) developed a technique that can simulate correlated random variables using a modified multivariate normal approach. The advantage of the Taylor and Bender method is the method preserves the marginal distributions of the random variables, regardless of the distribution, and accurately models the correlation structure. The Taylor and Bender method was used to simulate the compression strength, the tensile strength and the modulus of rupture for the lumber in the simulated test trusses.

One of the requirements of the Taylor and Bender method is the estimate of the correlation structure of the simulated variables. Estimating the correlations, also called concomitance, between the lumber properties is somewhat complex. Since the strength

properties of lumber are derived from destructive test, and a specimen cannot be "broken twice" alternative techniques must be used. Galligan et al. (1979) presented a method that proofloaded lumber to a certain level. If the member did not fail at the proof loading level, the member was then tested in the other failure mode. Using this technique, the researchers could estimate the concomitance of the lumber strength properties. One of the problems with the Galligan research was the estimates of the correlations had very wide confidence intervals. Green et al. (1984) expanded on the Galligan research with a series of Monte Carlo simulations attempting to find a theoretical optimum proof loading level and sample size. One of the more interesting findings of the Galligan research was the estimate for the correlation between the compression and bending strength for southern pine lumber was -0.3; however, the 95 percent confidence interval covered zero (-0.5, 0.1).

The Taylor and Bender method (1988) was used as follows. Compression members under combined loading are influenced by three variables -- the bending strength, the compression strength and the modulus of elasticity. To generate the lumber properties for the top chord of a truss, first by using the goodness of fit statistics, the best fit distributions were chosen from the In Grade data (Greene and Evans, 1987) for the bending strength (B), the compression strength (C) and the modulus of elasticity (E), denoted as  $F_B(x)$ ,  $F_C(x)$ , and  $F_E(x)$ , respectively. Next, the correlation structure between the random variables were estimated. These values were denoted as  $r_{BC}$ ,  $r_{BE}$ , and  $r_{CE}$ . The previous notation represents the correlation ( $r$ ) between B, C and E, depending on the subscript. The correlations estimates involving E were taken from Ross and Pellerin (1994), and the correlation between B and C was assumed to be 0.30 which was identical to the correlation Gupta (1990) used.

Once the best fit distributions are found for B, C and E, the Taylor and Bender method (1988) can be implemented. The following steps were used to simulate the correlated random variables. First a vector of three standard normal random variables was generated using a sampling method from a standard normal distribution (Ahrens and Dieter, 1973). This method required a uniform random number generator; therefore, a random number generator developed by Marsaglia et al. (1990) was used. The random number generator used a combined lagged-Fibonacci generator and a linear congruential generator. Marsaglia et al. (1990) state that this combined generator passes all the standard statistical tests, and all of the latest-more stringent-tests for randomness, and has an incredibly long period of approximately  $2^{144}$ . The Marsaglia et al. (1990) generator was modified slightly to include error trapping. James (1990) gave a suggestion to modify the code to adjust a generated zero to a very small number to prevent possible errors in generating random variables.

The vector of independent standard normal deviates is signified by.

$$\mathbf{Z} = \begin{bmatrix} z_B \\ z_C \\ z_E \end{bmatrix} \sim N(0,1) \quad (5.1)$$

where:

$\mathbf{Z}$  = vector of independent standard normal random variables and  
 $z_i$  = specific random variable for the  $i^{\text{th}}$  strength property.

Once the independent normal deviates are generated, they can be manipulated so they follow the desired correlation structure by multiplying the vector  $\mathbf{Z}$  with a matrix  $\mathbf{C}_r$ . The  $\mathbf{C}_r$  matrix



represents the Cholesky factorization of the correlation matrix, P (capital, Greek  $\rho$ ). Cholesky factorization is also known as "taking the square root" of a matrix (Press et al., 1992). Equation 5.2 represents the relationship between  $C_r$  and P.

$$C_r C_r^T = P = \begin{bmatrix} \rho_{BB} & \rho_{BC} & \rho_{BE} \\ \rho_{CB} & \rho_{CC} & \rho_{CE} \\ \rho_{EB} & \rho_{EC} & \rho_{EE} \end{bmatrix} \quad (5.2)$$

where:

- $C_r$  = a lower triangular matrix representing the Cholesky factorization of the correlation matrix,
- $C_r^T$  = transpose of  $C_r$ ,
- P = correlation matrix, and
- $\rho_{ij}$  = element in P representing the correlation between the  $i^{\text{th}}$  and the  $j^{\text{th}}$  strength property.

The correlations estimated to fill P were similar to Gupta's (1990), which were taken from research literature (Galligan, et al., 84; Green et al., 84; Hoyle, 68). The correlation matrix differs from Gupta's for the value of  $r_{BE}$ . The correlation between B and E was assumed to be 0.65, which was taken from Ross and Pellerin (1994). The entire correlation matrix was assumed to be:

$$\hat{P} = \begin{bmatrix} 1.00 & 0.30 & 0.65 \\ 0.30 & 1.00 & 0.65 \\ 0.65 & 0.65 & 1.00 \end{bmatrix} \quad (5.3)$$

The Cholesky factorization was estimated using a subroutine listed in Numerical Recipes (Press et al., 1992). The requirements for Cholesky factorization are P must be symmetric and

positive definite. The correlation matrix is symmetric since  $\rho_{ij} = \rho_{ji}$ , by definition of linear correlation. Kumar et al. (In Press) presents a method to adjust a non-positive definite matrix to positive definite, so the factorization can be performed. Multiplying the lower triangular matrix,  $C_r$ , with  $Z$ , yields a vector of standard normal correlated variables  $Z^*$ . This operation is represented by:

$$Z^* = C_r Z \quad (5.4)$$

where:

$Z^*$  = a vector of standard multivariate normal random variables.

The steps up to this point have generated a multivariate normal distribution with means of zero and variance equal to one. These steps are fairly routine and are described in more detail by Law and Kelton (1992). The next step is the unique contribution by Taylor and Bender (1988). The vector  $Z^*$  is then converted to a uniform random number,  $U(0,1)$ , that has the desired correlation structure, signified as  $U^*$ . This operation is represented by:

$$U^* = \begin{bmatrix} u_B^* \\ u_C^* \\ u_E^* \end{bmatrix} = \begin{bmatrix} \Phi(z_B^*) \\ \Phi(z_C^*) \\ \Phi(z_E^*) \end{bmatrix} \quad (5.5)$$

where:

$U^*$  = a vector of correlated uniform random numbers,  $U(0,1)$ ,  
 $\Phi(x)$  = normal cumulative density function.

The evaluation of the normal cumulative density function was performed by evaluating:

$$u^* = \Phi(z^*) = \frac{1}{\sqrt{2\pi}} \int_{-\infty}^{z^*} \exp\left(-\frac{x^2}{2}\right) dx \quad (5.6)$$

Equation 5.6 was evaluated by using an identity listed in the IMSL/STAT manual. This identity relates the standard normal function to the compliment of the error function by the following identity.

$$\Phi(x) = 1 - \frac{\text{erfc}(x/\sqrt{2})}{2} \quad (5.7)$$

Where the compliment of the error function is defined by:

$$\text{erfc}(x) = \frac{2}{\sqrt{\pi}} \int_x^{\infty} \exp(-t^2) dt \quad (5.8)$$

The compliment of the error function was evaluated using a Numerical Recipes subroutine (Press et al., 1992), based on the fact the compliment of the error function is a special case of the incomplete gamma function.

Finally, the correlated uniform random numbers were then transformed to the best fit marginal distributions for B, C and T, using the inverse transformation method. Equation 5.9 represents this transformation.

$$\begin{bmatrix} B \\ C \\ E \end{bmatrix} = \begin{bmatrix} F_B^{-1}(u_B^*) \\ F_C^{-1}(u_C^*) \\ F_E^{-1}(u_E^*) \end{bmatrix} \quad (5.9)$$

These steps will simulate random variables that will preserve the integrity of the marginal distributions and will closely approximate the correlation structure.

The previous steps describe the general method to simulate correlated random variables; however, the truss test simulation implemented some improvements to increase efficiency and accuracy. If the chosen marginal distribution is either lognormal or normal, it is unnecessary to evaluate the standard normal cumulative distribution function, Equation 5.6., because the very next step would be to calculate the inverse of the standard normal cumulative distribution function. Therefore, the model only calculated  $\Phi(x)$  when it was absolutely necessary.

Gupta (1990) performed similar steps for the lumber model; however, the researcher used the more general form of the Taylor and Bender method (1988). Gupta used the covariance matrix, as opposed to the correlation matrix in Equation 5.2. Although this procedure more closely follows the original article written by Taylor and Bender (1988), the correlation matrix can be substituted for the covariance matrix. Gupta's method generates numbers from a multivariate normal with non-zero means and preserving the correct covariance structure. The next step for Gupta's model is to convert the multivariate normals to standard multivariate normals with means of zero and variances of one. Since the covariance and the correlation are directly related, the correlation matrix can be used in lieu of the covariance matrix, then the simulated variables are multivariate normals with means of zero and variances of one.

The strength properties for the tension members, the bottom chords of trusses, were generated in a similar fashion; however, the material property vectors were not of length

three. The strength of a combined tension and bending member is a function of the bending strength and the tensile strength, and it is not related to the modulus of elasticity. Therefore, the combined bending and tensile strength properties vectors only consisted of two random variables, modulus of rupture,  $B$ , and tensile strength,  $T$ . The assumed correlation between bending strength and tensile strength was 0.40.

### **Tooth Withdrawal**

Embedding the teeth of a metal-connector-plate into the wood to form a mechanical connection is the main concept of using a truss plate. To assure an adequate joint, the teeth of the metal-connector-plate need to resist tooth withdrawal forces by remaining embedded into the wood members. As the teeth withdraw from the wood, the strength of the joint is diminished. Numerous mathematical models have been used in an attempt to model this physical behavior; however, they are quite complex and limited in their ability to predict the ultimate strengths of the joint.

The design tooth withdrawal forces are based on the contact area of the plate. Two types of contact areas, gross and net, are used for design purposes. As the name implies, a tooth withdrawal strength based on the gross contact area assumes that the entire plate is 100 percent effective against tooth withdrawal forces. The net section tooth withdrawal resistance attempts to account for areas of the joint that are not fully effective. An example of an ineffective area would be the ends of two pieces of lumber for a tension splice joint. The teeth of the MCP do not resist any force within a small distance of the ends of the two pieces of lumber; therefore, the area is excluded from the calculations. The design values submitted to

the building code officials by the truss plate manufacturers will sometimes be based on gross contact area, and sometimes the design values will be on the net contact area, depending on the truss plate manufacturer and the plate configuration. If the contact area is based on the gross contact area, the ineffective area is accounted for by the magnitude of the design value. For example, if design values were listed for both gross contact area, and net contact area, the tooth withdrawal design value for gross area would be smaller than the design value for the net effective area.

The design values for tooth withdrawal are based on short term joint tests. Assuming strength controls the joint test, the design values are based on the average of the short term joint tests divided by 3.0. Tooth withdrawal is a wood failure, not a steel failure; therefore, the design values are subjected to a load duration factor. However, since the loading for a truss test are performed at short load durations, no adjustment to the joint test values will be needed for the truss model. If a model is developed to simulate longer duration loads, for example in-service conditions, the load duration factor would need to be included for the tooth withdrawal of the joints.

The tooth withdrawal strengths will be generated using a scaling technique described by Zhao et al. (1992). This technique extrapolates existing data (for instance Gupta, 1990 or Suddarth et al., 1981) to joints with different configurations. Equation 3.4 defines the Weibull parameters for the Suddarth et al. (1981) data scaled so the mean of the data will be 3.0. By using a Weibull shape parameter of 8.663 and the scale parameter of 3.174, a random number from the Weibull distribution can be generated with a mean of 3.0. By assuming that all metal-connector-plates failing in tooth withdrawal have a similar shape and COV as the Suddarth

et al., (1981) data and have a mean failure load of 3.0 times the design load, the tooth withdrawal strength of any metal connector plate joint can be simulated. The joint simulation is accomplished by multiplying the design load for the particular plate by a random number following the specified Weibull distribution with mean of 3.0. The design values for connector plates can be found in building code reports, for example ICBO report number 2949 (1991) contains tooth withdrawal strengths for several metal connector plates manufactured by TPI members.

### **Steel Properties**

The two potential limiting cases for metal plate connectors that are associated with steel failure are steel net section and steel shear. Both of these failures are related to the ultimate strength of the steel,  $F_u$ . The strength of the plate for the steel net section failure mode is directly related to  $F_u$  of the plate. The relationship between the shear strength and the ultimate strength is reduced by a factor of 0.577. Experimental data for metals indicate that the shearing yield strength is related to the tension yield strength by factors ranging from 0.5 to 0.577 (Boresi and Sidebottom, 1985). The 0.577 factor is commonly associated with an accurate failure criterion known as the maximum octahedral stress. TPI (1992) applied the 0.577 factor to the ultimate strength of steel plates to describe the ultimate shear strength of plates. The application of the 0.577 factor assumes that the factor is valid for the ultimate strength of the metal connector plates.

The steel properties study (Chapter 4) illustrated that samples of Grade B and Grade 60 steel have values greater than the ASTM minimum values for both yield and ultimate

strength. Since the truss model is attempting to model the construction and testing of actual trusses, the simulated metal connector plates should exhibit this type of variability. Therefore, the best fit distributions for the Grade B and the Grade 60 steels were used to model the metal connector plates.

The model generates the steel properties for the plates for each new truss. Since the within-coil variability of steel should be very small (as compared to between-coil variability), all plate strengths from the same coil of steel should be closely related. Therefore it was assumed that all plates of the same category had the same steel strength. For example, all tension splice joints have the same steel properties, and all of the heel joints have the same steel properties. Since plates are produced from coils of steel in batches, it is very likely that plates of the same size in one truss design and production unit would exhibit very similar properties. With this statement, it is assumed that the plates of the same size were produced in the same batch.

## **STRUCTURAL ANALYSES OF THE TRUSS**

Several methods are available to analyze structural systems. Regardless of the method, all methods must estimate the internal forces of all members. Gupta (1990) analyzed the simulated trusses using a finite element analysis procedure. Another method is to use a commercial structural analysis package to predict end forces of the members and use the results in the model. When using the commercial package the end forces are estimated one time; whereas, implementing finite element analysis into the truss test simulation will require the end forces to be calculated for at least the number of trials that will be simulated.



However, when analyzing the truss one time, it is necessary to assume that the modulus of elasticity is constant for the truss configuration, causing all trials of a simulated trusses to have identical end forces, given the same load. Although this effort may appear to be deterministic in nature, the stress analysis of all of the truss members and components will be simulated and analyzed on a probabilistic basis.

Although the end forces are generated using the average design value (book value) of modulus of elasticity,  $E$ , the combined stress analysis treats  $E$  as a random variable. A variable  $E$  has less effect on the predicted end forces than it does on the predicted strength of a long beam-column. Long column strength is dominated by Euler buckling, which is directly related to  $E$ . Therefore, the strength is directly related to  $E$ . The end forces are not directly related. For example, the validation truss, discussed in more detail in Chapter VI, was subjected to a sensitivity analysis to examine the effect of a higher than average  $E$  value on the predicted end forces. The end forces were calculated for the validation truss with all members having an average  $E$ , then the end forces were calculated for a top chord piece of lumber with higher than average  $E$ . An  $E$  value was assumed to be 30% higher than average, and it was in the heel end of one of the pieces of lumber in the top chord (as opposed to the peak end). This 30% increase in  $E$  value resulted in a less than 1 percent increase in the axial force in the first panel (closest to the heel joint), and less than a 12% increase in end force moments. Using a variable  $E$  to calculate end forces was judged to be unnecessary level of model detail for this study.

Zhao et al. (1992) also assumed constant  $E$  of the truss lumber to study the reliability of truss bottom chords using a version of PPSA. The structural analysis package PPSA is an

finite element program that has become the industry standard, and has many years of successful use. One advantage of PPSA as an analysis program is that it estimates, by accepted industry practice, the effective buckling length of the members. The estimated buckling length of the members is based on the stiffness of the ends of the members. The typical design approach is to assume idealized end conditions, either pinned or fixed, and estimate the effective buckling length. PPSA will be used to model the end conditions as rotational springs. The truss test model will use end forces calculated by PPSA4 (Triche and Suddarth, 1993). The credibility (Law and Kelton, 1992) of PPSA4 outweighs the potential value of using any other analysis procedure.

### **Estimating the End Forces**

For each truss studied for this research, two sets of PPSA4 analyses are required. The first analysis simulates loading the member under uniform dead load. This loading is applied to both the bottom and the top chords of the truss. The simulated dead load includes the weight of the lumber, plates, and the design dead load of the truss. The second analysis loads only the top chord of the truss with full design live load. The top chord live load simulates loading the truss with uniform live loads. Actual truss tests can be loaded in at least two ways. The traditional procedure is to load the top of a truss with weight (for instance, bags of soil) until the truss failed. Another method that requires more testing equipment is to place the truss in a test rack that prevents the truss from buckling out of plane. The truss is then subjected to an increasing load using hydraulic rams. The hydraulic rams are spaced fairly

close together (one truss plate manufacturer places them 24 in on-center) to simulate uniform load.

Since PPSA4 performs a linear analysis, end forces for the truss under full design load (dead and live) can be calculated using superposition. The superposition technique allows one to add the end forces caused by the dead loads and the end forces caused by the live loads to predict the end forces caused by full design load. The convenient aspect of using superposition of the dead loads and the live loads is that any multiple of live load can be added to the truss to simulate loading the truss top chord.

The two sets of end forces will be required as input into the truss test model. PPSA4 follows typical finite element notation for end forces (Allen and Haisler, 1985; Cook et al., 1989) and beam notation. Figure 5.1 illustrates the end forces, as well as the beam layout notation used for the remainder of this dissertation.

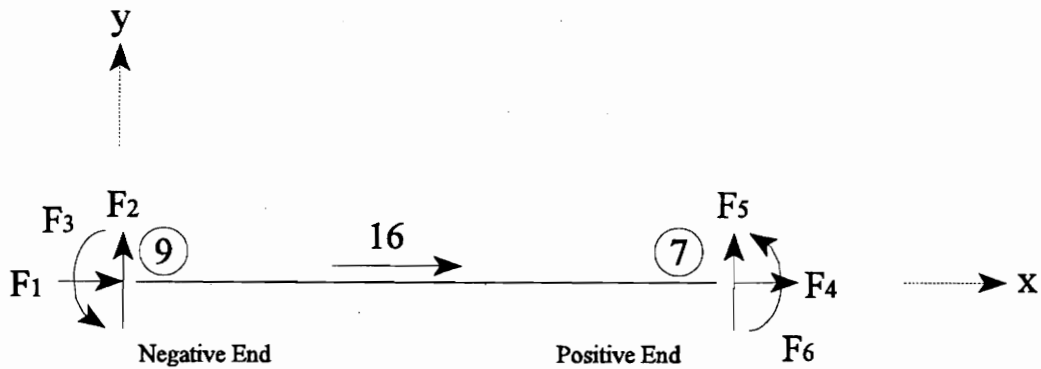


**Figure 5.1 Schematic diagram of a PPSA4 member showing end force notation.**

Figure 5.1 shows the beam having no depth, which is consistent with PPSA4 which assumes the beam elements located at the center lines of the actual beams. The depth of the beam is

accounted for in the stiffness matrix, but the beam element has no depth. There are several important notations illustrated in Figure 5.1. First the arrow above the middle of the beam, pointing right with a number 16 above it, illustrates the beam direction. The positive end of the beam is considered to be the end that the arrow is pointing toward, and the negative end of the beam is considered to be the other end. The number 16 above the arrow is the number of the member. The numbers with circles around them, 9 and 7, are the nodes that define the member ends and how they are connected to other truss members. Therefore, the negative end of beam 16 is connected to node 9, and the positive end is connected to node 7. The numbers 16, 9 and 7 have no special significance, they were used strictly for illustration purposes. The final notation from Figure 5.1 is the end forces, signified by  $F_i$ . The end forces, and loads (not shown) notation used by PPSA4 is strict "right-hand rule" based on the local coordinate system (x,y). The local coordinate system indicates that no matter what the beam angle is in the structural system, when the beam is drawn in local coordinates, the negative end of the beam will be on the left side of the drawing and the positive end of the beam will always be on the right side of the drawing. When the beam is drawn in the local coordinate system, right, upward, and counter-clockwise (CCW) are positive directions for the end forces. The axial forces in the beam are  $F_1$  and  $F_4$  for the negative and positive ends, respectively. The shear forces are  $F_2$  and  $F_5$  and the end moments are  $F_3$  and  $F_6$  for the negative and positive ends of the beam, respectively.

## **Modes of Failure and Failure Criteria**

Boresi and Sidebottom (1985) suggested that two things are required to describe the behavior of structural systems. The possible modes of failure and suitable failure criteria must be defined. The authors of the book were applying these two requirements in the terms of design, which would include an inherent factor of safety, but they are directly applicable to failure models. Developing a failure criteria attempts to relate material properties such as strength to the stresses caused by the applied loading. The following sections contain descriptions of the pertinent failure modes and the failure criteria related to the failure modes of a metal-plate-connected wood truss.

### Modelling Lumber Failures

Before the system can be fully analyzed for wood failures, the distribution of stresses in the truss must be characterized. Not only are the end forces required for live loading and dead loading, but also the boundary conditions of the truss analog are required. These include all of the coordinates of the nodes, the member layout (which member connects to which node), and the magnitude and members the uniform dead and live loads are applied. By using these properties, the internal moments for all members can be characterized along their length by using beam mechanics. There are a maximum of three areas that could possibly have maximum internal forces that must be checked for combined stress interaction in each structural member. These locations are both ends of the beam, and somewhere in the middle of the beam. The axial forces were also estimated at the three potential maximum internal

stress areas. Figure 5.2 illustrates a shear and moment diagram for a typical member of the a truss.

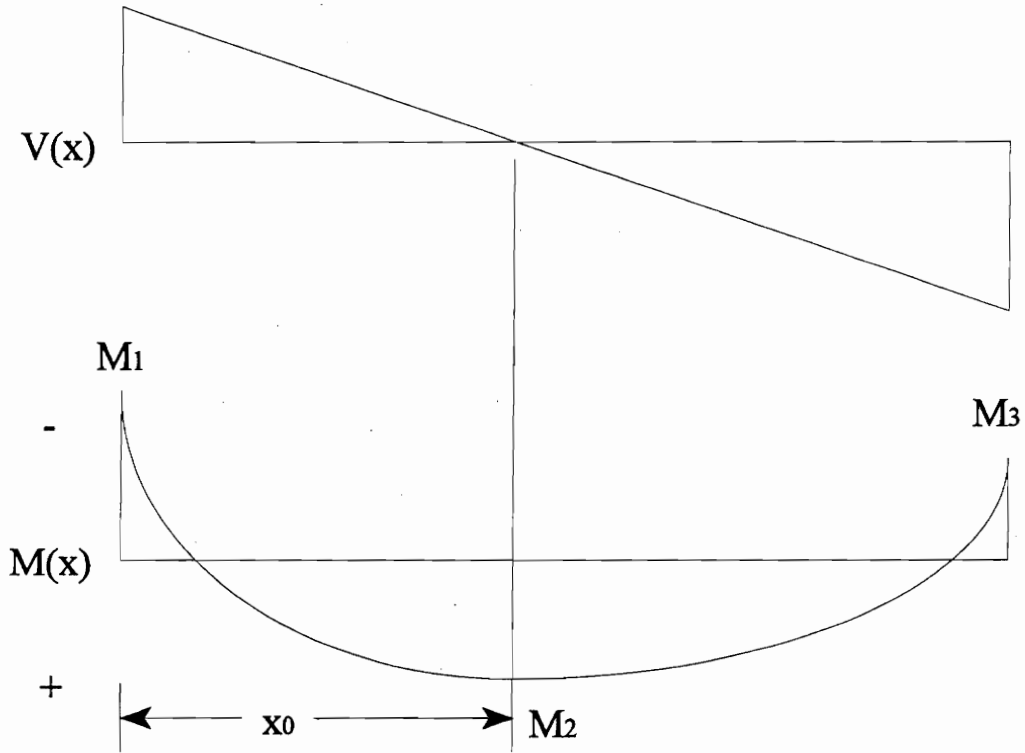


**Figure 5.2 Shear and moment diagrams for a typical truss panel.**

Figure 5.2 illustrates a general moment diagram for truss members caused by the uniform vertical load,  $w$  (note:  $w$  is pointing downward). The end moments  $M_1$  and  $M_3$  in a truss chord will not be equal; therefore they must both be checked. The other potential maximum moment in the beam is located somewhere in between the two ends of the member. The maximum moment can be located by using a relationship between the shear ( $V$ ) and moment ( $M$ ) diagrams along the length of the beam represented by:

$$V(x) = \frac{dM(x)}{dx} \quad (5.10)$$

where:

$V(x)$  = shear along the length of the beam, and  
 $M(x)$  = moment along the length of the beam.

The potential maximum moment will occur when the slope of the moment diagram is equal to zero. This can be found by examining the bending moment in the beam at a location of zero shear. Since one of the assumptions of the truss test model is that the loadings are uniform, this implies that the shear diagram will be linear. Therefore, to estimate the location where the shear diagram is zero, and moment is potentially maximum, can be calculated by Equation 5.11.

$$x_0 = \frac{F_2}{w} \quad (5.11)$$

where:

$x_0$  = distance from negative end of the beam to the potential maximum moment,  
 $w$  = uniform vertical load on the member, and  
 $F_2$  = shear end force on the negative end of the member.

$M_2$  is calculated as follows:

$$\begin{aligned}
 M_2 &= -F_3 + \frac{x_0 * F_2}{2} \\
 &= M_1 + \frac{x_0 * F_2}{2}
 \end{aligned}
 \tag{5.12}$$

where:

- $M_2$  = potential maximum moment,
- $F_3$  = moment at the negative end of the beam, (CCW positive),
- $M_1$  =  $-F_3$ , converted to the more common beam notation, and
- $L$  = length of the member.

The axial forces are also important at the areas of possible maximum moment; therefore, they also were estimated. The axial forces associated with  $M_1$  and  $M_2$  were simply the end forces  $F_1$  and  $F_3$  from the member end forces. The only time a member for the truss test simulation will be subjected to a uniform horizontal load is when the member load is on an angle, for instance the top chord of a pitched chord truss. Since the uniform horizontal load is linear, the axial force at any location in the member can be obtained by using linear interpolation between the two axial end forces.

Once all of the moments and axial forces have been estimated, the internal forces can then be related to the ultimate strength of the members by the appropriate failure mechanisms. The design of members having a combined loading (bending and axial loading) is covered in the NDS (NFPA, 1991). Since these equations are derived for design situations, a safety factor is built into the equations so the designs have an adequate safety margin. To accurately model the failure of a member, the safety factor should be removed. A method that has been



used successfully to model combined failure mechanisms is to use the NDS combined loading equations with ultimate strengths substituted in for design strengths. This substitution removes the safety factor on the strength component. It should be noted that many of the equations in the current NDS do not contain safety factors, because the safety factors are already included in the allowable design properties of the members.

Gupta and Gebremedhin (1992) and Suddarth et al. (1978) used this technique to model bending and tension. Equation 5.13 is similar to the NDS combined loading equation (Equation 3.9-1) with the ultimate tensile strength and the modulus of rupture substituted for the design tensile and the design bending stresses, respectively.

$$\frac{f_t}{T} + \frac{f_b}{B} \geq 1.0 \quad (5.13)$$

where:

$f_t$	=	actual tensile stress,
$T$	=	ultimate tensile strength,
$f_b$	=	actual bending stress, and
$B$	=	modulus of rupture.

$$f_t = \frac{P}{b d} \quad (5.14)$$

where:

$P$	=	axial load in member,
$b$	=	base, or width, of the member, and
$d$	=	depth of the member.

$$f_b = \frac{6M}{bd^2} \quad (5.15)$$

where:

M = internal moment at the point in question.

Equation 5.13 assumes that lateral bending stability is not a potential failure or strength reducing mechanism combined with the tension failure mechanism. Bending stability is not considered pertinent for combined tension and bending because all external members, top and bottom chords, are assumed to be braced laterally by sheathing. Even though some segments of truss lower chords have compression on the top, TPI (1992) does not require an adjustment to bending strength provided that the chord is 2 x 12 or smaller with drywall attached. This assumption simulates the true loading conditions of a truss test. Equation 5.13 was used to model the combined tension and bending loading conditions for the truss test model. The actual tensile and bending stresses will be calculated from the member end forces obtained from the PPSA4 end force calculations. Each tension member is checked at the ends of the member and at the location  $x_0$ . When Equation 5.13 is true (left hand side is greater than or equal to 1.0) the member will be considered failed at that particular location in the member and the truss.

Equation 5.16 will be used to model the failure mechanism of the truss where column buckling is not a factor, for instance the heel-joint region, or panel points.

$$\left(\frac{f_c}{C}\right)^2 + \frac{f_b}{B} \geq 1.0 \quad (5.16)$$

where:

$$\begin{aligned} f_c &= \text{actual compression stress, and} \\ C &= \text{ultimate compressive strength,} \end{aligned}$$

Equation 5.16 assumes that the member is braced at joints so that it can not buckle or twist; therefore, column and beam stability is not a factor, The equation is identical to the NDS equation for a totally braced beam column with the compression strength and bending strengths substituted for the design compression and bending strengths, respectively. Similarly to Equation 5.13, when Equation 5.16 holds true (left hand side greater or equal to 1.0) the member is considered to be failed at the point in question. The actual axial compression  $f_c$  stress found in Equation 5.16 is calculated identically to the axial tension stress, Equation 5.14.

Although the top-chord will be assumed to be braced about the weak axis, as a truss test would be, the top chord can still buckle in the plane of the truss, due to compression, about the strong axis. The NDS combined compression and bending equation is a direct application of research conducted by Zahn (1986). A more general form of Equation 5.16 is Equation 5.17 that also considers combined compression and bending.

$$\left( \frac{f_c}{C'} \right)^2 + \frac{f_b}{\theta_c B'} \geq 1.0 \quad (5.17)$$

where:

$$\begin{aligned} C' &= \text{ultimate compressive strength reduced for slenderness,} \\ \theta_c &= \text{moment modification factor, and} \\ B' &= B \text{ for fully supported members (i.e. top chord of truss during test).} \end{aligned}$$

For the case of the top chord of a truss which is braced from buckling about the weak axis, the modulus of rupture is not adjusted for stability since plywood sheathing does not allow the member between panel points to twist. Failure will be considered in a similar fashion as that used for Equations 5.13 and 5.16.

Equation 5.18 calculates a term needed for Equation 5.17. This equation follows the general format of the original research (Zahn, 1986); however, the equation is very similar to NDS Equation 3.7-1 with C factored out.

$$C' = \frac{C + C''}{2c} - \sqrt{\left(\frac{C + C''}{2c}\right)^2 - \frac{CC''}{2c}} \quad (5.18)$$

where:

- $C''$  = elastic buckling ultimate compressive strength, and
- $c$  = parameter in Ylinen's column formula
- = 0.8 for sawn lumber.

Equation 5.19 gives the Euler buckling strength of a column without a safety factor included. Again this equation is based on research presented by Zahn (1986).

$$C'' = \frac{0.822 E}{\left(\frac{l_e}{d}\right)} \quad (5.19)$$

where:

- E = modulus of elasticity,
- $l_e$  = effective buckling length, and
- d = depth of compression member.

The effective buckling length of the compression member is estimated using PPSA4. This method is used because it considers the stiffness of the end members when calculating effective buckling length. A common way to estimate the effective buckling length is to assume that the ends of the columns are ideally connected (either pinned, free or fixed); however, these idealized connections do not accurately model the end conditions of the beam-columns. Although these idealized assumptions are adequate for design, for this research a more precise method is desired.

Finally Equation 5.20 is used to calculate the moment modification factor (Zahn, 1986).

$$\theta_c = 1 - \frac{f_c}{C''} \quad (5.20)$$

Although the Zahn (1986) ultimate strength equations may appear very different from the design equation represented in the NDS, the only real difference is the NDS uses allowable design properties instead of ultimate strengths, and the Euler buckling equation (Equation 5.19) contains a factor applied to the modulus of elasticity, E. This factor converts the average E found in the NDS equations to a shear free fifth percentile E. Since visually graded lumber and machine stress rated (MSR) lumber have different variabilities for E, the NDS adjustment factors differ for the two types of grading. The ultimate Euler buckling equation does not distinguish between visually graded lumber and MSR graded lumber.

Equation 5.17 is the more general form between Equations 5.14 and 5.16; therefore it was used for all cases. When a compression member cannot buckle, for instance in the heel

joint region, the buckling length,  $l_b$ , was set to zero. If the buckling length is set equal to zero, Equation 5.17 is identical to Equation 5.16.

Equations 5.16 and 5.17 have the compression term of the equation squared. Zahn (1986) fit both a squared term and a linear term of the compression equation to historical test data. The researcher found that the squared compression term of the combined stress equation fit the data better than the linear compression term; however, no theoretical justification was given for squaring the compression term. The NDS also compares actual compression stresses to adjusted allowable compression stresses, not the squares. Therefore, for the case of pure compression, the truss test simulation used a linear compression equation. Equation 5.19 represents this failure criteria.

$$\frac{f_c}{C'} \geq 1.0 \quad (5.21)$$

Pure axial compression stress only occurs in the webs of trusses, since the ends of the members were assumed to be pinned. The truss plates that are used to connect the webs to the truss chords are typically small. These small metal connector plates cannot transfer large moments from the top and bottom chords of a truss into the webs. Therefore, the end conditions for webs in the truss test model were assumed to be pinned.

### Modelling Heel Joint Failures

Checking the heel joints in the truss for failure is similar to checking the truss for lumber failures. The end forces in the plated area are compared to the estimated ultimate

strength for the particular failure modes. The relationship between the heel joint strengths and the heel joint forces are related by using failure criteria. Figure 5.3 is a schematic diagram of a heel joint for a pitched chord truss with slope  $\theta$ , and an angle between top and bottom chords,  $\phi$ .

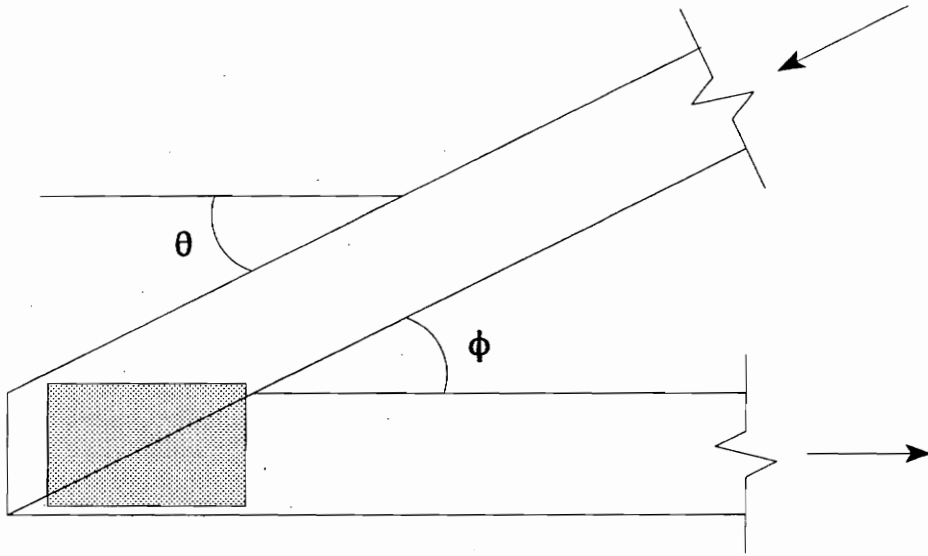


**Figure 5.3** Schematic view of a heel joint in a pitched chord truss.

First, it should be noted that the angle  $\phi$  is not necessarily the same angle as  $\theta$ . The angle  $\phi$  represents the angle between the top and the bottom chord; whereas, the angle  $\theta$  represents the top chord slope. In Figure 5.3, the two angles are equal; however, in some cases they will not be, for instance the bottom chord in a scissor truss is also pitched; thus, the angles would not be equal. The shaded rectangle in the bottom right corner represents the metal connector plate. Figure 5.4 is a closeup view of the metal connector plate with the forces that must be

resisted by the plate and the dimensions of the plate that will be used in calculating the ultimate strength for the different failure modes.

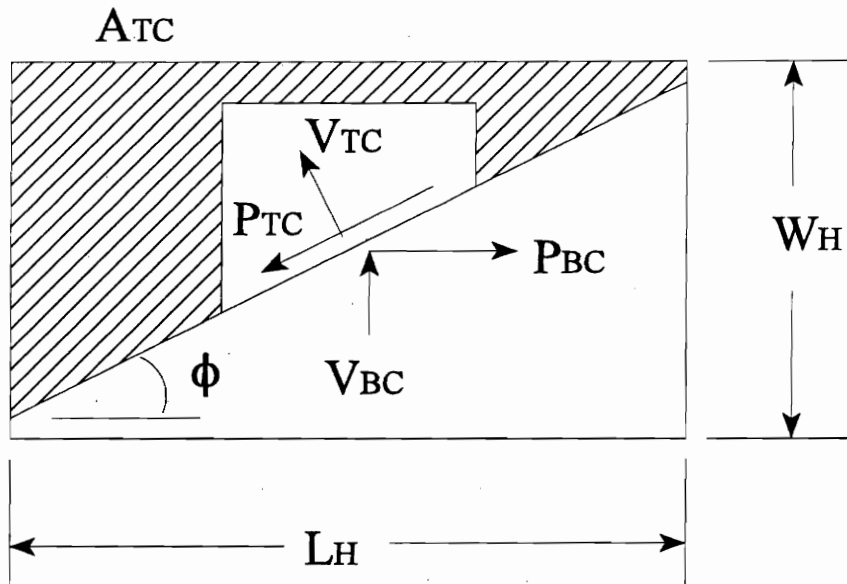


**Figure 5.4** Close up view of a truss plate used for a heel joint of a pitched chord truss.

The arrows in the middle of the truss plate represent the forces that must be resisted by the truss plate. The arrows labeled  $P_{BC}$  and  $P_{TC}$  represent the axial forces in the bottom chord and top chord, respectively. Similarly, the arrows labelled  $V_{BC}$  and  $V_{TC}$  represent the shear forces in the bottom chord and top chord respectively. The axial forces and the shear forces are the end forces for the members that represent the top and bottom chords from the PPSA4 output. The length and depth of the MCP heel plate are shown as  $L_H$  and  $W_H$ , respectively. These dimensions are used to calculate the strength of the plate. Finally, the shaded region in Figure 5.4 represents the contact area for the tooth withdrawal, which is



directly related to the length and the width of the plate. Figure 5.4 only shows the contact area on the top chord,  $A_{TC}$ , but there is also an area on the bottom chord,  $A_{BC}$ . When the plate is symmetrically located on the joint, the two areas will be equal.

Each heel joint was checked for four different failure modes: shear failure of the steel plate, net section tension failure of the steel plate, tooth withdrawal due to compression (Top chord), and finally tooth withdrawal due to tension (bottom chord). The shear failure of the plate was assumed to fail along the length where the bottom chord and top chord intersect. The shear length of the plate can be calculated as follows:

$$L_v = \min \left( \frac{L_H}{\cos \phi}, \frac{W_H}{\sin \phi} \right) \quad (5.22)$$

where:

- $L_v$  = shear length of the plate,
- $L_H$  = length of the heel plate,
- $\phi$  = the angle of the plane formed by the intersection of the top and bottom chords.
- $W_H$  = depth of the heel plate.

The failure criteria is based on the fact that the predicted shear strength of the joint must be greater than the shear force caused by the compressive stress,  $P_{TC}$ . To be consistent with the lumber failure criteria, the failure condition can be expressed as a ratio of the load and the shear strength, represented by Equation 5.23.

$$\frac{P_{TC}}{2 * (0.577 * F_u * L_v * t * e_v)} \geq 1.0 \quad (5.23)$$

where:

$P_{TC}$	=	axial load in the top chord member in the heel joint region (lbs),
$F_u$	=	simulated ultimate strength of the steel (psi),
$L_v$	=	length of the shear plane for the MCP (in),
$t$	=	thickness of the plate (in),
$e_v$	=	allowable design shear efficiency ratio, and

The load  $P_{TC}$  acts parallel to the shear plane; therefore, it is shear load that the joint must resist. The denominator of Equation 5.23 represents the strength of the plate. This is the ultimate shear strength of the steel ( $0.577F_u$ ), multiplied by the effective shear area ( $L_v * t * e_v$ ), multiplied by 2, for the fact that there are plates on both sides of the heel joint. The thickness of the plate ( $t$ ) and the allowable design shear efficiency ratio  $e_v$  can be found in building code reports, for the plates being simulated, for example BOCA (1991). The thickness of the plates will be listed as a gauge number, but the decimal equivalent for steel sheets can be found in ASTM A524 (1993b).

The steel net section criteria is similar to the shear criteria. The force perpendicular to the shear plane is compared to the estimated ultimate tensile strength of the plate for steel net section. Equation 5.24 represents this failure criteria.

$$\frac{P_{BC} \sin \phi + V_{BC} \cos \phi}{2 * (F_u * L_v * t * e_t)} \geq 1.0 \quad (5.24)$$

where:

$P_{BC}$	=	axial load in the bottom chord member in the heel joint region (lbs),
$V_{BC}$	=	shear load in bottom chord member in the heel joint region (lbs), and
$e_t$	=	allowable design tensile efficiency ratio.

The numerator of Equation 5.24 transforms the shear load and the axial load in the bottom chord to a resultant tensile stress in a plane normal to the shear plane. The denominator of Equation 5.24 represents the ultimate tensile strength of the MCP. The effective design tensile efficiency ratio can be found in building code reports (BOCA, 1991).

Tooth withdrawal is another possible failure mode of the heel joint. TPI (1992) specifies a reduction factor that is used for tooth withdrawal values. This equation takes into account the ineffective end and edge distances in the heel joint region. This reduction factor is represented by Equation 5.25.

$$H_R = 0.85 - 0.05 * (12 * \tan \phi - 2.0) \tag{5.25}$$

$$0.65 \leq H_R \leq 0.85$$

where:

HR = TPI heel reduction factor for tooth withdrawal, and  
 $\phi$  = the angle of the plane formed by the intersection of the top and bottom chords.

The forces that will cause compression tooth withdrawal are both the axial force and the shear force in the top chord member. One method to include the effects of both of these forces is to take the resultant of the forces and compare them to the predicted tooth withdrawal strengths. Equation 5.26 is the failure criteria for heel joint tooth withdrawal due to compression.

$$\frac{\sqrt{P_{TC}^2 + V_{TC}^2}}{2 * (TW * H_R * A_{TC})} \geq 1.0 \tag{5.26}$$

where:

- $P_{TC}$  = axial load in the top chord member in the heel joint region (lbs),
- $V_{TC}$  = shear load in top chord member in the heel joint region (lbs),
- $TW$  = simulated tooth withdrawal strength (lbs per square inch contact area),  
and
- $A_{TC}$  = contact area of the plate on the top chord member (in<sup>2</sup>).

The numerator takes into account the resultant force vector from the axial component and the shear component. The denominator in Equation 5.26 represents the tooth withdrawal strength over the effective area. The 2 in the denominator accounts for plates on both side of the joint. The contact area of the plate,  $A_{TC}$ , can be calculated using simple geometry. If the plate is symmetrically placed on the heel joint, the contact area will be half of the area of the plate.

The final failure mode checked for the heel joint in tooth withdrawal due to tension.

The forces that contribute to the tension withdrawal are the bottom chord axial force and shear force. The same methodology that was used to develop Equation 5.25 was used to develop failure criteria 5.26.

$$\frac{\sqrt{P_{BC}^2 + V_{BC}^2}}{2 * (TW * H_R * A_{BC})} \geq 1.0 \quad (5.27)$$

where:

- $P_{BC}$  = axial load in the bottom chord member in the heel joint region (lbs),
- $V_{BC}$  = shear load in bottom chord member in the heel joint region (lbs),
- $A_{BC}$  = contact area of the plate on the bottom chord member (in<sup>2</sup>).

The numerator and the denominator of equation 5.27 is almost identical to equation 5.26.

When Equations 5.23, 5.24, 5.26 and 5.27 yield ratios greater than one, they represent failure

due to steel shear, steel net section, tooth withdrawal due to compression, and tooth withdrawal due to tension, respectively, for metal-plate-connected heel joints in a wood trusses.

### Modelling Tension Splice Joint Failures

One of the advantages of using wood trusses is the fact that large clear spans are possible. As truss length increases, splice joints must be used to connect multiple pieces of lumber together. Figure 5.5 is a schematic diagram of a tension splice joint that could be found in the bottom chord of a truss.

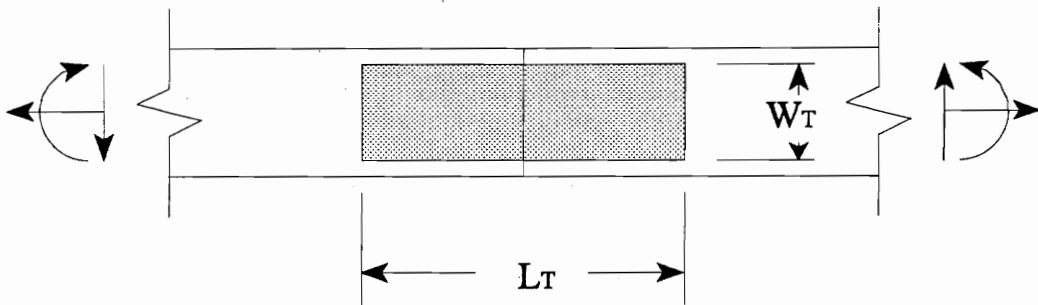


**Figure 5.5** Schematic view of a tension splice joint.

Figure 5.5 illustrates a tension joint that has been removed from a truss with end forces applied. The length of the tension plate is denoted by  $L_p$  and the width of the plate is labeled  $W_T$ . These dimensions will be used in developing strength criteria for the plate.

The tension plate failure criteria are similar to the heel joint failure criteria. The plates must resist steel net section failures and tooth withdrawal due to tension failures, very similar

to the heel joints. Figure 5.6 is a detailed view of the left half of the tension splice joint with the axial force, shear force, and moment applied to the plate.

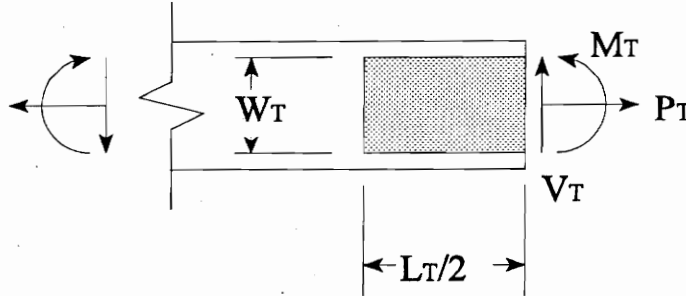


**Figure 5.6 Detailed view of half of the tension splice joint with forces applied.**

The first critical mode discussed is the plate failing in net section. For this failure mode, only the axial force,  $P_T$ , will be considered as contributing to steel net section. The local effects of bending stresses in the plate were ignored. The failure criteria is expressed by Equation 5.28.

$$\frac{P_T}{2 * (F_u * W_P * t * e_t)} \geq 1.0 \quad (5.28)$$

where:

- $P_T$  = axial force resisted by the tension joint (lbs), and
- $W_P$  = width of the tension plate (in).

Since the steel net section criteria is similar for heel joints and tension joints, Equation 5.28 is almost identical to Equation 5.24. There is no need to project the forces onto a plane

because the axial force is already normal to the failure plane. Secondly, the length of the failure plane is known and equal to the width of the plate,  $W_p$ .

The combined effects of tension and bending have been studied by several researchers (Wolfe et al., 1991, Wolfe, 1990; Gupta, 1994). These researchers developed failure criteria for splice joints loaded in combined tension and bending; however, their interaction equations were joint specific. Although these models fit specific joint data fairly well, no suggestion was given on how to extend the interaction equations to other tension joints. Another method to model the combined effect of bending and tension would be to use established engineering methods, such as mechanics of materials, to make simplifications so that a joint loaded under general conditions can be compared to joints that have been studied in great detail. The method used to model tooth withdrawal for splice joints loaded under tension and bending was similar to the method used to model tooth withdrawal in the heel plate region. All of the end forces were combined into one load vector, and the load vector was compared to the simulated joint strength; however, the moment is considered as a contributing factor in tooth withdrawal. The moment in the joint can be converted to an equivalent couple, as illustrated by Figure 5.7.

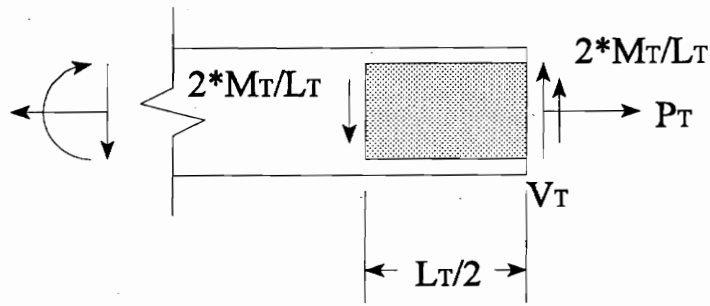


**Figure 5.7** Detailed view of half of the tension splice with the moment converted to an equivalent coupled force.

The magnitude of the moment is divided by half the length of the metal connector plate. Then one of the force couples is applied at the end of the plate, and the other force couple is applied at the end of the lumber, which corresponds to the middle of the plate. Once the force couple is applied, the resultant force can be found using vector mechanics. Equation 5.29 is the failure criteria for tooth withdrawal of a tension splice joint.

$$\frac{\sqrt{P_T^2 + \left( V_T + \frac{2 \cdot M_T}{L_T} \right)^2}}{2 \cdot (TW \cdot A_T)} \geq 1.0 \quad (5.29)$$

where:

- $V_T$  = shear force resisted by the tension joint (lbs),
- $M_T$  = moment resisted by the tension joint (in-lbs),
- $L_T$  = length of the tension plate(in), and
- $A_T$  = effective area of the tension plate (in<sup>2</sup>).



Equation 5.29 is very similar to equation 5.27, which would be expected since the same methodology was used to develop the two. One of the main differences is the fact that the effective area of the plate is not necessarily half of the plate area. If the tooth withdrawal strength used is based on the gross area, then the effective area of the plate is equal to half of the plate area. If the net section method is used to estimate the tooth withdrawal strength, then the effective area of the plate will be less than half of the area of the plate. Building Code reports (for instance BOCA, 1991) state which area was used when determining the tooth withdrawal strength of the plate.

### Modelling Compression Splice Joint Failures

Developing failure criteria for the compression splice joints is almost identical to the failure criteria used for the tension splice joints; however, there are a few differences. Failure of the plate in steel compression was not considered as a possible failure mode for two reasons. First, the plates are thin, causing a buckling failure mode. Stability problems are traditionally considerably more complex than simple net section fracture problems. Since no truss tests in the literature have reported problems with buckling of the compression splice plate, this complex problem was considered minute in the grand scheme of the truss test model; therefore this potential mode of failure was ignored. Secondly, when a splice joint is loaded in compression, some of the compression forces are transferred across the joint due to wood-to-wood bearing. This is not the case for tension failures. The true relative contribution of the wood-to-wood bearing is unknown, and it depends on several factors. For instance, the modulus of elasticity of the two wood members in the joint, and how tight the

joint was constructed. Hoyle and Woeste (1989) recommend that for the design of compression joints, if the joint is well constructed, 50% of the compression stress can be assumed to be resisted by wood-to-wood bearing. With this assumption, the failure criteria for tooth withdrawal of compression joints can be estimated by Equation 5.30.

$$\frac{\frac{1}{2} * \sqrt{P_C^2 + \left( V_C + \frac{2 * M_C}{L_C} \right)^2}}{2 * (TW * A_C)} \geq 1.0 \quad (5.30)$$

where:

- $P_C$  = axial force resisted by the compression joint (lbs),
- $V_C$  = shear force resisted by the compression joint (lbs),
- $M_C$  = moment resisted by the compression joint (in-lbs),
- $L_C$  = length of the compression plate(in), and
- $A_C$  = effective area of the compression plate (in<sup>2</sup>).

The ½ in the numerator of equation 5.30 represents the 50 percent reduction of the resultant force due to wood-to-wood bearing. The two in the denominator of the equation is based on two plates. As with the tension splice joint, the effective area  $A_C$  is not necessarily half of the area of the plate.

### Modelling Peak Joint Failures

The next joint in the truss test model that was considered as a possible failure was the peak joint. The peak joint, also known as the crown joint, occurs in pitched chord trusses. Figure 5.8 is a schematic diagram of a peak joint taken from a truss

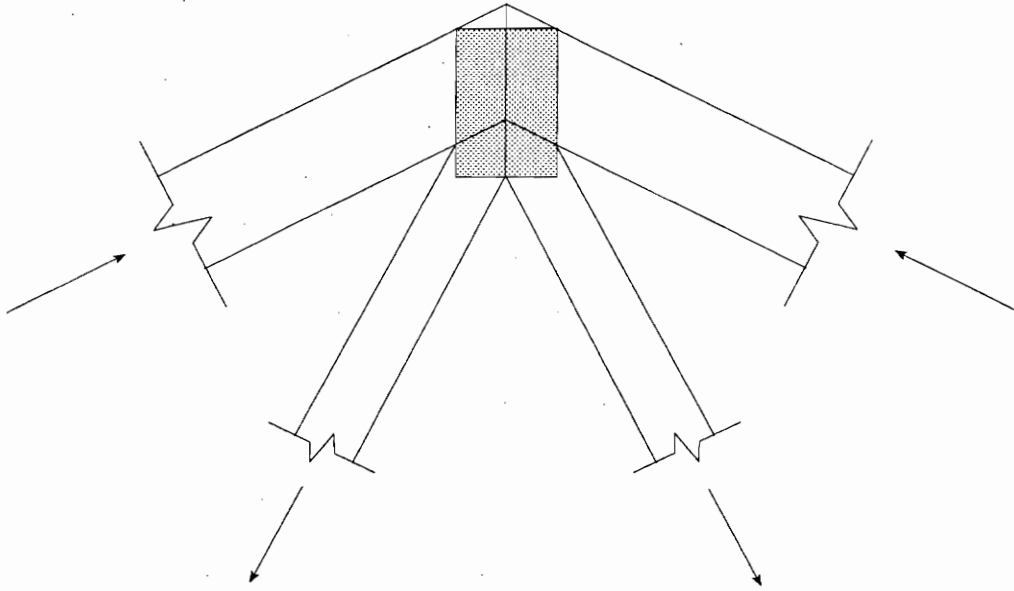


**Figure 5.8** Schematic view of a peak joint in a pitched chord truss.

Figure 5.8 shows compression forces going into the peak plate from the top chord, and tension forces from the bottom chord. Figure 5.9 is a more detailed view of the plate with the axial, and shear loads.

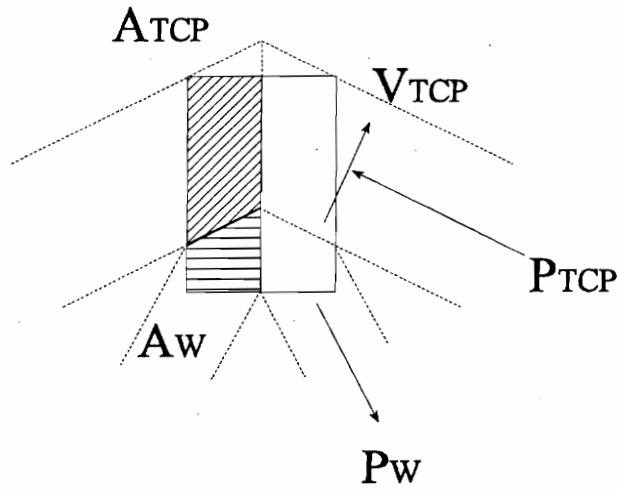


**Figure 5.9** Expanded view of the plate with the pertinent forces for possible failure modes.

The shaded areas  $A_{TCP}$  and  $A_W$  are the effective contact areas of the plate for the top chord and the webs, respectively. There is no general mathematical definition of these areas; therefore, they must be calculated using geometric properties for each truss. Assuming that the plate is symmetrically placed, the effective areas for both webs will be equal and the effective contact area of both top chords will be equal. The axial forces  $P_{TCP}$  and  $P_W$ , represent the compression force in the top chord, and the tension force from the webs, respectively. The shear force  $V_{TCP}$  is the shear force induced into the peak plate from the top chord of the truss. There is no shear from the webs, since the ends are considered pinned and there are no loads applied directly to the webs, only axial forces. There are also no moments on the ends of the

members, because it is assumed that no moment is transferred by the small plates typically used at the peak joint. The failure criteria for tooth withdrawal is very similar to the heel joint, tension splice joint, and compression joints, and is defined by:

$$\frac{\sqrt{P^2 + V^2}}{2 * (TW * A)} \geq 1.0 \quad (5.31)$$

where:

- P = the axial force in the top chord or the web,
- V = shear force in the top chord or the web (V = 0 for webs),
- TW = simulated tooth withdrawal strength and
- A = effective contact area on the top chord or web.

Equation 5.31 is more general than the other tooth withdrawal equation. This generality implies that the tooth withdrawal failure criteria equation is calculated exactly the same for both the compression loads due to the top chord and the tensile loads due to the webs. The equation takes the resulting force of the axial force and the shear force; however, for the web members, the shear force is zero. Secondly the equation assumes that no compressive force is transferred through the top chords. This assumption is conservative, but since the top chords have a large change in the angle, less compressive force would be transferred through the joint due to wood-to-wood bearing than would occur on a splice joint.

The other possible failure mode at the peak joint is fracture of the steel due to combined tension and shear. Figure 5.18 illustrates two lengths  $L_1$  and  $L_2$  that define the potential tension-shear failure path.

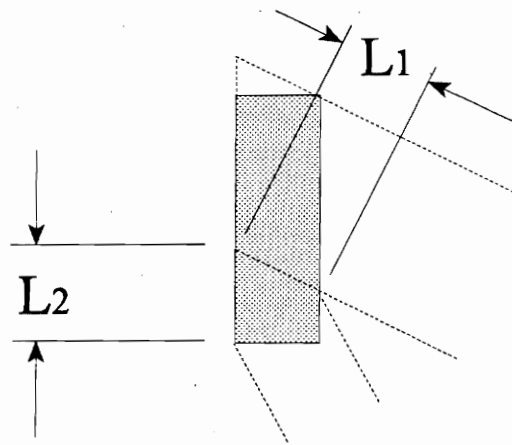


**Figure 5.10** Graphical representation of the lengths  $L_1$  and  $L_2$ .

Since it is not known which direction the combined tension-shear failure will occur, both must be checked. The two failure criteria are defined by:

$$\frac{P_w}{2 \cdot (0.577 \cdot L_1 \cdot e_v + L_2 \cdot e_t) F_u \cdot t} \geq 1.0 \quad (5.32)$$

$$\frac{P_w}{2 \cdot (L_1 \cdot e_t + 0.577 \cdot L_2 \cdot e_v) F_u \cdot t} \geq 1.0 \quad (5.33)$$

where:

- $P_w$  = axial force in the web (lbs),  
 $L_1$  = length of the plane defined by the intersection between the web and the top chord (in), and  
 $L_2$  = length of the plane defined by the intersection between the webs (in)

Equation 5.32 assumes that the steel fracture occurs in the shearing mode along the plane between the web and the top chord of length  $L_1$ , and has a tension failure along the plane defined by the intersection of the two webs of length  $L_2$ , simultaneously. Equation 5.33 assumes that the shearing failure occurs across  $L_2$  and the tension failure occurs across  $L_1$ .

### Modelling Web Joint Failures

The final joint in the truss test model that was analyzed was the web joint. The web joints were modelled identically to the peak joints. The assumed failure modes of the web members were tooth withdrawal and a combined tension and shear net section fracture, similarly to the peak plate. The compression members in the web region were assumed to only fail in the tooth withdrawal mode, also similar to the peak plate.

## **SIMULATED LOADING OF THE TRUSS**

To simulate the live loading of the truss, a loading scheme and a stopping criteria for when the truss has failed are required. The stopping criteria was considered any time any failure equations in the previous section exceeded one. The location and the failure mode were recorded. All trusses were analyzed twice with PPSA4. One of the output files from PPSA4 represented the end forces that would be generated by loading the truss with uniform

dead loads. The uniform dead loading is applied to both the top and bottom chords. The other PPSA4 output file contained the end forces from loading the top chord with the design live loads. This step is to simulate actual testing conditions, by loading the top chord of the truss with live load. TPI (1993) suggest that actual truss tests should be loaded to design dead load, then the design live load should be applied at increments of 0.1 times the total design live load until the truss is fully loaded. The full design load should be held for at least five minutes, then the load should be increased in increments of no more than 0.1 times the full design load, until the truss fails.

A truss test model could simulate incrementally loading the truss at 0.1 times the total load, until a failure occurs. This method has one disadvantage. If an precise measurement of failure load is required, a smaller increment would be needed, requiring many iterations. The truss test model used during this research implements a secant method to find the load required to fail the truss. All the lumber and joints in the simulated truss are first checked for failure at dead load. Checking for dead load assumes that the multiple of the live load is zero ( $MLL_0 = 0.0$ ). The maximum failure criterion ratio is recorded as  $CSI_0$ . The next iteration simulates applying one half of the live load on the truss ( $MLL_1 = 0.5$ ). Mathematically, the model checks the joints and the lumber for the internal forces caused by applying full dead load and half of the live load. The maximum failure criterion is recorded as  $CSI_1$ . The next multiple of live load is estimated using the secant method.

$$MLL_{i+1} = MLL_i - \frac{(1 - CSI_i)(MLL_{i-1} - MLL_i)}{CSI_{i-1} - CSI_i} \quad (5.34)$$



where:

$MLL_i$  = the multiple of live load applied to the truss at the  $i^{\text{th}}$  iteration.  
 $CSI_i$  = the combined stress index factor at the  $i^{\text{th}}$  iteration.

Chapra and Canale (1988) suggest that the secant method can be divergent for some functions; therefore, the method will stop after 30 iterations. The stopping requirement for the secant method is when the maximum combined stress index is within  $\pm 0.0001$  of 1.0. Although this criteria may seem tight, all trusses studied failed within 5 iterations. The secant method is based on estimating the multiple of live load that is required to reach a CSI equal to 1.0. The method considers the last two iterations for the next estimate, implying that the increment is based on a linear approximation. Since many of the failure modes are linear, the secant method finds the load required to fail the truss with very few iterations, even for a tight stopping criteria. The secant method proved to be a computationally efficient way to estimate the failure load of the truss.

## MODEL ASSUMPTIONS

Several assumptions were made for the model. Some of them were simplifying assumptions and some were made to reflect true truss test. These assumptions are:

- 1.) The top chord and bottom chord are laterally restrained from buckling out of plane; however the top chord can buckle in plane. The compression webs are free to buckle out of plane. These assumptions reflect actual truss tests.

- 2.) The lumber properties are constant within a piece, but lumber spanning multiple panels were considered as one piece. Each web was considered an individual piece of lumber. More accurate lumber property models were deemed too cumbersome for this model.
- 3.) For calculating the end forces, the modulus of elasticity was assumed to be constant for all members in a truss configuration. This simplifying assumption was required so the end forces could be calculated using PPSA4. For each trial in the truss configuration E was simulated for the top chords and the webs, since the strength of columns are related to E.
- 4.) The correlations between B, C and E were included to model the strength of top chord members using the Taylor and Bender (1988) modified multivariate normal method to generate random deviates. The correlation between B and T was simulated using the same method.
- 5.) Metal connector plates of the same size and thickness, have the same material properties. For instance, all heel joints in one truss trial are considered to have the same steel properties.
- 6.) No moment is transferred into the webs from the truss chords, and no moment is carried through the peak joint.

# CHAPTER VI

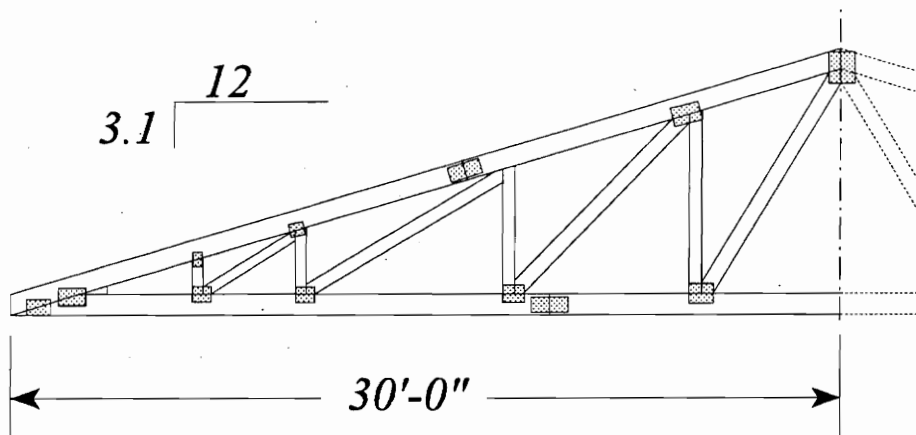
## MODEL VERIFICATION AND VALIDATION

### INTRODUCTION

Before a model can be used extensively, the model should be verified and validated. The process of verification is conducted by determining if the model is performing as intended (Law and Kelton, 1991). Verification can also be thought of as "debugging" the model. Although the idea of model verification may seem trivial, it is an important step that must be accomplished before the model can be validated.

The validation procedure is concerned with determining if the model accurately represents reality (Law and Kelton, 1991). This procedure is commonly accomplished by comparing the model to independent results or known results. A boundary of possible truss safety factors are known. If the model consistently predicts truss safety factors less than 1.0, the model is not representing reality because properly constructed trusses very seldom if ever fail below design load. The same argument holds for an unreasonable upper bound on the truss safety factor.

A truss plate manufacturer provided the author and his major advisor a very detailed test report. The following is a general test description of the truss, without releasing the test results. Figure 6.1 is a diagram of the left half of the test truss.



*Note: Drawing not to scale*

**Figure 6.1 Schematic diagram of a truss used for verification and validation of the truss test model.**

Figure 6.1 only shows half of the truss since the truss is symmetric about the centerline. The tested trusses were 60 ft in length. The truss had a top chord slope of 3.1 in 12. The top chord had one compression splice plate, and the bottom chord had one tension splice plate. The heel joints were double plated. All of the diagonal webs were constructed of 2 x 6 southern pine MSR grade 2250f-1.9E except for the shortest diagonal web which was constructed with 2 x 4 southern pine No. 2 KD15. All of the vertical webs were constructed with No. 2 southern pine 2 x 4s. The top chord was constructed from southern pine Dense Select Structural 2 x 10. The bottom chord was constructed from southern pine MSR grade 2250f-1.9E 2 x 10. Before the fabrication of the trusses, the truss plate manufacturer measured and recorded the modulus of elasticity of all truss chord members.

The two heel plates were 12" x 12" and 12" x 13.3", and the peak plate was 12" x 13.3". The tension splice plate was a 8" x 14", with a special punching pattern of the teeth for high tensile regions, and finally the compression splice joint was an 8" x 10" plate. Table 6.1 lists the plate values used by the truss test simulation for the validation truss.

**Table 6.1 Plate values used for the validation truss.**

Location	L	W	TW <sup>a</sup>	Steel Grade	t	e <sub>t</sub>	e <sub>v</sub>
	(in)	(in)	(psi) <sup>b</sup>		(in)		
Heel Joint	12.0	12.0	249.	B	0.0635	0.591	0.548
	12.0	13.3	249.	B	0.0635	0.591	0.548
Tension Splice	8.0	14.0	200.	B	0.0635	0.625	0.420
Compression Splice	8.0	10.0	200.	B	0.0635	0.560	0.340
Peak	12.0	13.3	249.	B	0.0635	0.591	0.548

<sup>a</sup> Tooth withdrawal values are based on gross area, unless otherwise noted.

<sup>b</sup> Pounds per square inch, contact area.

The validation truss was analyzed with a dead load applied to the top and bottom chord of 7.25 plf. This load represented the dead load weight of the truss, and the test equipment. The live load applied to the top chord was 258.5 plf. Although the test report did not specify, it appears that the truss was designed for a 30 psf top chord load, with truss spacing of 8 ft on center.

The PPSA4 analog for the heel joint was a series of four fictitious members (Hoyle and Woeste, 1989). The ends of the webs located on the bottom chords were also modelled as fictitious members. These fictitious members were used to model the lumber between the

center line of the members, as modelled by PPSA4. They were also used to model the eccentricity of the heel joint. An analog was developed that used the E of the top and bottom chords. The truss plate manufacturer's report included bottom chord deflections at certain loading levels. By using these deflections, the fictitious members were manually calibrated until the predicted deflections using PPSA4 closely matched the deflections measured during the truss test.

## **MODEL VERIFICATION**

Before the model could be validated, the model was tested to see if the simulated values were as expected. First the lumber strength properties were checked. Histograms of the lumber properties were visually compared to the simulated lumber properties, and the correlations between the simulated strength properties were calculated. The histograms of the simulated lumber properties were very similar to the density functions of the parent distributions; therefore, they were deemed to be generated properly. The correlation structure of the strength properties were also very close to the desired correlation structure. The same procedure was used to check the simulated tooth withdrawal strengths and the steel ultimate strengths.

The lumber failure criteria was checked as follows. The Euler buckling equation was changed so a safety factor was included. This step in effect transforms the failure criteria for combined bending and compression similar to the NDS design equation except the design values for the lumber are substituted with the simulated ultimate strength values. The safety factor in the Euler buckling equation was added by using the design factors specified by the

NDS. These factors differed for the visually graded lumber and the MSR graded lumber. Trusses were then simulated using the truss test model. The joints in the truss were adjusted so they could not control the truss failure; thus, forcing only lumber failures. The truss model then calculated the multiple of live load that would be required to make one of the lumber failure criteria equal to 1.0. Once the truss had "failed", the generated strength properties of the lumber, the multiple of live load factor, and the location of the failure was output to a file.

Next PPSA4 analyses were conducted with the dead load plus the multiple of live load applied to the truss. The simulated ultimate strengths were substituted for the design strengths used by PPSA4. The failure mode matched the failure mode predicted by the model, and the combined stress index calculated using PPSA4 was 1.0. This verification procedure was performed for several different failure locations, and the predicted failure locations predicted by PPSA4 always matched the truss test model. The maximum lumber CSIs calculated by PPSA4 were always 1.0.

This verification checked for two things. First, the superposition technique used by the model, i.e. combining end forces calculated for dead load, and some multiple of live load, is valid. Recall that the truss test model uses end forces calculated from two PPSA4 analyses, but the verification procedure used only one PPSA4 analysis with the dead and the multiple of live load applied to the truss analog. Secondly, the strength criteria used by the model is correct, or at least it is correct using the Euler buckling equation with a safety factor. After the lumber model was verified, the Euler buckling safety factor was removed from the model to simulate true compression failure.

The failure criteria for joints were verified by a hand example. One truss was simulated, and the end forces were output for the appropriate members. The failure criteria from Chapter V were then calculated for both heel joints, the peak joint, the two tension splice joints, and the two compression splice joints. The failure criteria calculated by hand matched the failure criteria calculated by the model. These procedures verified that the truss test model generates lumber values as specified with the correct correlation structure. The model also generates tooth withdrawal values, and steel strength values, as expected. Finally, the failure criteria used by the model matches independent analyses of the components. Therefore, the model was performing as intended.

## **MODEL VALIDATION**

After the truss test model was verified, the model was executed for the validation truss. The first model executed was to see what types of lumber failures would occur if the joints were adjusted so they could not fail. This scenario could theoretical occur if the ultimate strength of the joints was as strong as the ultimate strengths of the lumber; however, generally a mechanical joint acts as the weakest link in the system. Figure 6.2 is a histogram of this test case, for 1000 trials.



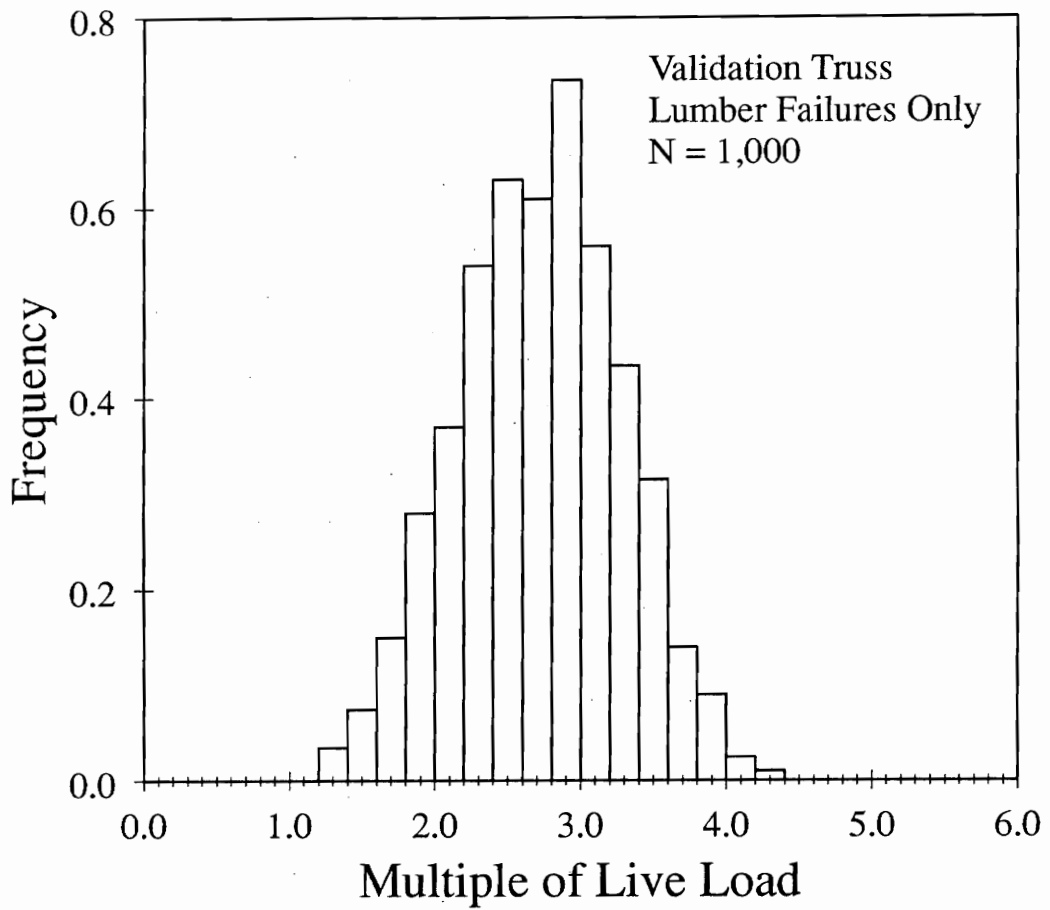


**Figure 6.2** Histogram of the multiple of live load capacity for the validation truss, lumber failure controlled for all trials.

The model simulated that 108 failures out of 1000 trials in the range of live load multiples of 1.0 and 2.0. There were 577 failures out of 1000 trials in the range of a live load multiples of 2.0 to 3.0. It appears that if the lumber models are accurate, that there is a reasonable probability that the truss will achieve 3.0 times the live load. The histogram represents the amount of live load applied to the top chord. Since the dead load was so small compared to the live load, the multiple of dead load and the multiple of total load are almost identical.

The second series of validation trials was conducted by including the joint failures. Figure 6.3 is a histogram of these failures.

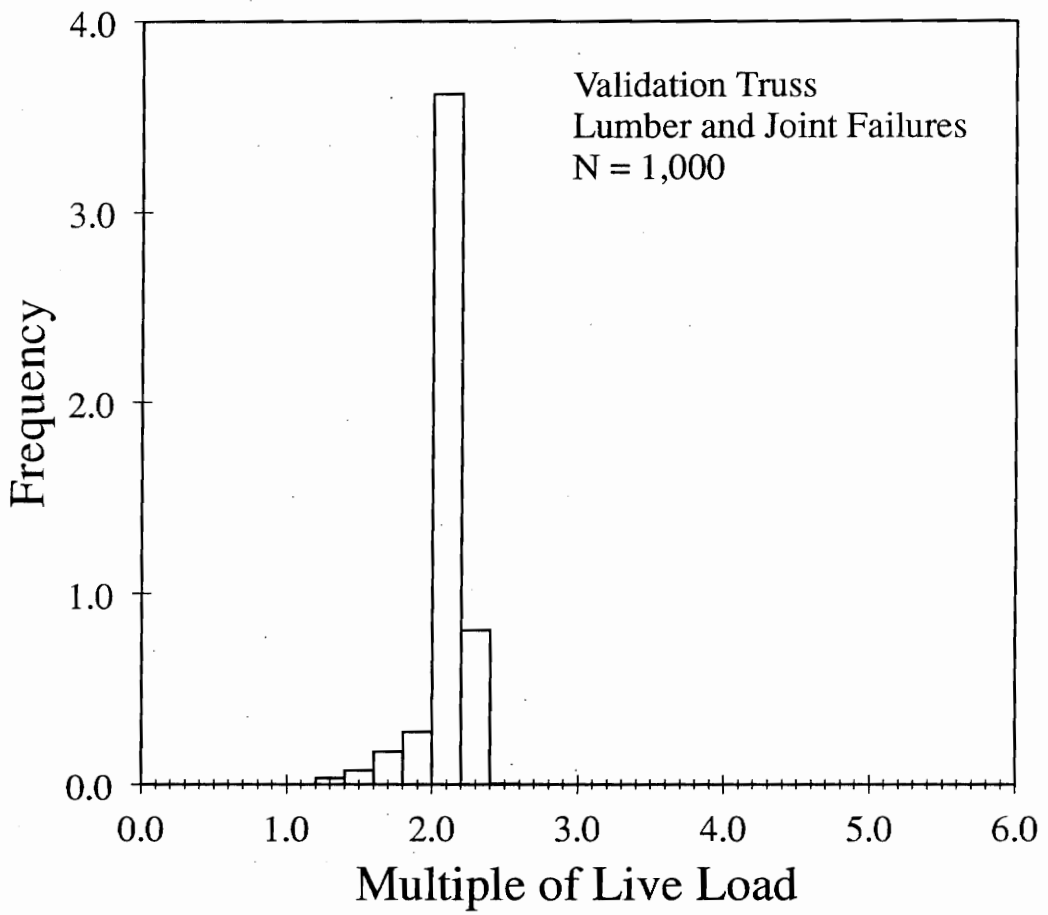


**Figure 6.3** Histogram of the multiple of live load for the validation truss.

These trials were performed using the same random number stream as the first trials, as a variance reduction technique (Law and Kelton, 1992). Figure 6.3 illustrates the effect that metal plate connected joints have on the strength of the truss. It is apparent that the joints are usually the weakest link of the structural system. Adding metal plate connected joints to the model effectively truncates the multiple-of-live load distribution carried by the truss. It is also interesting to note, that although lumber has a smaller safety factor than the joints, the joints still controlled almost all of the simulated truss failures. The histogram in Figure 6.3 has a much smaller spread than the histogram in Figure 6.2. There were 113 failures in the multiple of live load range of 1.0 to 2.0, and the rest of the failures occurred between a multiples of live load range of 2.0 to 2.5. If the model is accurate and the trusses were not over-plated, it is unlikely that test trusses similar to the validation truss will achieve the UBC(1991b) standard of 3.0 times the total load plus dead. None of the trials achieved 2.5 times live load plus dead. This indicates that this truss configuration might not pass the BOCA standard.

The truss plate manufacturer tested three trusses with the above configuration. The three actual truss test failures occurred in the range of 2.0 to 2.5 times the live load plus the dead load. Also two of the actual test trusses failed in the bottom chord splice joints and one of the trusses failed in buckling about the top chord. Table 6.2 summarizes the failures for the simulated trusses.

**Table 6.2 Summary of simulated failures for the validation truss.**

Failure Mode	Number of Simulated Failures	Comments
Compression Joint	0	
Heel Joint	0	
Lumber	163	150 of these were web failures
Peak Joint	1	
Tension Joint	831	830 were steel net section
Web Joint	5	

Out of the 1000 trials, 831 of them were caused by a tension joint failure. The other results were 1 peak joint failure, no heel joint failures, no compression splice joint failures, 5 web joint failures, and 163 lumber failures.

The model predicted a vast majority of failures in the tension joint region. Of these simulated failures, all but one was a steel net section failure. The actual truss test failures were tooth withdrawal of the tension joint. This discrepancy might be attributed to ignoring the bending stresses in the net section model and transforming the moment into an equivalent couple for the tooth withdrawal failure model. Secondly, out of the 163 simulated lumber failures, 150 of them were in the webs, and no failures occurred in the top cord. This result could indicate that the simulated lumber properties in the truss do not match the lumber properties used for the test trusses.

The model gives accurate prediction as compared to the test trusses. The magnitude of the load predicted by the test trusses was very close to the measured magnitude of the loads. The truss test model performed well under the rigorous conditions of inputting the

measured modulus of elasticity of the members and calibrating the size and stiffness of the fictitious members to match measured deflections. The end forces estimated using PPSA4 should be very accurate for the truss validation trials. However, the truss test model should be examined for robustness. These analyses are presented in Chapter VII.

# CHAPTER VII

## RESULTS AND DISCUSSION

### VALIDATION TRUSS

The 60 ft validation trusses analyzed in Chapter VI were reanalyzed to examine the sensitivity of the truss test model to the structural analog used by PPSA4. The truss analog influences the end forces calculated by PPSA4. The truss was reanalyzed with NDS (book value) E values for all lumber, and the fictitious members at the bottoms of the webs and the heel plate area were re-sized. The size of the fictitious members in the heel joint area were changed to the same dimensions as the top and bottom chords (1.5 x 9.25), and the E of the fictitious members were changed to the book value E of the top and bottom chords (1.9 Mpsi). The fictitious members used at the ends of the webs were changed to the same size and E of the webs. Figure 7.1 is a histogram similar to Figure 6.2 for wood failures only, and Figure 7.2 is similar to Figure 6.3 except the Figures 7.1 and 7.2 were generated with non-calibrated fictitious members.

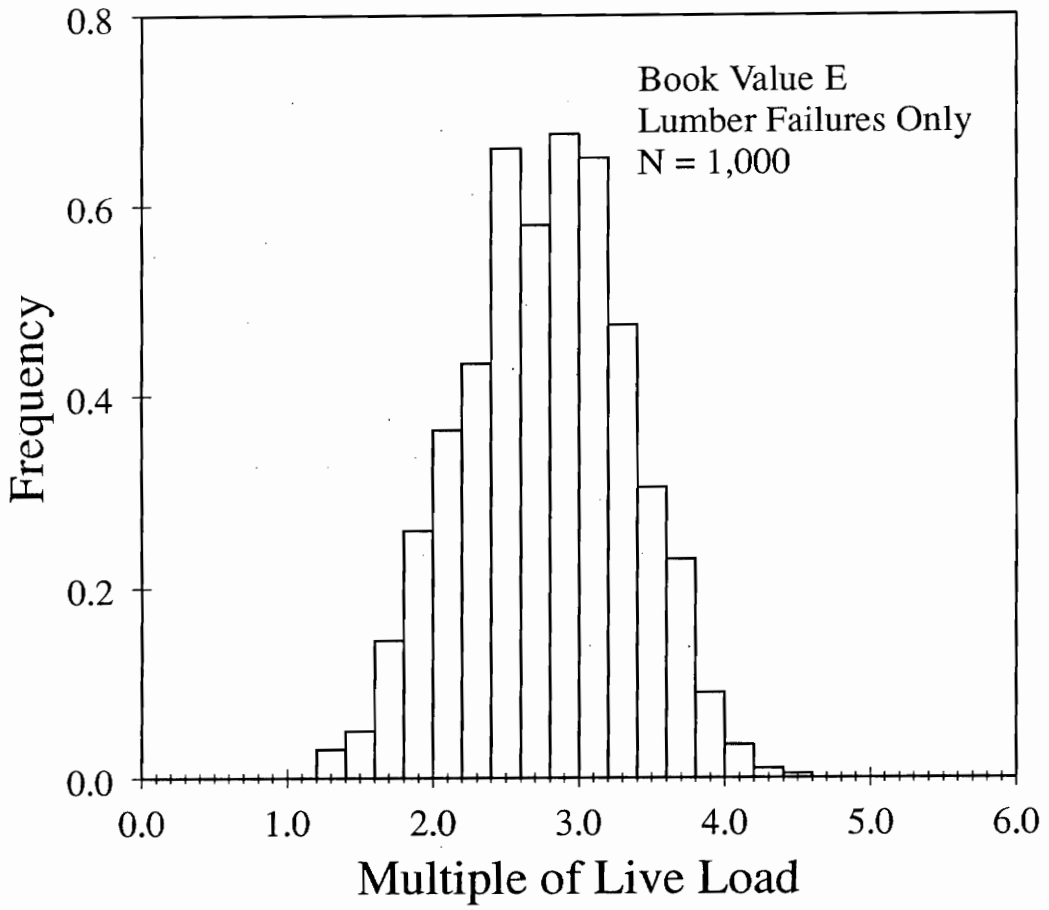


**Figure 7.1.** Histogram of the multiple of live load capacity for the validation truss, lumber failure controlled for all trials with no calibration of the fictitious members.



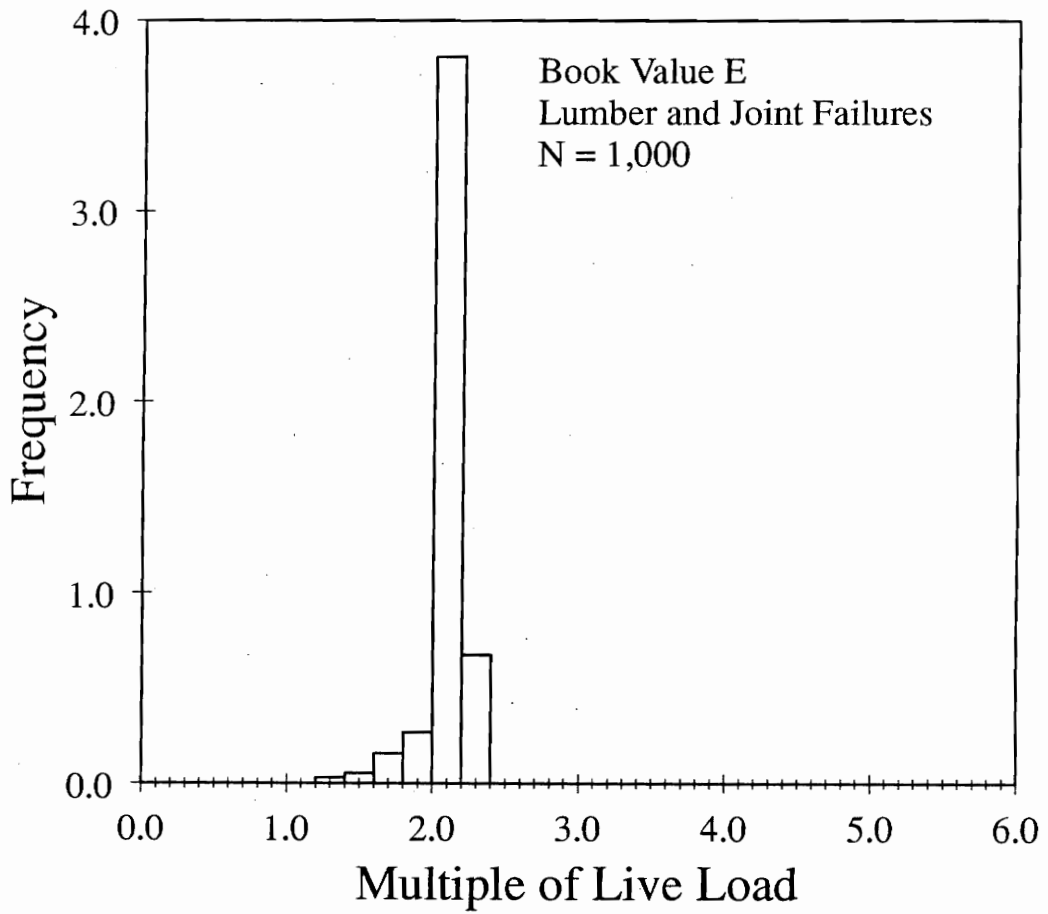


**Figure 7.2** Histogram of the multiple of live load for the validation truss with no calibration of the fictitious members.

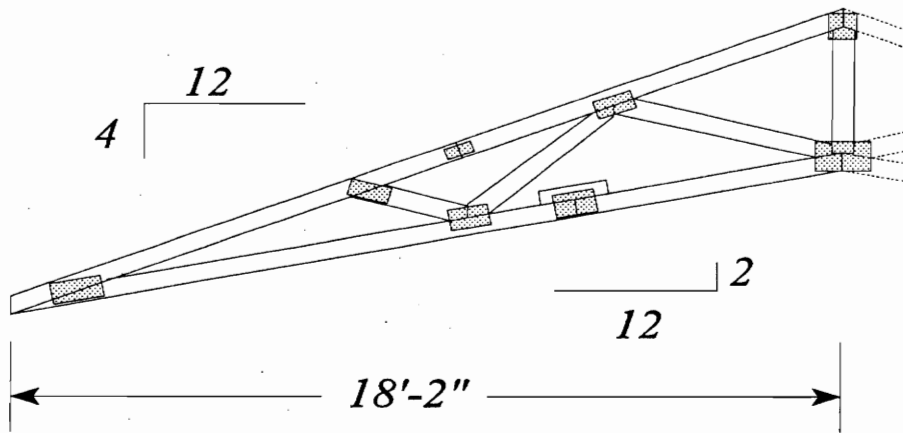
Figures 7.1 and 7.2 are almost identical to Figures 6.2 and 6.3. This indicates that the model is insensitive to using calibrated fictitious members for estimating the end forces with PPSA4. This an important finding because the fictitious members will not need to be calibrated to truss test deflections for the PPSA4 end force analyses. Fictitious members will be used to model the heel joints for the rest of the trusses. This is to aid in modelling the eccentricity of the heel joints.

Figures 7.1 and 7.2 are a more realistic simulation for the 60 ft truss used for the validation procedure, because the average E was used to calculated the end forces. Figure 7.1 indicates that very few lumber failures are expected below 2.0 times the live load. Figure 7.2 illustrates that simulated 60 ft trusses almost always failed above 2.0 times the live load. From the analysis that was used to generate the histogram in Figure 7.2, there were 103 failures below 2 times the live load plus dead. Of these 103 simulated failures, 97 were lumber failures.

## **SCISSOR TRUSS**

The author of this dissertation and his major advisor received another detailed report on a truss test conducted by a truss plate manufacturer. This truss test was for a scissor truss. The objectives of this test were to test the truss plate manufacturer's structural analog in terms of truss deflection for a wide range of loads. Since a wide range of loads were desired, the truss joints were over-plated to prevent premature joint failures. The scissor truss was 36' 4" wide and all members were constructed from southern pine No. 1 2 x 4. Generally, webs

would not be constructed with this high of a grade; however, the company did not want this truss to fail at a smaller than expected load. Figure 7.3 is a diagram of half of the scissor truss.



*Note: Drawing not to scale*

**Figure 7.3** Schematic diagram of a truss used for verification and validation of the truss test model.

The scissor truss had a top chord pitch of 4 in 12, and a bottom chord pitch of 2 in 12. The truss was designed for 16 psf top chord live, 7 psf top chord dead, and 10 psf bottom chord dead. The heel joint was modelled as a series of four fictitious members. Table 7.1 contains the plate properties for the scissor truss.

**Table 7.1 Plate values used for the scissor truss trials.**

Location	L	W	TW <sup>a</sup>	Steel Grade	t	e <sub>t</sub>	e <sub>v</sub>
	(in)	(in)	(psi) <sup>b</sup>		(in)		
Heel Joint	9.0	3.2	281.	B	0.0396	0.57	0.36
Tension Splice	5.2	4.8	237.	B	0.0635	0.62	0.26
Compression Splice	4.5	3.2	281.	B	0.0396	0.57	0.36
BC Peak	7.5	5.6	281.	B	0.0396	0.57	0.36
TC Peak	4.5	4.0	281.	B	0.0396	0.57	0.36

<sup>a</sup> Tooth withdrawal values are based on gross area, unless otherwise noted.

<sup>b</sup> Pounds per square inch, contact area.

The truss test model analyzed this truss exactly like the 60 ft truss with the exception of the bottom chord peak plate. The bottom chord peak plate was modelled exactly the same way as the top chord peak plate. Figure 7.4 is a histogram for the predicted multiple of live load required to fail the scissor truss.

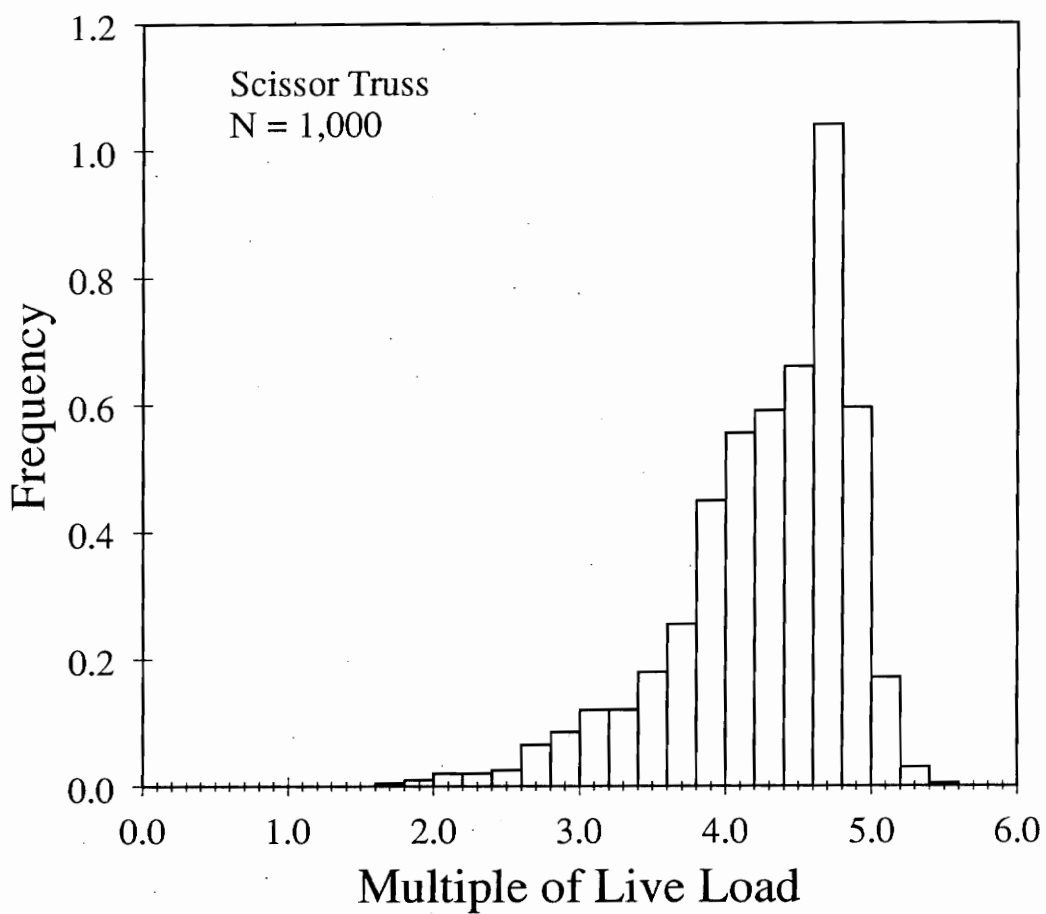


**Figure 7.4** Histogram of the multiple of live load capacity for the scissor truss.

The multiple of live loads predicted for this truss is considerably greater than for the 60 ft truss; however, this truss was specially built for deflection measurements, and does not reflect a truss test to verify design criteria. Nonetheless, the loads were greater than expected; therefore, more analyses was warranted.

An interesting comment was made in the truss test report. All three trusses failed in the bottom chord peak joint. One of these failures was due to tooth withdrawal, and the other two were due to net section fracture of the truss plate. After the first two bottom chord peak joints failed, the truss plate manufacturer took a close-up video of the bottom chord peak joint for the third truss test. After reviewing the video tape in slow motion, the report stated that it appeared that the peak joints failed in tension first, then in shear, not simultaneously. If the failures did not occur simultaneously, this would cause the failure criteria given by equation 5.32 and 5.33 to be invalid.

A second simulation was performed, assuming that the tension member in the peak joint failed in tension only, as opposed to combined tension and shear failure in the first simulation analysis. Figure 7.5 is a histogram of the results from the revised simulation analysis.

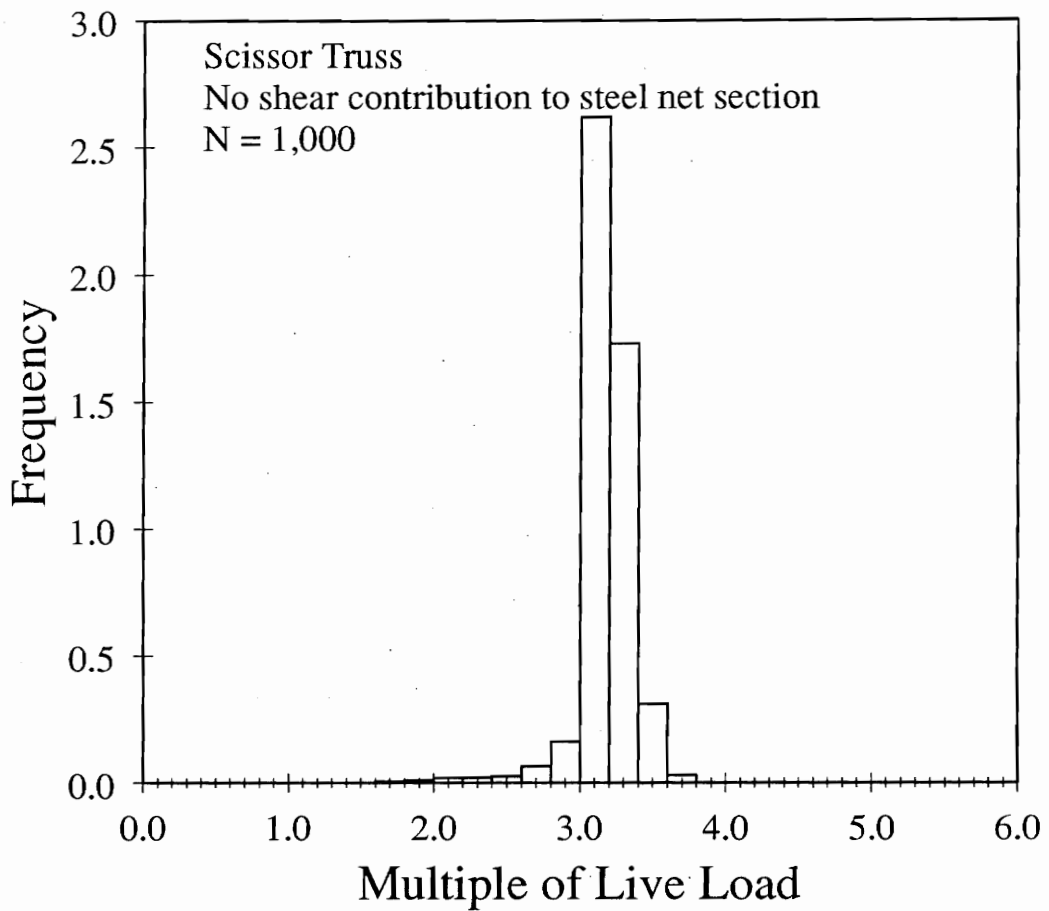


**Figure 7.5** Histogram of the multiple of live load for the scissor truss assuming that there is no interaction between the tensile strength and the shear strength in the peak joints.

Two of the actual truss failures occurred at greater than 2.5 times live load plus dead load and the third truss failed at greater than 2.0 times live load plus dead load. The truss test model predicted that a large majority of the failures would occur between 3.0 and 3.5 times live load, plus dead load. A summary of the simulated scissor truss failures is listed in Table 7.2.

**Table 7.2 Summary of simulated failures for the scissor truss.**

Failure Mode	Number of Simulated Failures	Comments
Compression Joint	0	
Heel Joint	0	
Lumber	7	
Peak Joint	987	923 were steel failures
Tension Joint	4	
Web Joint	2	

The truss test model predicted that out of 1000 trials, 987 were bottom chord peak failures. Of these, 923 were steel tension failures, and the other 64 were tooth withdrawal failures due to tension. Although the truss test model slightly overpredicted the actual failure loads, the modes and locations of failure are similar, and the magnitudes are fairly close to the actual truss failures. Since the truss test model predicts loads fairly close to the actual test trusses, it leads one to question the validity of assuming a peak plate will fail in combined tension and shear. The actual interaction between the shear strength of the plate and the tension strength of the plate is not known. Theoretically there should be some beneficial shear contribution to strength of the plate, but the amount of the contribution is unknown, at this time.



## CHAPTER VIII

### SUMMARY AND CONCLUSIONS

#### SUMMARY

A model was developed that simulates testing metal plate connected wood trusses. The model expanded on previous successful research efforts that transformed design criteria to ultimate strength criteria. This concept has been applied to lumber ultimate strength models for many years, and was applied to the joint strengths for this research. These ultimate strength models were developed using basic fundamental engineering properties to predict the strength of structural systems. Using these general principles allows the model to be used for many truss configurations. The model used actual steel properties data collected from truss plate manufactures for modelling the strength of the joints, and used the most current, up to data lumber data to model the lumber in the trusses.

Another finding was that the truss test model was insensitive to the structural analog used to calculate end forces. For the validation truss studied in detail fictitious members can be used to model eccentricities in the truss joints, and the properties of the members do not need to be calibrated to actual truss deflections. Many truss configurations do not have deflection data available to researchers to calibrate fictitious members. Models that require joint calibration are severely restricted in their potential usage.

Although lumber has the smallest safety factor of the components in terms of magnitude, many of the simulated truss failures were controlled by joints. This is partially due to the method that safety factors are calculated, but it illustrates that safety factors alone, do

not provide much information. The simulated outcome suggests that plates are generally the weakest link in the system. To increase the overall strength safety factor of the truss, the strengths of the joints should be increased.

Two different truss configurations were used for the simulations. Both of the trusses performed well, as compared to actual test data.

## CONCLUSIONS

- 1.) The safety factors used to design the components of trusses are not consistent in either the magnitude or the method of estimating the safety factors.
- 2.) Safety factors alone, do not indicate which mode of failure dominates truss tests. The different failure modes must be accompanied by statistical distributions and stress distributions in the truss to aid in identifying the probable failure mode.
- 3.) A truss simulation aimed at evaluating code specified truss test safety factors should include steel that is close to minimum specified strengths.
- 4.) The truss test model performed well when compared to actual test trusses. Although the two configurations studied appear similar, the behavior of the trusses are very different.

## MODEL LIMITATIONS

- 1.) The truss test model did not consider moment effects in any of the joints, except for tooth withdrawal for the tension and compression splice joints.
- 2.) The model did not consider the effect of steel buckling in the joint region due to compression forces.
- 3.) The truss test model treated the trusses as linear systems to failure; however, actual truss tests and joint tests have a non-linear load deflection response.
- 4.) The end forces were estimated only one time with the book value  $E$ . Although  $E$  was simulated for the members in the truss, the corresponding end forces for the simulated  $E$  were not re-estimated.
- 5.) The lumber model assumed constant properties throughout each individual piece of lumber.
- 6.) The tooth withdrawal strength of the joints extrapolated historical data to all metal connector plates. This assumes that all tooth withdrawal failure density functions have approximately the same shape.

- 7.) The properties used to generate the joint strengths were based on laboratory controlled test specimens. The joints in an actual truss may not exhibit the same joint quality.

## **FUTURE RESEARCH**

- 1.) Perform the truss test simulation on more trusses. The truss test model performed well for the trusses analyzed; however, more trusses need to be modelled.
- 2.) Analyze the interaction between shear failures and tension failures. It appears that adding the shear strength across a shearing plane, and the tensile strength along the tension failure plane may results in unrealistically high strength values for joints loaded in tension.
- 3.) Develop a model, based on engineering properties, to account for the effects of bending moment in the joint regions of trusses.
- 4.) Develop a model to account for steel buckling in the joint region due to compression stresses.

- 5.) Create a program that will aid in creating input files for the model. The current model requires extensive input, and these files are cumbersome to create. Programs were written in the C programming language and the UNIX operating system to aid in converting data from PPSA4 analyses to input files; however, the programs are fairly crude and still require manual editing of the input files.

## REFERENCES

- Ahrens, J. H. and U. Dieter. 1973. Extensions of Forsythe's method for random sampling from the normal distribution. *Mathematics of Computation*. 27(124):927-937.
- Allen, D. H. and W. E. Haisler. 1985. *Introduction to Aerospace Structural Analysis*. John Wiley and Sons, New York, N.Y.
- American Forest and Paper Association. 1991. National Design Specification. AFPA, Washington, D.C.
- American Iron and Steel Institute (AISI). 1978. Proposed criteria for load and resistance factor design of steel buildings structures. AISI Bulletin No. 27, New York, N.Y.
- American Institute of Steel Construction (AISC). 1986. *Manual of steel construction - Load and resistance factor design, 1<sup>st</sup> ed.* AISC, Chicago, IL.
- American Society of Testing and Materials (ASTM). 1993a. *Standard specification for steel sheet, zinc-coated (galvanized) by the hot-dip process, structural (physical) quality - A 446-91*. ASTM, Philadelphia, Pa.
- ASTM. 1993b. *Standard specifications for general requirements for steel sheet, zinc-coated (Galvanized) by the hot-dip process - A 525-93*. ASTM, Philadelphia, Pa.
- ASTM. 1993c. *Standard specification for steel sheet, zinc-coated (galvanized) by the hot-dip process, high strength, low alloy - A 816-91*. ASTM, Philadelphia, Pa.
- ASTM. 1993d. *Standard practice for establishing structural grades and related allowable properties for visually graded lumber- D 245-92*. ASTM, Philadelphia, Pa.
- Beineke, L. A. and S. K. Suddarth. 1979. Modeling joints made with light-gage metal connector plates. *Forest Products Journal* 29(8):39-45.
- Boresi, A. P. and O. M. Sidebottom. 1985. *Advanced Mechanics of Materials, 4<sup>th</sup> ed.* John Wiley and Sons, New York, N.Y.
- Breyer, D. E. 1993. *Design of Wood Structures, 3<sup>rd</sup> ed.* McGraw-Hill, Inc., New York, N.Y.
- Building Officials Code Administrators (BOCA). 1993. The BOCA national building code. BOCA, Country Club Hills, Ill.
- BOCA. 1991. Research Report No. 91-38. BOCA Evaluation Services, Inc. Country Club Hills, Ill.

- Canadian Standard Association (CSA). 1980. Method of test for evaluation of truss plates used in lumber joints. S347-M80, CSA, Rexdale, Ont.
- Chapra, S. C. and R. P. Canale. 1988. *Numerical methods for engineers*, 2<sup>nd</sup> ed., McGraw-Hill, New York, N. Y.
- Cook, R. D., D. S. Malkus and M. E. Plesha. 1989. Concepts and *Applications of Finite Element Analysis*, 3<sup>rd</sup> ed. John Wiley and Sons, New York, N. Y.
- Cooke, R. A., S. Mostaghimi and F. E. Woeste. 1993. VTFIT: A microcomputer-based routine for fitting probability distribution functions to data. *Applied Engineering in Agriculture* 9(4):401-408.
- Corotis, R. B. and V. A. Doshi. 1977. Probability models for live-load survey results. *Journal of the Structural Division, ASCE* 103(ST6):1257-1274.
- Cramer, S. M., D. Shrestha and W. B. Fohrell. 1990. Theoretical consideration of metal-plate-connected wood-splice joints. *Journal of Structural Engineering, ASCE* 116(ST12):3458-3474
- Crovella, P. L. and K. G. Gebremedhin. 1990. Analyses of light frame wood truss tension joint stiffness. *Forest Products Journal* 40(4):41-47.
- Dunn, O. J. and V. A. Clark. 1987. *Applied statistics: analysis of variance and regression*, 2<sup>nd</sup> ed., John Wiley and Sons, New York, N.Y.
- Edwards, A. L. 1984. *An Introduction to Linear Regression and Correlation*, 2nd ed., W. H. Freeman and Company, New York, N.Y.
- Ellingwood, B., T. V. Galambos, J. G. MacGregor and C. A. Cornell. 1980. Development of a probability based load criterion for American national standard A58. National Bureau of Standards special publication 577, U. S. Department of Commerce, Washington, D.C.
- Evans, J. W., R. A. Johnson and D. W. Green. 1989. Two- and three- parameter Weibull goodness-of-fit tests. Research Paper FPL-RP-493. U. S. Forest Products Laboratory, Madison, Wisc.
- Forest Products Laboratory. 1987. Wood Handbook: Wood as an engineering material. Agriculture Handbook No. 72, U. S. Forest Products Laboratory, Madison, Wisc.
- Foschi, R. O. 1977a. Analysis of wood diaphragms and trusses. Part I: diaphragms. *Canadian Journal of Civil Engineering* 4:345-352.

- Foschi, R. O. 1977b. Analysis of wood diaphragms and trusses. Part II: truss-plate connections *Canadian Journal of Civil Engineering* 4:353-362.
- Galambos, T. V. and M. K. Ravindra. 1978. Properties of steel for use in LRFD, *Journal of the Structural Division, ASCE* 104(ST9):1459-1468.
- Galligan, W. L., R. J. Hoyle, R. F. Pellerin, J. H. Haskell and J. R. Taylor. 1986. Characterizing the properties of 2-inch softwood dimension lumber with regressions and probability distributions: project completion report. U. S. Forest Products Laboratory, Madison, Wisc.
- Galligan, W. L., R. A. Johnson and J. R. Taylor. 1979. Examination of the concomitant properties of lumber. In *Proceedings of Metal Plate Wood Truss Conference*, P-79-28. Forest Products Society, Madison, Wisc.
- Gebremedhin, K. G., M. C. Jorgensen and C. B. Woelfel. 1992. Load-slip characteristics of metal plate connected wood joints tested in tension and shear. *Wood and Fiber Science* 24(2):118-132.
- Gibbons, J. D. 1993. *Nonparametric Measures of Association*, Sage University Paper series on Quantitative Application in the Social Sciences, 07-091. Newbury Park, Calif.
- Green, D. W. and J. W. Evans. 1987. Mechanical properties of visually graded lumber: Volume 4 southern pine. US. Forest Products Laboratory, Madison, Wisc.
- Green, D. W., J. W. Evans and R. A. Johnson. 1984. Investigation of the procedure for estimating concomitance of lumber strength properties. *Wood and Fiber Science* 16(3):427-440
- Groom, L. and A. Polensek. Nonlinear modeling of truss-plate joints. *Journal of Structural Engineering, ASCE* 118(ST9):2514-2531.
- Gupta, R. 1994. Metal-plate connected tension joints under different loading conditions. *Wood and Fiber Science* 26(2):212-222.
- Gupta, R. 1990. Reliability analysis of semirigidly connected metal plate residential wood trusses. Ph.D. Thesis, Cornell University, Ithaca, NY.
- Gupta, R. and K. G. Gebremedhin. 1992. Resistance distributions of a metal-plate-connected wood truss. *Forest Products Journal* 42(7/8):11-16.
- Gupta, R. and K. G. Gebremedhin. 1990. Destructive testing of metal-plate-connected wood truss joints. *Journal of Structural Engineering, ASCE* 116(ST7):1971-1982.



- Gupta, R., K. G. Gebremedhin and M. D. Grigoriu. 1992. Characterizing the strength of wood truss joints. *Transactions of the ASAE* 35(4):1286-1290.
- Gutshall, S. T. 1994. Monotonic and cyclic short-term performance of nailed and bolted timber connections. M. S. Thesis, Virginia Polytechnic Institute and State University, Blacksburg, Va.
- Hamon, D. C., F. E. Woeste and D. W. Green. 1985. Influence of lumber property correlations on roof truss reliability. *Transactions of the ASAE* 28(5):1618-1625.
- Hankinson, R. L. 1921. Investigation of crushing strength of spruce at varying angles of grain. US. Air Service Information Circular No. 259.
- Hoyle, R. J. 1968. Background to machine stress grading. *Forest Products Journal*, 18(4):87-97.
- Hoyle, R. J., W. L. Galligan and J. H. Haskell. 1979. Characterizing lumber properties for truss research, Appendix I: specific Weibull distribution concerns. In *Proceedings of Metal Plate Wood Truss Conference*, P-79-28. Forest Products Society, Madison, Wisc.
- Hoyle, R. J. and F. E. Woeste. 1989. *Wood technology in the design of structures, 5th ed.* Iowa State University Press, Ames, Ia.
- International Conference of Building Officials ICBO. 1991a. The uniform building code. ICBO, Whittier, Calif.
- ICBO. 1991b. Uniform building code standards. ICBO, Whittier, Calif.
- ICBO Evaluation Service (ES). 1991. Evaluation report no. 2949. ICBO ES, Whittier, Calif.
- ICBO ES. 1993. Evaluation report nos. 2059, 4443, 4451, 4542, 4805, 4922, 4994, 5039. ICBO ES, Whittier, Calif.
- ICBO ES. 1992. Evaluation report nos. 1329, 1591, 1607, 2342, 2929, 3777, 4211, 4420. ICBO ES, Whittier, Calif.
- IMSL. 1987. *FORTTRAN subroutines for statistical analysis*, IMSL, Houston, Tex.
- James, F. 1990. A review of pseudorandom number generators. *Computer Physics Communications* 60:329-344.
- Kennedy, D. J. L. and K. A. Baker. 1984. Resistance factors for steel highway bridges. *Canadian Journal of Civil Engineering* 11:324-334.

- Kennedy, D. J. L. and M. M. A. Gad Aly. 1980. Limit states design of steel structures performance factors. *Canadian Journal of Civil Engineering* 7:45-77.
- Kline, D. E. and D. A. Bender. 1990. Maximum likelihood estimation for shifted Weibull and lognormal distributions. *Transactions of the ASAE* 33(1):330-335.
- Kline, D. E., F. E. Woeste and B. A. Bendtsen. 1986. Stochastic model for modulus of elasticity of lumber. *Wood and Fiber Science* 18(2):228-238.
- Kumar, D., C. D. Heatwole, A. C. Bruggeman and F. E. Woeste. 1995. Assessing correlation structures with subjective information - an interactive approach. *Simulation*. In press.
- Lau, P. W. C. 1987. Factors affecting the behaviour and modelling of toothed metal-plate joints. *Canadian Journal of Civil Engineering* 14:183-195.
- Law, A. M. and W. D. Kelton. 1991. *Simulation Modeling and Analysis, 2<sup>nd</sup> ed.*, McGraw-Hill, Inc. New York, N.Y.
- Lewis, S. L. 1993. Personal conversation.
- Maraghechi, K. and R. Y. Itani. 1984. Influence of truss plate connectors on the analysis of light frame structures. *Wood and Fiber Science* 16(3):306-322.
- Marsaglia, G., A. Zaman and W. W. Tsang. 1990. Toward a universal random number generator. *Statistics and Probability Letters* 8:35-39.
- McAllister, R. H. 1989. Interaction between truss plate design and type of truss framing. *Forest Products Journal* 39(7/8):17-24.
- McCarthy, M. and R. W. Wolfe. 1987. Assessment of truss plate performance model applied to southern pine truss joints. Res. Pap. FPL 483, US. Forest Products Laboratory, Madison, Wisc.
- Ott, L. 1988. *An Introduction to Statistical Methods and Data Analysis, 3<sup>rd</sup> ed.*, PWS-Kent Publishing Company, Boston, Mass.
- Press, W. H., S. A. Teukolsky, W. T. Vetterling and B. P. Flannery. *Numerical recipes in fortran: the art of scientific computing, 2<sup>nd</sup> ed.* Cambridge University Press, New York, N.Y.
- Rao, N. R. M., M. Lohrmann and L. Tall. 1966. Effects of strain rate on the yield stress of structural steels. *Journal of Materials (ASTM)*, 1(1):241-262.

- Rojiani, K. B., K. A. Tarbell. 1985. Analysis of the reliability of wood roof trusses. In *Proceedings 4th International Conference on Structural Safety and Reliability*.
- Ross, R. J. and R. F. Pellerin. 1994. Nondestructive testing for assessing wood members in structures: a review. FPL-GTR-70, US. Forest Products Laboratory, Madison, Wisc.
- Salmon, C. G. and J. E. Johnson. 1990. *Steel Structures Design and Behavior, Emphasizing Load and Resistance Factor Design, 3<sup>rd</sup> ed.*, Harper and Row, New York, N.Y.
- SAS Institute Inc. 1989. *SAS/STAT User's Guide, version 6, 4<sup>th</sup> ed., volume 2*, SAS Institute Inc. Cary, N.C.
- SAS Institute Inc. 1990. *SAS Procedures Guide, version 6, 3<sup>th</sup> ed.*, SAS Institute Inc. Cary, N.C.
- Schuëller, G. I. 1985. Current trends in systems reliability. In *Proceedings 4th International Conference on Structural Safety and Reliability*.
- Seely, F. B. 1935. *Resistance of Materials, 2<sup>nd</sup> ed.* John Wiley and Sons, Inc., London.
- Sheppard, I. 1969. An analytical and experimental investigation of contact area stress distribution and buckling strength of light gauge punched metal heel plates for timber trusses. Ph.D. Thesis, Michigan State University, East Lansing, Mich.
- Showalter, K. L., F. E. Woeste and B. A. Bendtsen. 1987. Effect of length on tensile strength in structural lumber. Res. Pap. FPL 482, U.S. Forest Products Laboratory, Madison, Wisc.
- Southern Building Code Congress International (SBCCI). 1991. Standard Building Code. SBCCI, Birmingham, Ala.
- Suddarth, S. K., D. H. Percival and Q. B. Comus. 1981. Testing and analysis of 4 x 2 parallel chord metal-plate-connected trusses. Research Report 81-1, Small Homes Council-Building Research Council. University of Illinois, Urbana-Champaign, Ill.
- Suddarth, S. K., F. E. Woeste and W. L. Galligan. 1978. Differential reliability: probabilistic engineering applied to wood members in bending/tension. Res. Pap. FPL 302, U.S. Forest Products Laboratory, Madison, Wisc.
- Suddarth, S. K. and R. W. Wolfe. 1984. Purdue Plane Structures Analyzer II - A computerized wood engineering system. General Technical Report. FPL 40, US. Forest Products Laboratory, Madison, Wisc.

- Taylor, S. E. and D. A. Bender. 1988. Simulating correlated lumber properties using a modified multivariate normal approach. *Transactions of the ASAE* 31(1):182-186.
- Triche, M. H. 1984. Analysis and design of metal plate connections. M.S. Thesis, Purdue University, West Lafayette, IN.
- Triche, M. H. and S. K. Suddarth. 1993. Purdue plane structures analyzer (PPSA), Version 4.0. Purdue Research Foundation, West Lafayette, Ind.
- Triche, M. H. and S. K. Suddarth. 1988. Advanced design of metal plate connector joints. *Forest Products Journal* 38(9):7-12.
- Truss Plate Institute (TPI). 1993. BSR/TPI 2-1993 Standard for testing performance of metal-plate-connected wood trusses, TPI, Madison, Wisc.
- TPI. 1992. BSR/TPI 1-199x National design standard for metal plate connected wood truss construction, TPI, Madison, Wisc.
- TPI. 1987 *Design specifications for metal plate connected parallel chord wood trusses, PCT-80*, TPI, Madison, Wisc.
- Wolfe, R. W. 1990. Metal-plate connections loaded in combined bending and tension. *Forest Products Journal* 40(9):17-23.
- Wolfe, R. W., M. Hall and D. Lyles. 1991. Test apparatus for simulating interactive loads on metal plate wood connections. *Journal of Testing and Evaluation* 19(6):421-428.
- Worley, J. W., J. A. Bollinger, F. E. Woeste and K. S. Kline. 1990. Graphic distribution analysis (GDA). *Applied Engineering in Agriculture* 6(3):367-371.
- Zahn, J. J. 1986. Design of wood members under combined loading. *Journal of the Structural Division ASCE* 112(9):2109-2126.
- Zhao, W., F. E. Woeste and D. A. Bender. 1992. Effect of span-length on the reliability of truss bottom chords. *Transactions of the ASAE* 35(1):303-310.

# APPENDIX I

## TRUSS TEST MODEL SOURCE CODE

```
program truss
  common /cjoint/ clength,cwidth,ncsplice,cmem,cend,ctype
  common /define/ coord,connect,mtype,ngroup,nmem,grade,usetype
  common /force/ dforce,dload,lforce,lload,totforce,totload
  common /heel/ heelarea,heelvl,heelmem,heelend,heeltype
  common /peak/ peakarea,ptlen,pvlen,peakmem,mempeak,
+       peakend,peaktype,npeak
  common /props/ depth,e,fball,fcall,ftall,loverd,width
  common /tjoint/ tlength,twidth,ntsplice,tmem,tend,ttype
  common /trusstat/ newtruss
  common /webj/ webtl,webvl,webarea,nwebp,locweb,webmem,
+       webend,webtype
  character*3 heelend(2,2),cend(4),peakend(4,5),tend(4),
+       webend(30,2)
  character*4 usetype(50)
  character*10 grade(50),heeltype(2),peaktype(4),ctype(4),ttype(4),
+       webtype(30)
  integer connect(100,2),cmem(4),heelmem(2,2),mtype(100),
+       peakmem(4,5),tmem(4),mempeak(4),webmem(30,2),locweb(2)
  logical newtruss
  real coord(100,2),clength(4),cwidth(4),depth(50),
+       dforce(100,6),dload(100,2),e(50),fball(50),
+       fcall(50),ftall(50),heelarea(2),heelvl(2),ldf,lforce(100,6),
+       lload(100,2),loverd(100),peakarea(4,5),totforce(100,6),
+       totload(100,2),twidth(4),tlength(4),width(50),ptlen(4),
+       pvlen(4),webarea(30),webtl(30),webvl(30)
  data dload, lload, loverd /200*0., 200*0., 100*0./
  open (unit=50,file='woodfail.out',status='unknown')
  open (unit=51,file='heelfail.out',status='unknown')
  open (unit=52,file='cmpfail.out',status='unknown')
  open (unit=53,file='tenfail.out',status='unknown')
  open (unit=54,file='peakfail.out',status='unknown')
  open (unit=55,file='webfail.out',status='unknown')
  open (unit=60,file='factor.out',status='unknown')
  ldf = 1.6
  newtruss = .true.
  call rmarin(7390,9373)
  call input
  do 200 itruss=1,1000
    call secant(itruss,ldf)
200  continue
  stop
end

subroutine secant(itruss,ldf)
  common /cjoint/ clength,cwidth,ncsplice,cmem,cend,ctype
  common /define/ coord,connect,mtype,ngroup,nmem,grade,usetype
  common /force/ dforce,dload,lforce,lload,totforce,totload
  common /heel/ heelarea,heelvl,heelmem,heelend,heeltype
  common /peak/ peakarea,ptlen,pvlen,peakmem,mempeak,
+       peakend,peaktype,npeak
  common /props/ depth,e,fball,fcall,ftall,loverd,width
```

```

common /tjoint/ tlength,twidth,ntsplICE,tmem,tend,ttype
common /trusstat/ newtruss
common /webj/ webtl,webvl,webarea,nwebp,locweb,webmem,
+         webend,webtype
character*3 heelend(2,2),cend(4),peakend(4,5),tend(4),
+         webend(30,2)
character*4 usetype(50)
character*10 grade(50),heeltype(2),peaktype(4),ctype(4),ttype(4),
+         webtype(30)
integer connect(100,2),cmem(4),heelmem(2,2),mtype(100),
+         peakmem(4,5),tmem(4),index(5),imode(5),mempeak(4),
+         webmem(30,2),locweb(2)
logical newtruss
real coord(100,2),clength(4),cwidth(4),depth(50),
+         dforce(100,6),dload(100,2),e(50),fball(50),fcall(50),
+         ftall(50),heelarea(2),heelvl(2),ldf,lforce(100,6),
+         lload(100,2),loverd(100),lumcsi,ptlen(4),pvlen(4),
+         maxcsi, peakarea(4,5),totforce(100,6),plcsi(5),
+         totload(100,2),twidth(4),tlength(4),width(50),
+         webarea(30),webtl(30),webvl(30)
10  format (2x,i4,2x,i3,2x,i3,2(5x,f8.4))
    if (newtruss) call genprop
    oldfact = 0.
    oldfx = 0.
    factor = 0.
    fx = 0.
    do 130 itr=1,30
        do 110 i=1,nmem
            do 100 j=1,6
                totforce(i,j) = dforce(i,j)+factor*lforce(i,j)
            do 110 j=1,2
                totload(i,j) = dload(i,j)+factor*lload(i,j)
110         call chkIum(lumcsi,ldf,member,mode)
            call chkplate(plcsi,index,imode)
            newtruss = .false.
            maxcsi = 0.
            do 120 i=1,5
                if (plcsi(i).gt.maxcsi) then
                    maxcsi = plcsi(i)
                    ifail = i
                endif
120         continue
            if (lumcsi.gt.maxcsi) then
                maxcsi = lumcsi
                ifail = 0
            endif
            fx = maxcsi - 1.0
            if (itr.ne.1) then
                if (fx.eq.0.) goto 140
                dx = fx*(oldfact-factor)/(oldfx-fx)
                if (abs(dx).lt.0.0001) goto 140
            else
                dx = -0.5
            endif
            oldfact = factor
            oldfx = fx
            factor = factor-dx
130         continue
        write (*,*) ' This loading situation failed to converge'
        ifail = -1

```

```

140  if (ifail.eq.0) then
      write(50,10) itruss, member,mode,factor
    elseif (ifail.eq.1) then
      write(51,*) itruss,heelmem(index(1),1),imode(1),factor
    elseif (ifail.eq.2) then
      write(52,*) itruss,cmem(index(2)),factor
    elseif (ifail.eq.3) then
      write(53,*) itruss,tmem(index(3)),imode(3),factor
    elseif (ifail.eq.4) then
      write(54,*) itruss,index(4),imode(4),factor
    elseif (ifail.eq.5) then
      write(55,*) itruss,index(5),locweb,imode(5),factor
    endif
  write (60,*) factor
  newtruss = .true.
  return
end

subroutine chkplate(plcsi,index,imode)
common /cjoint/ clength,cwidth,ncsplice,cmem,cend,ctype
common /define/ coord,connect,mtype,ngroup,nmem,grade,usetype
common /force/ dforce,dload,lforce,lload,totforce,totload
common /heel/ heelarea,heelvl,heelmem,heelend,heeltype
common /peak/ peakarea,ptlen,pvlen,peakmem,mempeak,
+ peakend,peaktype,npeak
common /tjoint/ tlength,twidth,ntsplice,tmem,tend,ttype
common /trusstat/ newtruss
common /webj/ webtl,webvl,webarea,nwebp,locweb,webmem,
+ webend,webtype
character*3 heelend(2,2),cend(4),peakend(4,5),tend(4),
+ webend(30,2)
character*4 usetype(50)
character*10 grade(50),heeltype(2),peaktype(4),ctype(4),ttype(4),
+ webtype(30)
integer connect(100,2),cmem(4),heelmem(2,2),mtype(100),
+ peakmem(4,5),tmem(4),index(5),imode(5),mempeak(4),
+ webmem(30,2),locweb(2)
logical newtruss
real coord(100,2),clength(4),cwidth(4),
+ dforce(100,6),dload(100,2),
+ heelarea(2),heelvl(2),lforce(100,6),
+ lload(100,2),peakarea(4,5),plcsi(5),totforce(100,6),
+ totload(100,2),twidth(4),tlength(4),ptlen(4),pvlen(4),
+ webarea(30),webtl(30),webvl(30)
call chkheel(plcsi(1),index(1),imode(1))
call chkcmpj(plcsi(2),index(2))
call chktenj(plcsi(3),index(3),imode(3))
call chkpeak(plcsi(4),index(4),imode(4))
call chkweb(plcsi(5),index(5),imode(5))
return
end

subroutine chkweb(maxcsi,imem,mode)
common /define/ coord,connect,mtype,ngroup,nmem,grade,usetype
common /force/ dforce,dload,lforce,lload,totforce,totload
common /trusstat/ newtruss
common /webj/ webtl,webvl,webarea,nwebp,locweb,webmem,
+ webend,webtype
character*3 webend(30,2)
character*4 usetype(50)

```

```

character*10 grade(50),webtype(30)
integer connect(100,2),mtype(100),webmem(30,2),ncritmem(2),
+   locweb(2)
logical newtruss
real coord(100,2),dforce(100,6),dload(100,2),
+   lforce(100,6),lload(100,2),totforce(100,6),toothfac(30),
+   totload(100,2),webarea(30),webtl(30),webvl(30),fu(30),
+   tmpsi(2),maxcsi,webcsi(2)
if (newtruss) then
  do 90 i=1,nwebp
    toothfac(i) = gentfact()
90    fu(i) = genfu(webtype(i))
  endif
  do 110 i=1,2
110    tmpsi(i) = 0.
    maxcsi = 0.
    do 120 i=1,nwebp
      call platepro(webtype(i),t,twith,educt,teff,veff)
      do 120 j=1,2
        ten = 0.
        if (webend(i,j).eq.'NEG') then
          axial = abs(totforce(webmem(i,j),1))
          if (totforce(webmem(i,j),1).lt.0.) ten = axial
        elseif (webend(i,j).eq.'POS') then
          axial = abs(totforce(webmem(i,j),4))
          if (totforce(webmem(i,j),4).gt.0.) ten = axial
        else
          write (*,*) 'Error in Web Plate definition'
          stop
        endif
        thold = 2.*webarea(i)*twith*toothfac(i)
        if (webvl(i).le.0.) then
          tall = 2.*webtl(i)*teff*fu(i)*t
        else
          tall1 = 2.*(webvl(i)*0.577*veff+webtl(i)*teff)*fu(i)*t
          tall2 = 2.*(webtl(i)*0.577*veff+webvl(i)*teff)*fu(i)*t
          tall = min(tall1,tall2)
        endif
        webcsi(1) = axial/thold
        webcsi(2) = ten/tall
c-> this loop finds the most critical member in the peak joint for
c-> each individual failure mode
        do 120 k=1,2
          if (webcsi(k).gt.tmpsi(k)) then
            tmpsi(k) = webcsi(k)
            ncritmem(k) = j
            jmem = i
          endif
120    continue
        do 130 i=1,2
          if (tmpsi(i).gt.maxcsi) then
            maxcsi = tmpsi(i)
            imem = webmem(jmem,ncritmem(i))
            locweb(1) = webmem(jmem,1)
            locweb(2) = webmem(jmem,2)
            mode = i
          endif
130    continue
      return
    end

```



```

subroutine chkheel(maxcsi, iside, mode)
common /define/ coord, connect, mtype, ngroup, nmem, grade, usetype
common /force/ dforce, dload, lforce, lload, totforce, totload
common /heel/ heelarea, heelvl, heelmem, heelend, heeltype
common /trusstat/ newtruss
character*3 heelend(2,2)
character*4 usetype(50)
character*10 grade(50), heeltype(2)
integer connect(100,2), heelmem(2,2), mtype(100), maxside(4)
logical newtruss
real coord(100,2), dforce(100,6), dload(100,2), lforce(100,6),
+   lload(100,2), heelarea(2), heelvl(2), totforce(100,6),
+   totload(100,2), toothfac(2), heelcsi(4), maxcsi, tmpsi(4)
c->heelcsi(1) = shear
c->heelcsi(2) = tension
c->heelcsi(3) = toothcomp
c->heelcsi(4) = toothtens
    if (newtruss) then
        do 90 i=1,2
90         toothfac(i) = gentfact()
            fu = genfu(heeltype(1))
        endif
        maxcsi = 0.
        do 100 i=1,4
100        tmpsi(i) = 0.
        do 110 i=1,2
            call platepro(heeltype(i), t, twith, reduct, teff, veff)
            if (heelend(i,1).eq.'NEG') then
                vactual = totforce(heelmem(i,1),1)
                thcmp = sqrt(totforce(heelmem(i,1),1)**2+
+                   totforce(heelmem(i,1),2)**2)
            elseif (heelend(i,1).eq.'POS') then
                vactual = -totforce(heelmem(i,1),4)
                thcmp = sqrt(totforce(heelmem(i,1),4)**2+
+                   totforce(heelmem(i,1),5)**2)
            else
                write (*,*) 'Error in Heel Plate definition'
                stop
            endif
            if (heelend(i,2).eq.'NEG') then
                xlength = coord(connect(heelmem(i,1),2),1)-
+                   coord(connect(heelmem(i,1),1),1)
                ylength = coord(connect(heelmem(i,1),2),2)-
+                   coord(connect(heelmem(i,1),1),2)
                theta1 = atan2(ylength,xlength)
                xlength = coord(connect(heelmem(i,2),2),1)-
+                   coord(connect(heelmem(i,2),1),1)
                ylength = coord(connect(heelmem(i,2),2),2)-
+                   coord(connect(heelmem(i,2),1),2)
                theta2 = atan2(ylength,xlength)
                phi = abs(theta1-theta2)
                tactual = -totforce(heelmem(i,2),1)*sin(phi)+
+                   totforce(heelmem(i,2),2)*cos(phi)
                thten = sqrt(totforce(heelmem(i,2),1)**2+
+                   totforce(heelmem(i,2),2)**2)
            elseif (heelend(i,2).eq.'POS') then
                tactual = -totforce(heelmem(i,2),4)*sin(phi)+
+                   totforce(heelmem(i,2),5)*cos(phi)
                thten = sqrt(totforce(heelmem(i,2),4)**2+
+                   totforce(heelmem(i,2),5)**2)

```

```

else
  write (*,*) 'Error in Heel Plate definition'
  stop
endif
tall = 2.*heelyl(i)*t*fu*teff
vall = 2.*heelvl(i)*t*fu*veff*0.577
heelred = 0.85-0.05*(12.*abs(tan(phi))-2.)
if (heelred.gt.0.85) heelred = 0.85
if (heelred.lt.0.65) heelred = 0.65
thold = 2.*heelarea(i)*heelred*twith*toothfac(i)
heelcsi(1) = vactual/vall
heelcsi(2) = tactual/tall
heelcsi(3) = thcmp/thold
heelcsi(4) = thten/thold
do 110 j=1,4
  if (heelcsi(j).gt.tmpcsi(j)) then
    tmpcsi(j) = heelcsi(j)
    maxside(j) = i
  endif
110 continue
do 120 i=1,4
  if (tmpcsi(i).gt.maxcsi) then
    maxcsi = tmpcsi(i)
    iside = maxside(i)
    mode = i
  endif
120 continue
return
end

subroutine chkcmpj(maxcsi,iplate)
common /cjoint/ clength,cwidth,ncsplice,cmem,cend,ctype
common /define/ coord,connect,mtype,ngroup,nmem,grade,usetype
common /force/ dforce,dload,lforce,lload,totforce,totload
common /trussstat/ newtruss
character*3 cend(4)
character*4 usetype(50)
character*10 grade(50),ctype(4)
integer connect(100,2),cmem(4),mtype(100)
logical newtruss
real coord(100,2),clength(4),cwidth(4),
+   dforce(100,6),dload(100,2),lforce(100,6),maxcsi,
+   lload(100,2),totforce(100,6),totload(100,2),toothfac(4)
if (newtruss) then
  do 100 i=1,ncsplice
100   toothfac(i) = gentfact()
c-> assumes that all plates are identical to the first plate in terms
c-> of steel ultimate strength
  fu = genfu(ctype(1))
endif
maxcsi = 0.
do 110 i=1,ncsplice
  call platepro(ctype(i),t,twith,reduct,teff,veff)
  if (cend(i).eq.'NEG') then
    cmp = sqrt(totforce(cmem(i),1)**2+
+      (abs(totforce(cmem(i),2)))+
+      abs(totforce(cmem(i),3)*2./clength(i)))**2)
  elseif (cend(i).eq.'POS') then
    cmp = sqrt(totforce(cmem(i),4)**2+

```

```

+          (abs(totforce(cmem(i),5))+
+          abs(totforce(cmem(i),6)*2./clength(i)))**2)
else
  write (*,*) 'Error in Compression Splice Plate definition'
  stop
endif
thold = 2.*(clength(i)-reduct)*cwidth(i)*twidth*toothfac(i)
csi = cmp/thold
if (csi.gt.maxcsi) then
  maxcsi = csi
  iplate = i
endif
110 continue
return
end

```

```

subroutine chktenj(maxcsi,iplate,mode)
common /define/ coord,connect,mtype,ngroup,nmem,grade,usetype
common /force/ dforce,dload,lforce,lload,totforce,totload
common /tjoint/ tlength,twidth,ntsplice,tmem,tend,ttype
common /trusstat/ newtruss
character*3 tend(4)
character*4 usetype(50)
character*10 grade(50),ttype(4)
integer connect(100,2),mtype(100),tmem(4),nplate(2)
logical newtruss
real coord(100,2),dforce(100,6),dload(100,2),tencsi(2),
+   lforce(100,6),lload(100,2),maxcsi,totforce(100,6),
+   totload(100,2),tmpsi(2),twidth(4),tlength(4),toothfac(4)
if (newtruss) then
  do 100 i=1,ntsplice
100    toothfac(i) = gentfact()
    fu = genfu(ttype(1))
  endif
  do 110 i=1,2
110    tmpsi(i) = 0.
  maxcsi = 0.
  do 120 i=1,ntsplice
    call platepro(ttype(i),t,twidth,reduct,teff,veff)
    if (tend(i).eq.'NEG') then
      ten = sqrt(totforce(tmem(i),1)**2+
+      (abs(totforce(tmem(i),2))+
+      abs(totforce(tmem(i),3)*2./tlength(i)))**2)
    elseif (tend(i).eq.'POS') then
      ten = sqrt(totforce(tmem(i),4)**2+
+      (abs(totforce(tmem(i),5))+
+      abs(totforce(tmem(i),6)*2./tlength(i)))**2)
    else
      write (*,*) 'Error in Tension Splice Plate definition'
      stop
    endif
    tall = 2.*twidth(i)*teff*t*fu
    thold = (tlength(i)-reduct)*twidth(i)*twidth*toothfac(i)
    tencsi(1) = ten/tall
    tencsi(2) = ten/thold
c-> this loop finds the most critical tension plate in the truss for
c-> each individual failure mode
    do 120 j=1,2
      if (tencsi(j).gt.tmpsi(j)) then
        tmpsi(j) = tencsi(j)
      endif
    enddo
  enddo
endif

```

```

        nplate(j) = i
    endif
120  continue
    do 130 i=1,2
        if (tmpcsi(i).gt.maxcsi) then
            maxcsi = tmpcsi(i)
            iplate = nplate(i)
            mode = i
        endif
130  continue
    return
end

subroutine chkpeak(maxcsi, imem, mode)
common /define/ coord, connect, mtype, ngroup, nmem, grade, usetype
common /force/ dforce, dload, lforce, lload, totforce, totload
common /peak/ peakarea, ptlen, pvlen, peakmem, mempeak,
+             peakend, peaktype, npeak
common /trusstat/ newtruss
character*3 peakend(4,5)
character*4 usetype(50)
character*10 grade(50), peaktype(4)
integer connect(100,2), mtype(100), peakmem(4,5),
+         ncritmem(2), mempeak(4), numpeak(2)
logical newtruss
real coord(100,2), dforce(100,6), dload(100,2), peakcsi(2),
+     lforce(100,6), lload(100,2), peakarea(4,5), maxcsi,
+     totforce(100,6), totload(100,2), toothfac(4), tmpcsi(2),
+     ptlen(4), pvlen(4)
if (newtruss) then
    do 100 i=1, npeak
        toothfac(i) = gentfact()
        fu = genfu(peaktype)
    endif
110  do 110 i=1,2
        tmpcsi(i) = 0.
    maxcsi = 0.
    do 120 i=1, npeak
        call platepro(peaktype(i), t, twith, reduct, teff, veff)
        do 120 j=1, mempeak(i)
            ten = 0.
            if (peakend(i,j).eq.'NEG') then
                axial = sqrt(totforce(peakmem(i,j),1)**2+
+                totforce(peakmem(i,j),2)**2)
                if (totforce(peakmem(i,j),1).lt.0.) ten = axial
            elseif (peakend(i,j).eq.'POS') then
                axial = sqrt(totforce(peakmem(i,j),4)**2+
+                totforce(peakmem(i,j),5)**2)
                if (totforce(peakmem(i,j),4).gt.0.) ten = axial
            else
                write (*,*) 'Error in Peak Plate definition'
                stop
            endif
            thold = 2.*peakarea(i,j)*twith*toothfac(i)
            tall1 = 2.*(pvlen(i)*0.577*veff+ptlen(i)*teff)*fu*t
            tall2 = 2.*(ptlen(i)*0.577*veff+pvlen(i)*teff)*fu*t
            tall = min(tall1,tall2)
            peakcsi(1) = axial/thold
            peakcsi(2) = ten/tall
        enddo
    enddo
enddo
enddo

```

c-> this loop finds the most critical member in the peak joint for  
c-> each individual failure mode

```
      do 120 k=1,2
        if (peakcsi(k).gt.tmpcsi(k)) then
          tmpcsi(k) = peakcsi(k)
          ncritmem(k) = j
          numpeak(k) = i
        endif
120    continue
c->mark
      do 130 i=1,2
        if (tmpcsi(i).gt.maxcsi) then
          maxcsi = tmpcsi(i)
          imem = peakmem(numpeak(i),ncritmem(i))
          mode = i
        endif
130    continue
      return
      end

      function gentfact()
      scale = 3.174
      shape = 8.663
      gentfact = scale*(-alog(1.-ranmar()))**(1./shape)
      return
      end

      function genfu(pltype)
      character*10 pltype
      real loc
      if (pltype(1:2).eq.'HS') then
        loc = 66216.3
        scale = 7644.2
        shape = 3.53363
      else
        loc = 52107.3
        scale = 3352.8
        shape = 1.87944
      endif
      genfu = loc+scale*(-alog(1.-ranmar()))**(1./shape)
      return
      end

      subroutine platepro(pltype,t,twith,reduct,teff,veff)
      character*10 pltype
      if (pltype(1:3).eq.'LMK') then
        t = 0.0635
        twith = 249.
        reduct = 0.
        teff = 0.591
        veff = 0.548
      elseif (pltype(1:3).eq.'LMS') then
        t = 0.0635
        twith = 200.
        reduct = 0.
```

c-> The LMS plate is a special plate. It is 680 16 gauge plate with  
c-> only two rows of teeth instead of three/inch. This plate is used  
c-> in places that require high tensile strength (bottom chord of a  
c-> truss). The efficiency ratio is theoretical based on a failure  
c-> path crossing two holes with a width of 3/16.  $1-2*3/16 = 0.625$

```

    teff = 0.625
    veff = 0.350
elseif (pltype(1:3).eq.'LMT') then
    t = 0.0396
    twith = 232.
    reduct = 0.
    teff = 0.67
    veff = 0.420
elseif (pltype(1:5).eq.'68020') then
    t = 0.0396
    twith = 200.
    reduct = 0.
    teff = 0.56
    veff = 0.34
elseif (pltype(1:5).eq.'68018') then
    t = 0.0516
    twith = 240.
    reduct = 0.
    teff = 0.59
    veff = 0.35
elseif (pltype(1:5).eq.'68016') then
    t = 0.0635
    twith = 200.
    reduct = 0.
    teff = 0.56
    veff = 0.34
elseif (pltype(1:7).eq.'R500020') then
    t = 0.0396
    twith = 211.*4./3.
    reduct = 0.5
    teff = 0.57
    veff = 0.36
elseif (pltype(1:4).eq.'TW16') then
    t = 0.0635
    twith = 178.*4./3.
    reduct = 0.5
    teff = 0.62
    veff = 0.26
else
    write (*,*) 'Incorrect Plate Type'
    stop
endif
return
end

subroutine chk lum(maxcsi,ldf,itmpmem,itmpmode)
common /define/ coord,connect,mtype,ngroup,nmem,grade,usetype
common /force/ dforce,dload,lforce,lload,totforce,totload
common /props/ depth,e,fball,fcall,ftall,loverd,width
character*4 memid,usetype(50)
character*10 grade(50)
integer connect(100,2),mtype(100)
real axltemp(3),coord(100,2),depth(50),e(50),
+ fball(50),fcall(50),ftall(50),dforce(100,6),
+ dload(100,2),ldf,length,lforce(100,6),
+ lload(100,2),loverd(100),
+ maxcsi,maxmom,momtemp(3),
+ totforce(100,6),totload(100,2),width(50)
maxcsi = 0.
do 120 i=1,nmem

```

```

inx = mtype(i)
memid = usetype(inx)
if (memid(1:2).ne.'FI') then
  xlength = coord(connect(i,2),1)-coord(connect(i,1),1)
  ylength = coord(connect(i,2),2)-coord(connect(i,1),2)
  length = sqrt(xlength*xlength+ylength*ylength)
  ctheta = xlength/length
  stheta = ylength/length
  uniformx = totload(i,1)*abs(stheta)*ctheta+
+           totload(i,2)*abs(ctheta)*stheta
  uniformy =-totload(i,1)*abs(stheta)*stheta+
+           totload(i,2)*abs(ctheta)*ctheta
  if (uniformy.ne.0..and.totforce(i,2).gt.0.) then
    distmax = -totforce(i,2)/uniformy
    if (distmax.gt.length) distmax = length
  else
    distmax = 0.
  endif
  momtemp(1) = -totforce(i,3)
  momtemp(2) = -totforce(i,3)+(totforce(i,2))*distmax/2.
  momtemp(3) = totforce(i,6)
  axltemp(1) = -totforce(i,1)
  axltemp(2) = -totforce(i,1)-uniformx*distmax
  axltemp(3) = totforce(i,4)
c-> This section of code was used for verifying the model under design
c-> loads with PPSA4. The maxmom variable was used to calculate the
c-> CSI at the maximum moment region in the member.
  maxmom = momtemp(1)
  mode = 1
  do 100 j=2,3
    if (abs(maxmom).lt.abs(momtemp(j))) then
      maxmom = momtemp(j)
      mode = j
    endif
100  continue
  do 110 jj=1,3
    if (jj.eq.2) then
      blength = 0.
c      blength = length
    else
      blength = 0.
    endif
    fb = fbprime(blength,width(inx),depth(inx),
+           e(inx),fball(inx),ldf,memid)
    ft = ftall(inx)*ldf
c-> If the axial load on the negative end of the member is greater than
c-> zero, and the axial load on the positive end of the member is less
c-> than zero than he member is loaded in compression.
    if (totforce(i,1).ge.0..and.totforce(i,4).lt.0.) then
      if (jj.eq.2) then
        cblength = loverd(i)
      else
        cblength = 0.
c      cblength = loverd(i)
    endif
    fc = fcprime(cblength,e(inx),fcall(inx),ldf,memid)
    cstress = axltemp(jj)/(width(inx)*depth(inx))
c-> checks if the member is an interior member. If it is an interior
c-> member, both ends should be 'pinned'; therefore should have no
c-> moment. Thus CSI is equal to actual stress over allowable stress,

```

```

c-> instead of squaring the term.
      if (memid(2:2).ne.'I') then
          bstress = momtemp(jj)/(width(inx)*depth(inx)*
+              depth(inx)/6.)
          csi = (cstress/fc)**2+
+              abs(bstress)/(fb*(1.+cstress/
+              euler(e(inx),loverd(i),memid)))
      else
          csi = -cstress/fc
      endif
      elseif(totforce(i,1).lt.0..and.totforce(i,4).ge.0.)then
+          bstress = momtemp(jj)/(width(inx)*depth(inx)*
          depth(inx)/6.)
          tstress = axltemp(jj)/(width(inx)*depth(inx))
          csit1 = tstress/ft+abs(bstress)/(fball(inx)*ldf)
          csit2 = (abs(bstress)-tstress)/fb
          csi = amax1(csit1,csit2)
      else
          write(*,*) 'load reversal'
          stop
      endif
      if (csi.gt.maxcsi) then
          maxcsi = csi
          itmpmem = i
          itmpmode = jj
      endif
110      continue
      endif
120      continue
      return
      end

      function euler(e,loverd,memid)
      character*4 memid
      real kce, loverd
      if (memid(2:2).eq.'1'.or.memid(3:3).eq.'1') then
c          kce = 0.418
          kce = 0.822
      else
c          kce = 0.3
          kce = 0.822
      endif
      euler = kce*e/(loverd*loverd)
      return
      end

```

c This function calculates the bending allowable design stress.  
c The Beam Stability Factor, C<sub>L</sub>, (section 3.3.3 c 1991 NDS.  
c The effective buckling length is calculated using equations  
c provided in the footnotes of Table 3.3.3.  
c

```

      function fbprime(lu,width,depth,e,fball,ldf,memid)
      character*4 memid
      real kbe, le,ldf,lu
      if(memid(1:1).eq.'S') lu = 0.
      if (lu.eq.0..or.width.ge.depth) then
          cl = 1.0
      else
          if (lu/depth.lt.7.) then

```



```

        le = 2.06*lu
    elseif (lu/depth.le.14.3) then
        le = 1.63*lu+3.*depth
    else
        le = 1.84*lu
    endif
    if (memid(2:2).eq.'1'.or.memid(3:3).eq.'1') then
c       kbe = 0.609
c       kbe = 1.44
    else
c       kbe = 0.438
c       kbe = 1.44
    endif
    ratio = (kbe*e/(le*depth/(width*width)))/(fball*ldf)
    c1 = ((1+ratio)/1.9)-sqrt(
+       ((1+ratio)/1.9)**2-(ratio/0.95))
    endif
    fbprime = fball*ldf*c1
    return
end

```

c This function calculates the compression parallel to grain  
c allowable design stress. The Column Stability Factor, C<sub>P</sub>,  
c (section 3.7.1, 1991 NDS). The effective column length over  
c depth is estimated by PPSA4. This function is only intended  
c for solid sawn, visually graded lumber.

c234567

```

function fcprime(loverd,e,fcall,ldf,memid)
character*4 memid
real loverd,ldf
if (loverd.eq.0.) then
    cp = 1.0
else
    ratio = euler(e,loverd,memid)/(fcall*ldf)
    cp = ((1+ratio)/1.6)-sqrt(
+       ((1+ratio)/1.6)**2-(ratio/0.8))
endif
fcprime = fcall*ldf*cp
return
end

```

c This subroutine reads input from a file named TRUSS.INP, and  
c LUMBER.INP.

```

subroutine input
common /cjoint/ clength,cwidth,ncsplice,cmem,cend,ctype
common /define/ coord,connect,mtype,ngroup,nmem,grade,usetype
common /force/ dforce,dload,lforce,lload,totforce,totload
common /heel/ heelarea,heelvl,heelmem,heelend,heeltype
common /peak/ peakarea,ptlen,pvlen,peakmem,mempeak,
+       peakend,peaktype,npeak
common /props/ depth,e,fball,fcall,ftall,loverd,width
common /tjoint/ tlength,twidth,ntsplice,tmem,tend,ttype
common /webj/ webtl,webvl,webarea,nwebp,locweb,webmem,
+       webend,webtype
character*3 heelend(2,2),cend(4),peakend(4,5),tend(4),
+       webend(30,2)
character*4 usetype(50)
character*10 grade(50),heeltype(2),peaktype(4),ctype(4),ttype(4),
+       webtype(30)
character*80 junk

```

```

integer connect(100,2),cmem(4),heelmem(2,2),mtype(100),
+   peakmem(4,5),tmem(4),mempeak(4),webmem(30,2),locweb(2)
real coord(100,2),clength(4),cwidth(4),depth(50),
+   dforce(100,6),dload(100,2),e(50),fball(50),
+   fcall(50),ftall(50),heelarea(2),heelvl(2),lforce(100,6),
+   lload(100,2),loverd(100),peakarea(4,5),totforce(100,6),
+   totload(100,2),twidth(4),tlength(4),width(50),ptlen(4),
+   pvlen(4),webarea(30),webtl(30),webvl(30)
open (unit=10,file='truss.inp',status='old')
open (unit=20,file='lumber.inp',status='old')
open (unit=30,file='plates.inp',status='old')
10  format(a)
20  format(2x,i2,5x,a4,3(2x,f5.0),2(2x,f6.3),1x,e9.4)
30  format(2x,i2,5x,a10)
40  format(1x,i2,6x,a3,4x,i2,6x,a3,3x,f7.3,3x,f7.3,3x,a10)
50  format(1x,i5,5x,f5.2,6x,f5.2,6x,a10)
60  format(1x,i2,6x,a3,4x,f7.3)
70  format(1x,i2,6x,a3,3x,f6.3,2x,f6.3,3x,a10)
80  format(1x,i2,6x,a3,4x,i2,6x,a3,4x,f5.2,4x,f5.2,6x,f5.2,4x,a10)
read (10,10) junk
read (10,10) junk
read (10,*) nnode, nmem, ngroup, nrealm, ndload, nlload
read (10,10) junk
read (10,10) junk
do 100 i=1,ngroup
100  read (10,20) ijunk, usetype(i), fball(i), fcall(i),
+     ftall(i), width(i), depth(i), e(i)
read (20,10) junk
read (20,10) junk
do 110 i=1,ngroup
110  read (20,30) ijunk, grade(i)
read (10,10) junk
read (10,10) junk
do 120 i=1,nnode
120  read (10,*) ijunk, coord(i,1), coord(i,2)
read (10,10) junk
read (10,10) junk
do 130 i=1,nmem
130  read (10,*) ijunk, (connect(i,j), j=1,2), mtype(i)
read (10,10) junk
read (10,10) junk
do 140 i=1,ndload
140  read (10,*) imem, (dload(imem,j), j=1,2)
read (10,10) junk
read (10,10) junk
do 150 i=1,nmem
read (10,*) ijunk, (dforce(i,j), j=1,3)
150  read (10,*) (dforce(i,j), j=4,6)
read (10,10) junk
read (10,10) junk
do 160 i=1,nlload
160  read (10,*) imem, (lload(imem,j), j=1,2)
read (10,10) junk
read (10,10) junk
do 170 i=1,nmem
read (10,*) ijunk, (lforce(i,j), j=1,3)
170  read (10,*) (lforce(i,j), j=4,6)
read (10,10) junk
read (10,10) junk
do 180 i=1,nrealm

```

```

180     read (10,*) imem, loverd(imem)
       read (30,10) junk
       read (30,10) junk
       read (30,*) npeak, ncspllice, ntspllice, nwebp
       read (30,10) junk
       read (30,10) junk
       do 190 i=1,2
190     read (30,40) heelemem(i,1),heelend(i,1),heelemem(i,2),
+       heelend(i,2),heelvl(i),heelarea(i),heeltype(i)
       do 200 i=1,npeak
         read (30,10) junk
         read (30,10) junk
         read (30,50) mempeak(i),ptlen(i), pvlen(i), peaktype(i)
         read (30,10) junk
         read (30,10) junk
         do 200 j=1,mempeak(i)
200         read (30,60) peakmem(i,j), peakend(i,j), peakarea(i,j)
         read (30,10) junk
         read (30,10) junk
         do 210 i=1,ncspllice
210         read (30,70) cmem(i),cend(i),cwidth(i),clength(i),ctype(i)
         read (30,10) junk
         read (30,10) junk
         do 220 i=1,ntspllice
220         read (30,70) tmem(i),tend(i),twidth(i),tlength(i),ttype(i)
         read (30,10) junk
         read (30,10) junk
         do 230 i=1,nwebp
230         read (30,80) webmem(i,1),webend(i,1),webmem(i,2),webend(i,2),
+       webtl(i),webvl(i),webarea(i),webtype(i)
       return
       end

subroutine genprop
common /define/ coord,connect,mtype,ngroup,nmem,grade,usetype
common /props/ depth,e,fball,fcall,ftall,loverd,width
parameter (lda = 4)
character*4 usetype(50)
character*10 grade(50), groupid
integer connect(100,2), mtype(100)
real corr(4,4), c(4,4), x(4), z(4),
+   coord(100,2), depth(50), e(50),
+   fball(50), fcall(50), ftall(50),
+   loverd(100),width(50)
data (corr(1,j),j=1,lda) /1.00, 0.30, 0.65, 0.40/
data (corr(2,j),j=1,lda) /0.30, 1.00, 0.65, 0.00/
data (corr(3,j),j=1,lda) /0.65, 0.65, 1.00, 0.00/
data (corr(4,j),j=1,lda) /0.40, 0.00, 0.00, 1.00/
call dcmpmatx(corr,lda,c)
do 200 jj=1,ngroup
  groupid = grade(jj)
  if (groupid(1:2).eq.'FI') then
    fball(jj) = 5555.
    fcall(jj) = 0.
    ftall(jj) = 0.
  else
100    do 100 i=1,lda
      z(i) = stdnor()
    do 120 i=1,lda
      sum = 0.

```

```

do 110 j=1,i
110     sum = sum+z(j)*c(i,j)
120     x(i) = sum
        if (groupid(1:9).eq.'SPDSS2X10') then
c-> These values are based on southern pine select structural 2x10s.
c-> they were scaled by the design values for DSS/SS.
        bloc = 1.858
        bscale = 6.46
        bshape = 4.37
        factor = 1000.*2150./2050.
        fball(jj) = genweib(bloc,bscale,bshape,factor,x(1))
        cloc = 0.
        cmean = 1.748
        cstdev = 0.178
        factor = 1000.*2000./1850.
        fcall(jj) = genln(cloc,cmean,cstdev,factor,x(2))
        eloc = 0.811
        escale = 1.16
        eshape = 3.63
        factor = 1000000.*1.9/1.8
        e(jj) = genweib(eloc,escale,eshape,factor,x(3))
        tloc = 0.
        tscale = 5.70
        tshape = 4.80
        factor = 1000.*1200./1100.
        ftall(jj) = genweib(tloc,tscale,tshape,factor,x(4))
elseif (groupid(1:9).eq.'SPMSR2X10') then
        bloc = 1.858
        bscale = 6.46
        bshape = 4.37
        factor = 1000.*2250./2050.
        fball(jj) = genweib(bloc,bscale,bshape,factor,x(1))
        cloc = 0.
        cmean = 1.748
        cstdev = 0.178
        factor = 1000.*1925./1850.
        fcall(jj) = genln(cloc,cmean,cstdev,factor,x(2))
c-> The COV_E for this distribution was 0.16. May be too wide for an
c-> MSR graded piece of lumber.
        eloc = 0.811
        escale = 1.16
        eshape = 3.63
        factor = 1000000.*1.9/1.8
        e(jj) = genweib(eloc,escale,eshape,factor,x(3))
        tloc = 0.
        tscale = 5.70
        tshape = 4.80
        factor = 1000.*1750./1100.
        ftall(jj) = genweib(tloc,tscale,tshape,factor,x(4))
elseif (groupid(1:7).eq.'SPN12X4') then
        bloc = 0.
        bmean = 2.241
        bstdev = 0.314
        factor = 1000.
        fball(jj) = genln(bloc,bmean,bstdev,factor,x(1))
        cloc = 0.
        cmean = 1.593
        cstdev = 0.166
        factor = 1000.
        fcall(jj) = genln(cloc,cmean,cstdev,factor,x(2))

```

```

    eloc = 1.030
    escale = 0.77
    eshape = 2.07
    factor = 1000000.
    e(jj) = genweib(eloc, escale, eshape, factor, x(3))
    tloc = 0.
    tmean = 1.288
    tstdev = 0.352
    factor = 1000.
    ftall(jj) = genln(tloc, tmean, tstdev, factor, x(4))
elseif (groupid(1:7).eq.'SPN22X4') then
    bloc = 1.619
    bscale = 7.75
    bshape = 2.09
    factor = 1000.
    fball(jj) = genweib(bloc, bscale, bshape, factor, x(1))
    cloc = 0.
    cmean = 1.573
    cstdev = 0.230
    factor = 1000.
    fcall(jj) = genln(cloc, cmean, cstdev, factor, x(2))
    eloc = 0.532
    escale = 1.20
    eshape = 3.03
    factor = 1000000.*1.9/1.8
    e(jj) = genweib(eloc, escale, eshape, factor, x(3))
    tloc = 0.
    tmean = 1.246
    tstdev = 0.464
    factor = 1000.
    ftall(jj) = genln(tloc, tmean, tstdev, factor, x(4))
elseif (groupid(1:8).eq.'SPMSR2X6') then
c-> These values are based on southern pine select structural 2x6s.
c-> they were scaled by the design values for 2250f-1.9e/SS.
    bloc = 0.0
    bscale = 10.03
    bshape = 4.27
    factor = 1000.*2250./2300.
    fball(jj) = genweib(bloc, bscale, bshape, factor, x(1))
    cloc = 3.127
    cscale = 3.19
    cshape = 2.73
    factor = 1000.*1925./1900.
    fcall(jj) = genweib(cloc, cscale, cshape, factor, x(2))
c-> COV_E for this distribution is .23. This seems to large, but
c-> the this member is a tension member for the lumbermate truss;
c-> therefore, E is not used in the model!
    eloc = 0.407
    escale = 1.36
    eshape = 3.52
    factor = 1000000.*1.9/1.6
    e(jj) = genweib(eloc, escale, eshape, factor, x(3))
    tloc = 0.
    tscale = 6.120
    tshape = 3.85
    factor = 1000.*1750./1300.
    ftall(jj) = genweib(tloc, tscale, tshape, factor, x(4))
else
    write(*,*) 'LUMBER.INP has incorrect grade names'
    stop

```

```

                endif
            endif
200    continue
        end

c
c This subroutine performs a Cholesky decomposition of the correlation
c matrix, r(n,n). R is a positive definite, symmetric matrix. The
c subroutine returns the unique lower triangular matrix, c(n,n). The
c two matrices are related by the following:
c
c      r = cc'
c where:
c      c' is the transposed matrix c
c
c This subroutine uses a subroutine from Numerical Recipes (Press et
c al, 1992). CHOLDC was used to perform the decomposition; however,
c this program returns the decomposed matrix in the lower half of the
c original matrix. I wanted to keep the integrity of the original
c matrix.
c
c References:
c
c Fishman. 1978. Principles of Discrete Event Simulation. Wiley & Sons
c pub. pp.464-466.
c
        subroutine dcmpmatx(r,n,c)
        parameter (nl=3)
        real c(n,n), p(nl), r(n,n)
        do 100 i=1,n
            do 100 j=1,n
100         c(i,j) = r(i,j)
            call choldc(c,n,n,p)
            do 110 i=1,n
                c(i,i) = p(i)
                do 110 j=i+1,n
110         c(i,j) = 0.
            return
        end

c This function generates a random deviate following the Weibull
c distribution. The function is passed a N(0,1) random number,
c it uses the inverse transformation method to generate a Weibull
c deviate of given location, scale and shape. There is also a
c parameter called factor that will factor the Weibull parameters
c by a constant. The function was written for generating correlated
c random variables
c234567
        function genweib(loc,scale,shape,factor,x)
        real loc
        loc = loc*factor
        scale = scale*factor
        genweib = loc+scale*(-alog(1.-anorm(x)))**(1./shape)
        return
        end

c This function generates a random deviate following the Lognormal
c distribution. The function is passed a N(0,1) random number,
c and the function outputs a Lognormal deviate with give location,
c scale and shape. There is also a parameter called factor that will
c factor the lognormal parameters by a constant.

```

```

c234567
    function genln(loc,mean,stdev,factor,x)
    real loc, mean
    loc = loc*factor
    mean = mean+alog(factor)
    genln = loc+exp(mean+stdev*x)
    return
    end

c-> cut here
c-> numerical recipes subroutines below this point
    SUBROUTINE choldc(a,n,np,p)
    INTEGER n,np
    REAL a(np,np),p(n)
    INTEGER i,j,k
    REAL sum
    do 13 i=1,n
        do 12 j=i,n
            sum=a(i,j)
            do 11 k=i-1,1,-1
                sum=sum-a(i,k)*a(j,k)
11          continue
            if(i.eq.j)then
                if(sum.le.0.)pause 'choldc failed'
                p(i)=sqrt(sum)
            else
                a(j,i)=sum/p(i)
            endif
12          continue
13          continue
    return
    END
C (C) Copr. 1986-92 Numerical Recipes Software.

```

```

C=====
C
C                               Function:  RANMAR
C
C=====
C
C  This generator passes ALL of the test for random number
C  generators and has a period of 2^144, is completely portable
C  (gives bit identical results on all machines with at least
C  24-bit mantissas in the floating point representation).
C
C  The algorithm is a combination of a Fibonacci sequence (with
C  lags of 97 and 33, and operation "subtraction plus one, modulo
C
C  The original algorithm was developed by Marsaglia and Zaman
C  (1990).  This algorithm was developed as a function that required
C  four random number seeds.  James (1990) modified the original
C  algorithm by converting the function to a subroutine that
C  returned a vector of uniform random numbers.  James suggested
C  combining the four random number seeds into one, then split the
C  one seed into four.  The code received from Cooke (1994)
C  required two seeds, and contained error trapping to check if
C  the seeds were valid and if the random number generator had been
C  initialized by RANMAR().  The error trapping was modified by
C  Skaggs (1994).  Skaggs also converted the subroutine back to a
C  function

```

```

c
c REFERENCES:
c
c Cooke. R. A. 1994. Department of Biological Systems Engineering.
c Virginia Tech.
c
c James. F. 1990. A review of pseudorandom number generators.
c Computer Physics Communications 60:329-344.
c
c Marsaglia, G. and A. Zaman. 1990. Toward a universal random
c number generator. Statistics and Probability Letters 8:35-39.
c
c Skaggs. T. D. 1994. Department of Biological Systems Engineering.
c Virginia Tech.
c

```

```

c=====
c234567

```

```

function RANMAR()
real u(97)
logical test
common /raset1/ u, c, cd, cm, i97, j97, test
10 format (/,10x,'Must initialize RNG by calling RANMAR',/)
if( .not. test) then
write (*,10)
stop
endif
uni = u(i97) - u(j97)
if (uni.lt.0.) uni = uni + 1.0
u(i97) = uni
i97 = i97 - 1
if (i97.eq.0) i97 = 97
j97 = j97 - 1
if (j97.eq.0) j97 = 97
c = c - cd
if (c.lt.0.) c = c + cm
uni = uni - c
if (uni.lt.0.) uni = uni + 1.0
if (uni.eq.0.) uni = u(j97)*2.**(-24)
ranmar = uni
100 continue
return
end

```

```

c=====
c
c Subroutine: RMARIN
c

```

```

c=====
c
c This is the initialization routine for the random number
c generator RANMAR(). See RANMAR for more information on
c these subroutines.
c
c NOTE: The seed variables can have values between:
c
c 0 <= IJ <= 31328
c 0 <= KL <= 30081
c
c Use IJ = 1802 & KL = 9373 to test the random number generator.
c The subroutine RANMAR should be used to generate 20000 random
c numbers. Then display the next six random numbers generated.

```



```
c If the random number generator is working properly, the random
c numbers should be:
```

```
c          .3894503      .8475913      .4336278
c          .3678937      .4979669      .6337869
c
```

```
=====
c234567
```

```
      subroutine RMARIN(ij,kl)
      logical test
      real u(97)
      common /raset1/ u, c, cd, cm, i97, j97, test
10     format (/,10x,'Seed1 must be between 0 and 31328',/)
20     format (/,10x,'Seed2 must be between 0 and 30081',/)
      if (ij.lt.0.or.ij.gt.31328) then
          write (*,10)
          stop
      endif
      if (kl.lt.0.or.kl.gt.30081) then
          write (*,20)
          stop
      endif
      i = mod(ij/177, 177) + 2
      j = mod(ij      , 177) + 2
      k = mod(kl/169, 178) + 1
      l = mod(kl,      169)
      do 40 ii = 1, 97
          s = 0.
          t = .5
          do 30 jj = 1, 24
              m = mod(mod(i*j, 179)*k, 179)
              i = j
              j = k
              k = m
              l = mod(53*l+1, 169)
              if (mod(l*m, 64) .ge. 32) then
                  s = s + t
              endif
              t = 0.5 * t
30         continue
          u(ii) = s
40     continue
      c = 362436. / 16777216.
      cd = 7654321. / 16777216.
      cm = 16777213. /16777216.
      i97 = 97
      j97 = 33
      test = .true.
      return
      end
```

```
=====
c
c          Function:  STDNOR
c
=====
```

```
c
c All statement numbers correspond to the steps of algorithm 'fl'
c (m=5) in Ahrens and Dieter (1973). Slightly modified
```

```

c implementation. Modified by Barry W. Brown, Feb 3, 1988 to
c use RANF instead of SUNIF. The argument IR thus goes away.
c Modified by Thomas D. Skaggs, June 1994 to use RANMAR instead
c of RANF.

```

```

c REFERENCES:

```

```

c Ahrens, J.H. and U. Dieter. 1973. Extensions of forsythe's
c method for random sampling from the normal distribution.
c Mathematics of Computation, 27(124): 927-937.
c
c Skaggs. T. D. 1994. Department of Biological Systems Engineering.
c Virginia Tech.

```

```

c=====

```

```

c234567

```

```

function STDNOR()
dimension a(32),d(31),t(31),h(31)
c-> The definitions of the constants a(k), d(k), t(k) and
c-> h(k) are according to Ahrens and Dieter (1973).
data a/.0d0 ,.3917609d-1,.7841241d-1,.1177699d0,.1573107d0,
+ .1970991d0,.2372021d0, .2776904d0, .3186394d0,.3601299d0,
+ .4022501d0,.4450965d0, .4887764d0, .5334097d0,.5791322d0,
+ .6260990d0,.6744898d0, .7245144d0, .7764218d0,.8305109d0,
+ .8871466d0,.9467818d0,1.009990d0, 1.077516d0,1.150349d0,
+ 1.229859d0,1.318011d0, 1.417797d0, 1.534121d0,1.675940d0,
+ 1.862732d0,2.153875d0/
data d/5*0.0d0, .2636843d0, .2425085d0, .2255674d0,.2116342d0,
+ .1999243d0,.1899108d0, .1812252d0, .1736014d0,.1668419d0,
+ .1607967d0,.1553497d0, .1504094d0, .1459026d0,.1417700d0,
+ .1379632d0,.1344418d0, .1311722d0, .1281260d0,.1252791d0,
+ .1226109d0,.1201036d0, .1177417d0, .1155119d0,.1134023d0,
+ .1114027d0,.1095039d0/
data t/.7673828d-3,.2306870d-2,.3860618d-2,.5438454d-2,
+ .7050699d-2,.8708396d-2,.1042357d-1,.1220953d-1,.1408125d-1,
+ .1605579d-1,.1815290d-1,.2039573d-1,.2281177d-1,.2543407d-1,
+ .2830296d-1,.3146822d-1,.3499233d-1,.3895483d-1,.4345878d-1,
+ .4864035d-1,.5468334d-1,.6184222d-1,.7047983d-1,.8113195d-1,
+ .9462444d-1,.1123001d0,.1364980d0,.1716886d0,.2276241d0,
+ .3304980d0,.5847031d0/
DATA h/.3920617d-1,.3932705d-1,.3950999d-1,.3975703d-1,
+ .4007093d-1,.4045533d-1,.4091481d-1,.4145507d-1,.4208311d-1,
+ .4280748d-1,.4363863d-1,.4458932d-1,.4567523d-1,.4691571d-1,
+ .4833487d-1,.4996298d-1,.5183859d-1,.5401138d-1,.5654656d-1,
+ .5953130d-1,.6308489d-1,.6737503d-1,.7264544d-1,.7926471d-1,
+ .8781922d-1,.9930398d-1,.1155599d0,.1404344d0,.1836142d0,
+ .2790016d0,.7010474d0/
10 u = ranmar()
s = 0.d0
if (u.gt.0.5) s = 1.d0
u = u + u - s
20 u = 32.0*u
i = int(u)
if (i.eq.32) i = 31
if (i.eq.0) goto 100
c-> Start Center
30 ustar = u - float(i)
aa = a(i)
40 if (ustar.le.t(i)) goto 60
w = (ustar-t(i))*h(i)

```

```

c-> Exit (Both Cases)
50   y = aa + w
      stdnor = y
      if (s.eq.1.d0) stdnor = -y
      return
c-> Center Continued
60   u = ranmar()
      w = u* (a(i+1)-aa)
      tt = (0.5*w+aa)*w
      goto 80
70   tt = u
      ustar = ranmar()
80   if (ustar.gt.tt) goto 50
90   u = ranmar()
      if (ustar.ge.u) goto 70
      ustar = ranmar()
      goto 40
c-> Start Tail
100  i = 6
      aa = a(32)
      goto 120
110  aa = aa + d(i)
      i = i + 1
120  u = u + u
      if (u.lt.1.d0) goto 110
130  u = u - 1.d0
140  w = u*d(i)
      tt = (0.5*w+aa)*w
      goto 160
150  tt = u
160  ustar = ranmar()
      if (ustar.gt.tt) goto 50
170  u = ranmar()
      if (ustar.ge.u) goto 150
      u = ranmar()
      goto 140
      end

```

```

C=====
C
C                               Function:  ANORM
C
C=====
C
C  This function evaluates the standard normal function Phi(x).
C  It uses the following identity found in IMSL/STAT (1987):
C
C                                $\Phi(x) = 1.-\text{erfc}(x/\text{sqrt}(2.))/2.$ 
C
C  The complementary error function is a special case of the
C  incomplete gamma function.  Numerical Recipes Press et al. (1992)
C  was used to evaluate ERFC.
C
C  REFERENCES:
C
C  IMSL. 1987. Stat/library: FORTRAN subroutines for statistical
C  analysis. IMSL, Houston, Tex.
C
C  Press. W.H., S.A. Teukolsky, W.T. Vetterling and B.P. Flannery.

```

```
c 1992. Numerical recipes in FORTRAN: the art of scientific |
c computing. Cambridge Univesity Press, Cambridge, Mass. |
c |
```

```
=====
c234567
```

```
function ANORM(x)
  anorm = 1.-erfc(x/sqrt(2.))/2.
  return
end
```

```
FUNCTION erfc(x)
REAL erfc,x
CU USES gammp,gammq
REAL gammp,gammq
if(x.lt.0.)then
  erfc=1.+gammp(.5,x**2)
else
  erfc=gammq(.5,x**2)
endif
return
END
```

C (C) Copr. 1986-92 Numerical Recipes Software.

```
FUNCTION gammln(xx)
REAL gammln,xx
INTEGER j
DOUBLE PRECISION ser,stp,tmp,x,y,cof(6)
SAVE cof,stp
DATA cof,stp/76.18009172947146d0,-86.50532032941677d0,
*24.01409824083091d0,-1.231739572450155d0,.1208650973866179d-2,
*-.5395239384953d-5,2.5066282746310005d0/
x=xx
y=x
tmp=x+5.5d0
tmp=(x+0.5d0)*log(tmp)-tmp
ser=1.000000000190015d0
do 11 j=1,6
  y=y+1.d0
  ser=ser+cof(j)/y
11 continue
gammln=tmp+log(stp*ser/x)
return
END
```

C (C) Copr. 1986-92 Numerical Recipes Software.

```
FUNCTION gammp(a,x)
REAL a,gammp,x
CU USES gcf,gser
REAL gammcf,gamser,gln
if(x.lt.0..or.a.le.0.)pause 'bad arguments in gammp'
if(x.lt.a+1.)then
  call gser(gamser,a,x,gln)
  gammp=gamser
else
  call gcf(gammcf,a,x,gln)
  gammp=1.-gammcf
endif
return
END
```

C (C) Copr. 1986-92 Numerical Recipes Software.

```

FUNCTION gammq(a,x)
REAL a,gammq,x
CU  USES gcf,gser
REAL gammcf,gamser,gln
if(x.lt.0..or.a.le.0.)pause 'bad arguments in gammq'
if(x.lt.a+1.)then
  call gser(gamser,a,x,gln)
  gammq=1.-gamser
else
  call gcf(gammcf,a,x,gln)
  gammq=gammcf
endif
return
END

```

C (C) Copr. 1986-92 Numerical Recipes Software.

```

SUBROUTINE gcf(gammcf,a,x,gln)
INTEGER ITMAX
REAL a,gammcf,gln,x,EPS,FPMIN
PARAMETER (ITMAX=100,EPS=3.e-7,FPMIN=1.e-30)
CU  USES gammln
INTEGER i
REAL an,b,c,d,del,h,gammln
gln=gammln(a)
b=x+1.-a
c=1./FPMIN
d=1./b
h=d
do 11 i=1,ITMAX
  an=-i*(i-a)
  b=b+2.
  d=an*d+b
  if(abs(d).lt.FPMIN)d=FPMIN
  c=b+an/c
  if(abs(c).lt.FPMIN)c=FPMIN
  d=1./d
  del=d*c
  h=h*del
  if(abs(del-1.).lt.EPS)goto 1
11  continue
  pause 'a too large, ITMAX too small in gcf'
1   gammcf=exp(-x+a*log(x)-gln)*h
return
END

```

C (C) Copr. 1986-92 Numerical Recipes Software.

```

SUBROUTINE gser(gamser,a,x,gln)
INTEGER ITMAX
REAL a,gamser,gln,x,EPS
PARAMETER (ITMAX=100,EPS=3.e-7)
CU  USES gammln
INTEGER n
REAL ap,del,sum,gammln
gln=gammln(a)
if(x.le.0.)then
  if(x.lt.0.)pause 'x < 0 in gser'
  gamser=0.
  return
endif
ap=a

```

```
sum=1./a
del=sum
do 11 n=1,ITMAX
  ap=ap+1.
  del=del*x/ap
  sum=sum+del
  if(abs(del).lt.abs(sum)*EPS)goto 1
11 continue
  pause 'a too large, ITMAX too small in gser'
1 gamser=sum*exp(-x+a*log(x)-gln)
  return
  END
C (C) Copr. 1986-92 Numerical Recipes Software.
```

## VITA

Thomas D. Skaggs was born in Amarillo, Texas on August 10, 1967. He is the son of Grady and Nancy Skaggs of Adrian, Texas. After graduating from Adrian High School in May of 1985, Tom attended his fathers alma mater, Texas A&M University. He finished his undergraduate degree in Agricultural Engineering in December 1989. Tom stayed in the Agricultural Engineering department and completed his Master of Science Degree, specializing in Wood Structures, in December of 1991. Tom won second place in the Wood Award sponsored by the Forest Products Society for a paper describing his M.S. research at Texas A&M.

During Tom's tenure at Texas A&M, he was an active member of the Fraternity of Phi Gamma Delta. He was also a member of the following honor societies: Tau Beta Pi, Alpha Epsilon, Gamma Sigma Delta and Alpha Zeta.

Tom began pursuing his Doctor of Philosophy in January 1992 at Virginia Tech. Tom served on several departmental committees in the Department of Biological Systems Engineering (formerly Agricultural Engineering). Tom was Vice-President and then later President of Virginia Eta Chapter of Alpha Epsilon. He also had an opportunity to teach a senior level course in the department in the area of probabilistic engineering.

Tom has accepted a position with the Engineered Wood Association (formerly the American Plywood Association) in Tacoma, Washington. He will continue to perform research in the area of wood structures.

His permanent address is:

c/o Grady S. Skaggs  
P.O. Box 37  
Adrian, TX 79001.

